CATALYTIC SYNTHESIS OF NANOCELLULOSE FROM OIL PALM EMPTY FRUIT BUNCH FIBRES

MAZLITA BINTI YAHYA

INSTITUTE OF GRADUATE STUDIES
UNIVERSITY OF MALAYA
KUALA LUMPUR

2016

CATALYTIC SYNTHESIS OF NANOCELLULOSE FROM OIL PALM EMPTY FRUIT BUNCH FIBRES

MAZLITA BINTI YAHYA

DISSERTATION SUBMITTED IN FULFILMENT OF THE REQUIREMENTS FOR THE DEGREE OF MASTER OF PHILOSOPHY

INSTITUTE OF GRADUATE STUDIES
UNIVERSITY OF MALAYA
KUALA LUMPUR

2016

UNIVERSITY OF MALAYA

ORIGINAL LITERARY WORK DECLARATION

Name of Candidate: Mazlita binti Yahya

Matric No:HGA140001

Name of Degree: Master of Philosophy

Title of Project Paper/Research Report/Dissertation/Thesis ("this Work"): Catalytic Synthesis of Nanocellulose from Oil Palm Empty Fruit Bunch Fibres

Field of Study:Chemistry

I do solemnly and sincerely declare that:

(1) I am the sole author/writer of this Work;
(2) This Work is original;
(3) Any use of any work in which copyright exists was done by way of fair dealing and for permitted purposes and any excerpt or extract from, or reference to or reproduction of any copyright work has been disclosed expressly and sufficiently and the title of the Work and its authorship have been acknowledged in this Work;
(4) I do not have any actual knowledge nor do I ought reasonably to know that the making of this work constitutes an infringement of any copyright work;
(5) I hereby assign all and every rights in the copyright to this Work to the University of Malaya ("UM"), who henceforth shall be owner of the copyright in this Work and that any reproduction or use in any form or by any means whatsoever is prohibited without the written consent of UM having been first had and obtained;
(6) I am fully aware that if in the course of making this Work I have infringed any copyright whether intentionally or otherwise, I may be subject to legal action or any other action as may be determined by UM.

Candidate's Signature Date:

Subscribed and solemnly declared before,

Witness's Signature Date:

Name:

Designation:

ABSTRACT

Currently, Malaysia has substantially increased its reputation as a country developed for palm-based lignocellulosic biomass. Oil palm biomass is composed of cellulose, hemicellulose, and lignin. Generally, oil palm biomass can be divided into three categories: (i) oil palm frond (OPF), oil palm trunk (OPT) and empty fruit bunches (EFB) fibres. The presence of high cellulose content in oil palm biomass is potentially converted to nanocellulose, which is a promising bio-polymer that useful for various industrial applications (personal cares, chemicals, foods, pharmaceuticals and bio-composites). Objectives of this project are to study the effectiveness of catalytic conversion of oil palm biomass (EFB) into nanocellulose by using chemical route (inorganic acid: H_2SO_4 and inorganic salt: Ni $(NO_3)_2$) and also to optimize the nanocellulose yield by study different reaction parameters (reaction temperature ,reaction time and acidity of catalyst). Finally the objectives is to determine the physicochemical properties of produced nanocellulose by using Thermogravimetric Analyzer (TGA) and Derivatives Thermogravimetric(DTG), X-Ray Diffractometer (XRD), Fourier Transform Infrared (FTIR), High Resolution Transmission Electron Microscope (HR-TEM), Field Emission Scanning Electron Microscopy (FESEM), Atomic Force Microscopy(AFM), and Particle Size Analyzer (PSD) techniques. Nanocellulose was successfully yielded from oil palm biomass (EFB) via and strong acid hydrolysis (H_2SO_4) and Ni-salt catalyzed hydrolysis which annotated as SA-NC and Ni-NC respectively. The mild acid nickel-salt catalyzed hydrolysis capable to selectively depolymerized amorphous regions of cellulose and retained its crystalline region, thus improving the crystallinity index of the Ni-NC up to 80.75% compared to SA-NC (73.17%). The FTIR analysis confirmed that the basic cellulose structure of inorganic Ni-salt and H_2SO_4 treated products was maintained and no derivative was formed. Furthermore, FESEM images clearly display that outer layer (waxes, pectins and fats) of EFB fibres has been removed after pretreatment process. The

chemical pretreatment methods was performed followed by acid hydrolysis process to produce nano-scale dimension (SA-NC and Ni-NC). Chemical pretreatment process was executed in order to enhance both strong and mild acid hydrolysis process (SA-NC and Ni-NC). HR-TEM and AFM analyses showed that acid hydrolysis was capable to depolymerize cellulose micro-chain into average nano-dimensions in fibres length (< 700 nm) and fibres width dimension (< 50 nm). In addition, PSD results clearly showed the particle sizes had been reduced from EFB fibres(<5500 nm) to SA-NC and Ni-NC(<90.00 nm). This study concluded that Ni-salts is an efficient and selective catalyst for the hydrolysis of cellulose with high simplicity in operation as compared to inorganic acid (H_2SO_4). Optimization reaction conditions (reaction temperature, reaction time, and acidity of catalyst) were performed in order to obtain the optimized condition for nanocellulose production. Based on the reaction model generated from Response Surface Methodology-Face Central Composite Design (RSM-FCCD), the predicted nanocellulose yield was 81.40 % (60min, 45 °C, pH 3). Meanwhile, the experimental value (81.37 %) achieved was reasonably near to the predicted value generated from the model. It can be concluded that the generated model is near to predictability and close to precision for the nanocellulose yield in the experimental conditions used. In summary from the results above, it shows that nanoscale of cellulose (Ni-NC and SA-NC) was successfully produced, characterized as well as optimized from oil palm biomass (EFB) via Ni-Salt and H_2SO_4 catalyzed treatment.

ABSTRAK

Pada masa ini, reputasi Malaysia sebagai sebuah negara maju yang membangunkan biojisim lignoselulosa berasaskan sawit telah meningkat dengan ketara. Biojisim lignoselulosa kelapa sawit terdiri daripada selulosa, hemiselulosa dan lignin. Secara umumnya, biojisim sawit boleh dibahagikan kepada tiga kategori utama: (i) pelepah kelapa sawit (OPF), batang kelapa sawit (OPT) dan tandan kosong kelapa sawit (EFB). Kandungan selulosa yang tinggi dalam biojisim kelapa sawit berpotensi untuk menghasilkan nanocellulosa, iaitu bio-polimer yang berpotensi digunakan dalam pelbagai aplikasi industri (bahan sediaan jaga diri, bahan kimia, makanan, farmaseutikal dan bio-komposit). Objektif projek ini adalah mengkaji keberkesanan penukaran biomas kelapa sawit (EFB) kepada nanoselulosa menggunakan kaedah kimia (asid bukan organik: H_2SO_4 dan garam bukan organic: Ni $(NO_3)_2$)) serta pengoptimuman hasil nanoselulosa dengan mengkaji parameter tindakbalas yang berbeza (tindak balas suhu, masa, keasidan pemangkin). Pada akhir kajian ini, sifat-sifat fizikokimia nanoselulosa yang berjaya dihasilkan ditentukan menggunakan Termogravimetri Analisis (TGA) dan Derivatif Termogravimetri (DTG), Pembelauan Sinar-X (XRD), Spektroskopi Sinar Merah *Fourier Transform* (FTIR) , mikroskop transmisi elektron beresolusi tinggi (HR-TEM), mikroskop imbasan elektron pancaran medan (FESEM), mikroskop daya atom (AFM) dan distribusi saiz zarah (PSD). Nanoselulosa telah berjaya dihasilkan daripada biojisim kelapa sawit (EFB) melalui hidrolisis bermangkin asid kuat (H_2SO_4) dan garam nikel yang dijelaskan sebagai Ni-NC dan SA-NC masing-masing. Garam nikel adalah asid lemah yang bertindak sebagai pemangkin hidrolisis kerana kemampuannya untuk menyahpempolimeran(perbuatan) bahagian amorf daripada selulosa serta pada masa yang sama ia mengekalkan struktur kristalnya, iaitu berlaku peningkatan penghabluran daripada Ni-NC sehingga 80.75% berbanding SA-NC (73.17%). Analisis FTIR mengesahkan bahawa struktur organik selulosa yang dirawat menggunakan garam Nikel

dan H_2SO_4 sebagai pemangkin, berjaya dikekalkan serta tiada terbitan yang terbentuk. Tambahan pula, imej FESEM jelas memaparkan bahawa imej lapisan luar (lapisan lilin, pektin dan lemak) EFB biojisim berjaya disingkirkan selepas proses prarawatan. Kaedah prarawatan kimia dijalankan, diikuti dengan proses hidrolisis berasid untuk menghasilkan selulosa dengan dimensi berskala nano (SA-NC dan Ni-NC). Kaedah prarawatan dijalankan bagi meningkatkan kadar proses hidrolisis asid kuat dan lemah (SA-NC dan Ni-NC). HR-TEM dan analisis AFM menunjukkan bahawa asid hidrolisis mampu untuk menyahpolimer rantaian panjang serat dan lebar serat selulosa daripada saiz mikro kepada saiz purata dimensi nano masing-masing <700 nm dan <50 nm. .Di samping itu, keputusan PSD jelas menunjukkan saiz zarah berkurang daripada EFB (<5500 nm) kepada SA-NC dan Ni-NC (<90.00 nm). Kesimpulan daripada kajian ini menunjukkan bahawa garam Nikel adalah mangkin yang berkesan dan terpilih untuk pengendalian proses hidrolisis selulosa yang lebih mudah berbanding asid bukan organik (H_2SO_4). Keadaan optimum tindak balas kimia (suhu tindak balas, masa tindak balas, dan keasidan pemangkin) telah dijalankan untuk mendapatkan keadaan optimum untuk penghasilan nanoselulosa. Berdasarkan model tindak balas yang dijana melalui *Response Surface Methodology-Face Central Composite Design* (RSM-FCCD), hasil nanoselulosa yang diramalkan adalah 81.40% (60min, 45 ° C, pH 3). Sementara itu, hasil daripada eksperimen (81.37%) yang berjaya diperolehi adalah menghampiri nilai ramalan yang dijana daripada model tersebut. Dapat disimpulkan bahawa nilai model yang dijana adalah menghampiri nilai ketepatan hasil nanoselulosa yang diperolehi daripada kajian eksperimen. Secara ringkasnya daripada keputusan diatas, ia menunjukkan bahawa nanoselulosa (Ni-NC dan SA-NC) telah berjaya dihasilkan, dicirikan dan juga dioptimumkan daripada biojisim kelapa sawit (EFB) melalui rawatan bermangkin garam Nikel dan H_2SO_4 .

ACKNOWLEDGEMENTS

I am deeply grateful to both my supervisors, Dr. Lee Hwei Voon and Proffesor Sharifah Bee binti Abd Hamid for her detailed and constructive comments, and for her important support throughout my master. Their understanding, encouraging and personal guidance have provided a good basis for the present thesis.

My fellow friends from Nanotechnology and Catalysis Research Center (NANOCAT) should also be recognized for their support. My sincere appreciation also extends to all my colleagues and others who have provided assistance at various occasions.

The most importantly my beloved parents and family for their support in helping, giving limitless motivation, warm support in word of wisdom and the sacrifices they made for me to complete this thesis. Their views and tips are useful indeed. Finally yet importantly, the most Merciful and the Beneficent, Allah S.W.T for everything He showered me. Thank you.

.

TABLE OF CONTENTS

LIST OF FIGURES

LIST OF TABLES

LIST OF SYMBOLS AND ABBREVIATIONS

AFM	Atomic Force Microscopy
$Al(NO_3)_3$	Aluminium Nitrate
BC	Bacterial Cellulose
C_2H_5OH	Ethanol
C_3H_7OH	Isopropanol
C_6H_6	Benzene
C_7H_8	Toluene
$CaCl_2$	Calcium Chloride
CH_3COOH	Acetic Acid
CH_3OH	Methanol
CMC	Carboxymethyl Cellulose
C-MCC	Commercialized Microcrystalline Cellulose
CNC	Cellulose Nanocrystals
CNF	Cellulose Nanofibrils
CO	Carbon Monoxide
CO_2	Carbon Dioxide
CrI	Crystallinity Index
DTG	Derivatives Thermogravimetric
EFB	Empty Fruit Bunches
$Fe_2(SO_4)_3$	Iron(III) Sulfate
$FeCl_2$	Iron(II) Chloride
$FeCl_3$	Iron(III) Chloride
FESEM	Field Emission Scanning Electron Microscopy
$FeSO_4$	Iron(II) Sulfate

FTIR	Fourier Transform Infrared Spectroscopy
H_2O	Water
H_2O_2	Hydrogen Peroxide
H_2SO_4	Sulfuric Acid
H_3PO_4	Phosphoric acid
HCl	Hydrochloric Acid
HPH	High Pressure Homogenization
HR-TEM	High Resolution Transmission Electron Microscope
KCl	Potassium Chloride
KOH	Potassium Hydroxide
MCPF	Microcrystalline Cellulose Press Fiber
NaCl	Sodium Chloride
$NaClO_2$	Sodium Chlorite
NaOH	Sodium Hydroxide
NaOH-AQ	Sodium Hydroxide-Anthraquinone
NH_4OH	Ammonium Hydroxide
$Ni(NO_3)_2$	Nickel (II) Nitrate
Ni-NC	Nanocellulose From Ni-Salt Hydrolysis
OPEFB	Oil Palm Empty Fruit Bunch
OPEFB	Oil Palm Empty Fruit Bunch
OPF	Oil Palm Frond
OPT	Oil Palm Trunk
PKC	Palm Kernel Cake
PKS	Palm Kernel Shell
PSD	Particle Size Distribution
RSM	Response Surface Methodology

SA-NC	Nanocellulose From Acid Sulfuric Hydrolysis
SEM	Scanning Electron Microscopy
SMCA	Sodium Monochloroacetate
TEM	Transmission Electron Microscope
TGA	Thermogravimetric Analysis
XRD	X-Ray Diffraction

LIST OF EQUATIONS

CHAPTER 1: INTRODUCTION

1.1 Introduction

To date, transition from fossil-based technology to bio-resource technology is a crucial alternative seeing that the depletion of fossil fuel reserves and alarming of environmental problems to the society. Lignocellulosic biomass has become the most potential renewable feedstock for the chemicals and fuels production. It is defined as a complex bio-matrix, comprising many different polysaccharides, phenolic polymers and proteins, excluding a fossil-based resource, which is a non-starch based fibrous part of plant material that can be valorized into fuel(Agbor *et al.*, 2011) . As one of the largest producers and exporter of palm oil (approximately 20 MT/year), Malaysia's palm oil industry leaves behind a huge amount of biomass (46.6 MT) from its plantation and milling activity (Song *et al.*, 2013). The continuous expand of oil palm plantation area in Malaysia is concurrent with growing global demand for edible oil applications such as cooking oil, household products, personal care products, nutrition and transportation fuel usage. Thus, the amount of palm residues produced also shows a correspondingly increase from the palm utilization cycle . According to Shuit's case study, one hectare of oil palm plantation can generate about 50–70 tons of biomass residues from oil palm industry every year (Shuit *et al.*, 2009). For the whole palm tree, the majority empty fruit bunches (EFB), palm pressed fibres (PPF), oil palm fronds (OPF), oil palm trunks (OPT), palm kernel shells (PKS), oil palm leaves (OPL), oil palm roots (OPR) and palm oil mill effluent (POME) with less commercialization value (Figure 1.1). Minorities of the value product are palm oil, for edible oil applications such as cooking oil, household products, personal care products, nutrition and transportation fuel usage (Ng *et al.*, 2012) .

In another way, it can consider that each kg of palm oil, roughly another 4 kg of dry biomass is produced, which is a third attributed to EFB fibres while two thirds represented by trunk and frond material (Xiao-shu & Wen-xun, 1992). Up to now, palm biomass is

reaching to a large extent without high profit usage, and ultimately, it becomes a hazardous material to farmers (Ng *et al.*, 2012).

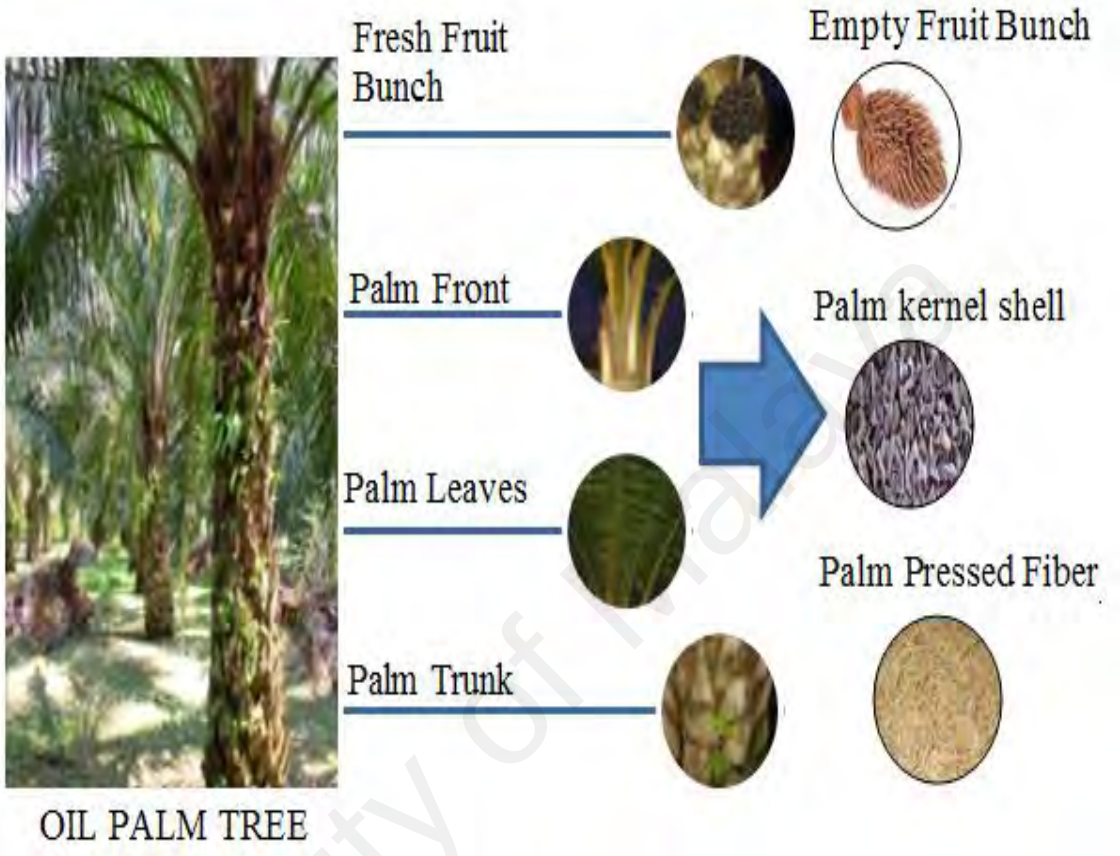

Figure 1.1: Various types of oil palm waste in Malaysia

In normal practice, the oil palm biomass are dumped into open areas, incinerated for fertilizer usage, applied as pellet fuel for industrial heating, bioelectricity generation and making pulp for paper and furniture (Table 1.1). However, the biomass burning lead to greenhouse gas (GHG) emission such as aerosol particles, CO_2, CO, volatile organic compounds and organic halogen compounds (Ng *et al.*, 2012).

Basically, oil palm biomass can be converted to a wide range of value-added products that can be clustered into bio-based chemical, nano-material, biofuel, and as direct fuel for power generation. Thus, research and development for sustainable technology is continued in order to select a wise route for biomass bio-refinery, while maintain an environmental friendly and green process (Ng *et al.*, 2012).

Table 1.1: Application of palm-based biomass in Malaysia

Palm biomass	Industrial application	References
EFB	Cigarette paper and bound paper(writing)	(Rosnah *et al.*, 2010; Singh *et al.*, 2013; Sulaiman *et al.*, 2011)
PKS	Industrial burner, road Tar, and activated carbon	(Shinoj *et al.*, 2011; Sulaiman *et al.*, 2011)
OPT	Plywood (blackboards)	(Khalil *et al.*, 2012; Shinoj *et al.*, 2011; Sulaiman *et al.*, 2011)
	Saw wood (furniture)	
OPT, EFB and PKS	Energy	(Shinoj *et al.*, 2011; Sulaiman *et al.*, 2011)
PKS	Briquettes	(Khalil *et al.*, 2012; Shinoj *et al.*, 2011)

Biomass bio-refinery is numerous types of technologies that able to fractionate biomass into different separated products for bio-based industry (fuels, power, heat, and value-added chemicals) via thermo-chemical (gasification, pyrolysis), physico-chemical (chemical synthesis), biochemical or biological (fermentation) conversion and separation. It is a similar concept with today's petroleum refinery, where various types of petroleum fractionation yielded for fuel and chemical synthesis (Figure 1.2).

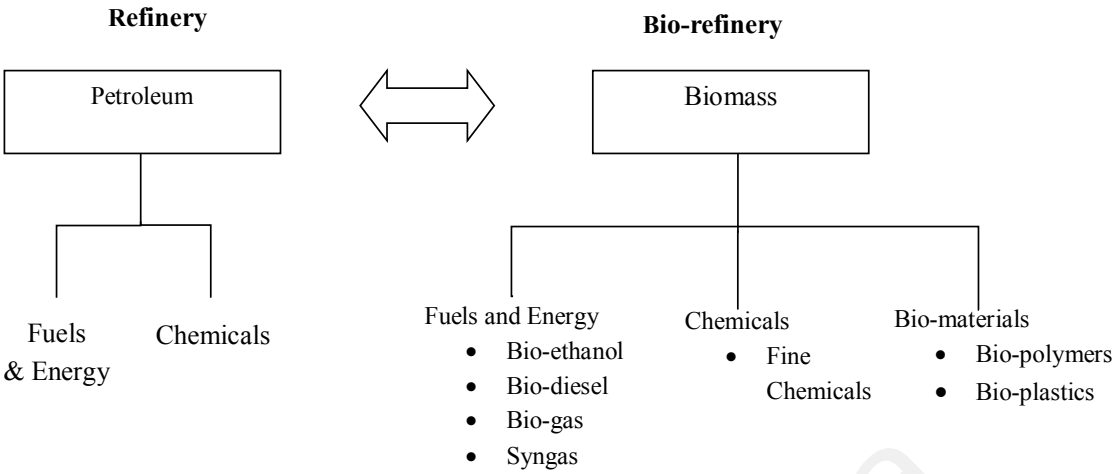

Figure 1.2: Inter-connectivity between petroleum refinery route and biomass refinery process

In this process, each technology is capable of generate diverse types of co-products (by-products that are produced simultaneously during biomass conversion), which can further transform into marketable end products (Figure 1.3). Thus, the main challenge is to discover efficient processing technologies that can convert the woody or non-woody biomass into finished products with higher value.

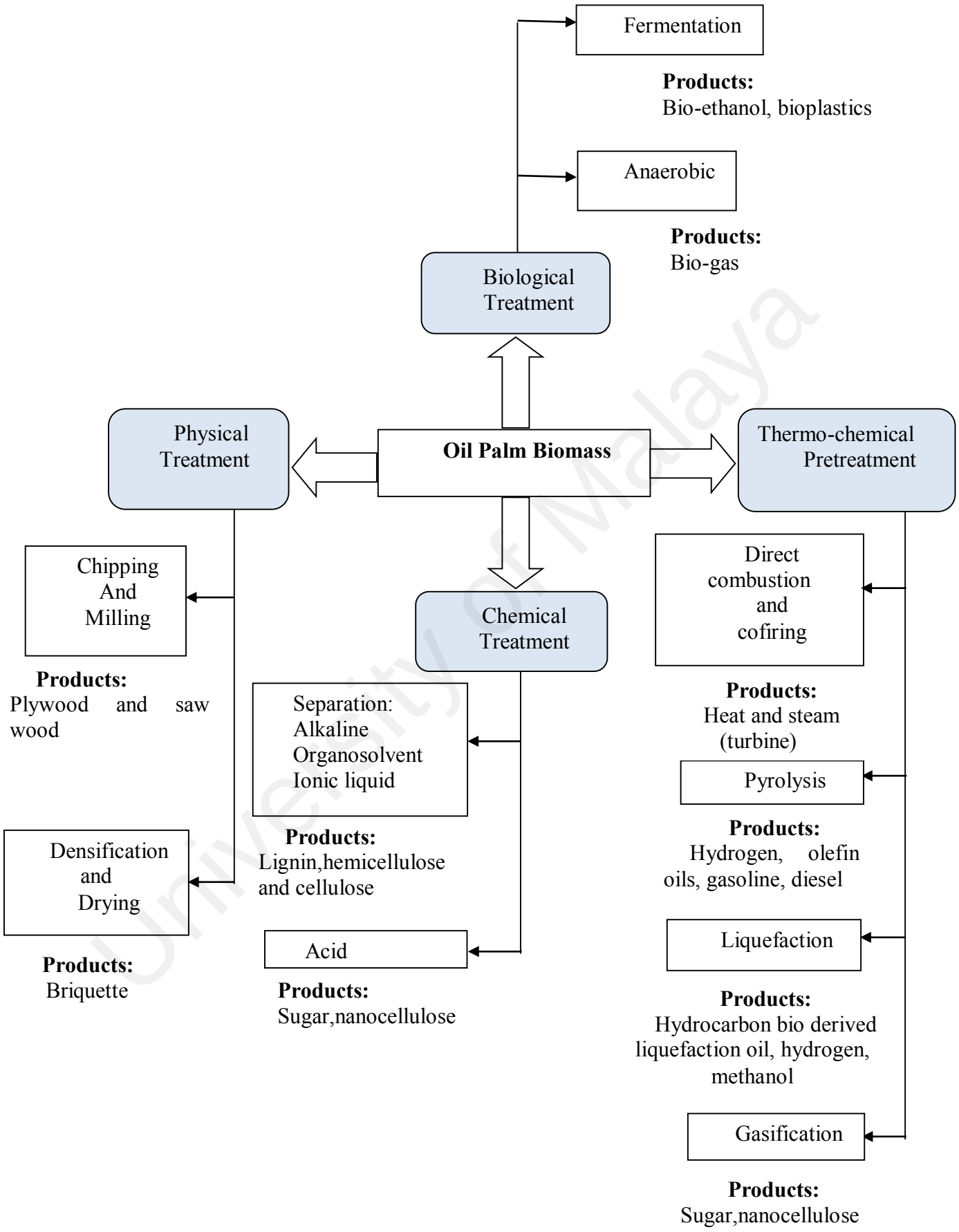

Figure 1.3: Bio-refinery of lignocellulosic biomass to fuels and chemicals

1.2 Problem statement

Lignocellulosic biomass (EFB) mainly composed of cellulose, hemicellulose and lignin, which are categorized into carbohydrate and aromatic polymer that contributed to various applications based on its composition. Among the bio-components presented in oil palm biomass, cellulose is the primary structural building block of trees, which can be extracted for pulp and paper industry. Cellulose is a polymeric carbohydrate that contains many monosaccharide units covalently bonded to each other. This polymer is a linear chain of anhydro-glucose monomer units connected through 1,4 β-linkages. The compact structure of cellulose mainly contributed by the linkage of intra- and inter-hydrogen bonds, which creating a spectacular mechanical strength to protect the plant structure(Lindman *et al.*, 2010).

Lately, cellulose in nanodimension has been getting attention by various industries due to its superior characteristic as a green polymer nanomaterial. The major advantages of nanocellulose are including excellent mechanical strength, non-toxic and biodegradability and high availability to diverse surface functionalities for different applications. With all these superior properties, nanocellulose has a great potential in applications such as strength enhancers in paper, as additives to composites, polymer reinforcement, films and barrier coating, water treatment, oxygen barriers for food packaging, electronics, cosmetic, pharmaceuticals and biomedical devices (e.g. scaffolds in tissue engineering, artificial skin and cartilage, wound healing and vessel substitutes) (L. Brinchi *et al.*, 2013; Alain Dufresne, 2013).

To produce nanocellulose from lignocellulosic biomass, the complexity of the biomass structure needs to be ruptured so that the accessibility of cellulose in the plant fibres can be increased for depolymerisation process (Kumar *et al.*, 2009). Ideally, chemical treatment is the most crucial route to obtain nanoscale cellulose from the complex

biomass. Various methods have been used to produce nanocellulose material from lignocellulosic biomass, this included acid, alkali, organosolv and ionic liquid treatment (Kumar *et al.*, 2009; H. V. Lee, S. B. A. Hamid, *et al.*, 2014). During biomass pretreatment process, the used of KOH solution make polymers (lignin, hemicellulose and cellulose) swelling, which partially breaking of inter- or intra hydrogen bonding from biomass structure occurred. The less ordered biomass structure lead to an increment of the active surface area (increase the number of available hydroxyl group) and accessibility to solvents for further hydrolysis process. Conventionally, acid sulfuric (H_2SO_4) or acid hydrochloric (HCl) were used for depolymerisation processing which acid will be the hydrolytic cleave, the glyosidic linkages between the two anhydroglucose units, dissolving the cellulose amorphous region and increase cellulose crystallinity (Morais *et al.*, 2013). However, a large amount of toxic waste water from the washing process has raised the environmental issues such as generation of acid rains pollutes the ground water and destroys aesthetic value. Thus, introduction of inorganic salt such as Ni-based catalyst offer an integrated approach of chemical techniques for the controlled structured degradation of natural cellulose into nanocellulose, which promote more reliable methods in degradation of cellulose into nanocellulose. As a conclusion, nanocellulose preparation via chemical route (Ni-salt) is potentially gives profits to Malaysia thus giving greener solution in generating nation profits.

1.3 Objectives of Research

1. To study the effectiveness of catalytic hydrolysis for the conversion of oil palm Empty Fruit Bunch biomass (EFB) into nanocellulose by using chemical route (inorganic acid: H_2SO_4 and inorganic salt: Ni $(NO_3)_2$).
2. To optimize the nanocellulose yield by studying different reaction parameters (reaction temperature, reaction time and acidity of catalyst).

3. To determine the physicochemical properties of the produced nanocellulose by using Thermogravimetric Analyzer (TGA) and Derivatives Thermogravimetric(DTG), X-Ray Diffractometer (XRD), Fourier Transform Infrared (FTIR), High Resolution Transmission Electron Microscope (HR-TEM), Field Emission Scanning Electron Microscopy (FESEM), Atomic Force Microscopy(AFM), and Particle Size Analyzer (PSD) techniques.

1.4 Scope of Research

The intention of this project was addressed to the process of cellulose extraction from EFB fibres and nanocellulose preparation from EFB derived cellulose. Furthermore, an effective process for nanocellulose preparation was developed by comparing inorganic acid (H_2SO_4) and inorganic salt ($Ni(NO_3)_2$) catalyzed hydrolysis process. In order to achieve the objectives of the study, the scope of research was discussed as follows:

1. Catalytic conversion of oil palm biomass into nanocellulose.

- Extraction of cellulose from EFB fibres
- Preparation of nanocellulose using chemical route (Ni-salt and H2SO4 catalyzed hydrolysis).

2. Optimization study by using Response Surface Methodology (RSM)

- Reaction temperature (^0C)
- Reaction time (min)
- Acidity of catalyst (pH)

3. Physicochemical study of produced nanocellulose

The produced cellulose and nanocellulose products will be washed several times with deionized water and dry in freeze drier for further analysis. The properties of treated product were analyzed as Table 1.2:

Table 1.2: The physicochemical study of nanocellulose

Analyzer	Function
Thermogravimetric Analyzer (TGA) and Derivatives Thermogravimetric(DTG)	Analyze thermal stability of samples
Fourier Transform Infrared (FTIR)	Identify chemical functional group of samples
High Resolution Transmission Electron Microscope (HR-TEM)	Analyze the morphology of samples (size distribution, nanocellulose dimensions and the surface structure).
Atomic Force Microscopy(AFM)	
Field Emission Scanning Electron Microscopy (FESEM)	
X-Ray Diffractometer (XRD)	Analyze the chemical characteristic, crystallinity index and crystallite size (nm)
Particle Size Analyzer (PSD)	Profiling particle size distribution

1.5 Rationale and Significance

Based on the research scopes mentioned above, the following rationale and significance of the research study was outlined as below:

- Effectiveness of inorganic salt (Ni $(NO_3)_2$) as a hydrolysis catalyst to selectively convert cellulose into nanocellulose under mild reaction condition.
- High yield of nanocellulose derived from EFB under optimized conditions (reaction time, temperature, acidity of catalyst).
- High quality of nanocellulose features (narrow particle size distribution, higher aspect ratio, better thermal stability) was obtained by using inorganic salt catalyzed hydrolysis route.

CHAPTER 2: LITERATURE REVIEW

2.1 Palm-Based Lignocellulosic Biomass and Architecture of Cellulose

Palm-based lignocellulose resourse is abundantly available in Malaysia, which composed majority of cellulose biopolymer. It consists of a defensive inner framework which contributed to the hydrolytic stability, structural robustness of plant cell walls and its resistance to microbial degradation. Generally, palm biomass can be divided into three main categories: (i) Oil palm frond (OPF), oil palm trunk (OPT) and empty fruit bunches (EFB). These biomass consist primarily of three biopolymers: cellulose (~30-50 % by weight), hemicelluloses (~19-45 % by weight), lignin (~15-35 % by weight) and a small amount of protein content (Table 2.1) (Umar *et al.*, 2013).

This chemical compositions of a lignocellulosic fiber are varied according to the species, growing conditions, fiber arrangement and many other factors (Khalil *et al.*, 2012). The presence of cross-link between the cellulose and hemicellulose with lignin via ester and ether linkages lead to the biomass recalcitrance (Figure 2.1) (Bozell *et al.*, 2011; Himmel *et al.*, 2007; Lange, 2007). Today, the biomass's hierarchical structure no longer holds any secrets. Each valuable biopolymer can be extracted with high recovery for various usage especially biofuel, biochemical and advance material. Lignin is an amorphous heteropolymer network of p-coumaryl, coniferyl and sinapyl alcohol that linked together by different bonding. This complex structure makes lignin to act as a physical barrier of the plant cell wall as it is rigid, insoluble in water, impermeable, resistance to microbial attack and oxidative stress.

Extraction of lignin (delignification) is an important process to cause biomass swelling, disruption of lignin structure, increase in internal surface area, and increase accessibility of hydrolysis reaction (Doherty *et al.*, 2011; Scheller & Ulvskov, 2010).

Table 2.1: Chemical composition of palm-based biomass (Umar *et al.*, 2013)

Oil Palm biomass chemical composition (wt%)			
Composition	EFB	OPF	OPT
Cellulose	43-65	40-50	29-37
Hemicellulose	17-33	34-38	12-17
Holocellulose	68-86	80-83	42-45
Lignin	13-37	20-21	18-23
Xylose	29-33	26-29	15-18
Glucose	60-66	62-67	30-32
Ash	1-6	2-3	2-3

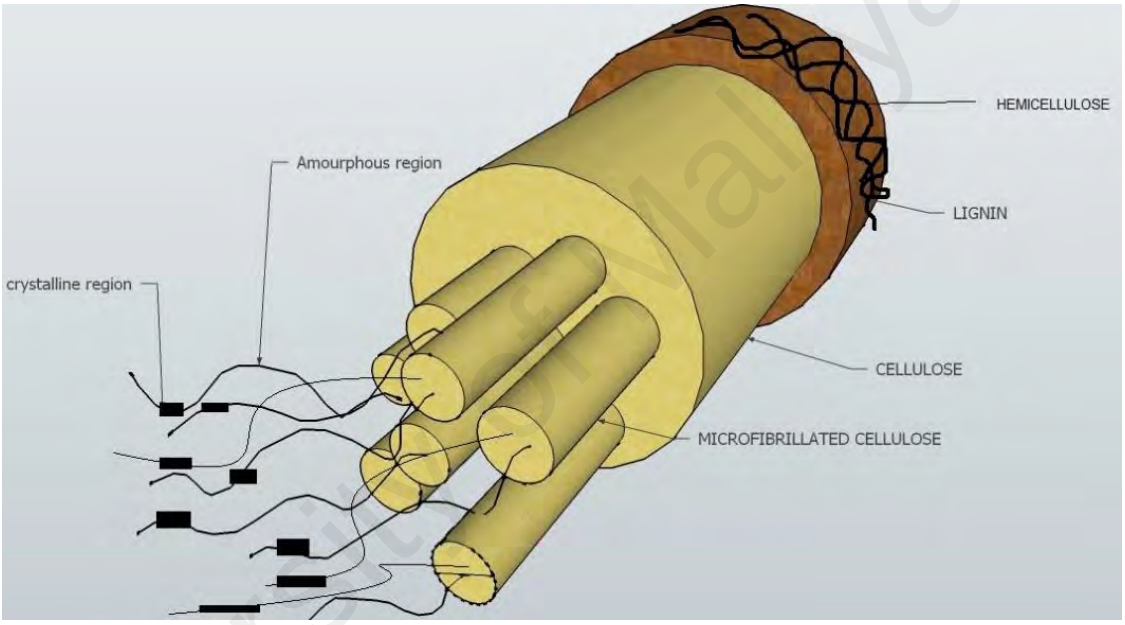

Figure 2.1: Schematic diagram of Lignocellulose Biomass.

Valorization of lignin plays a crucial role for the production of renewable fuels (power, fuel pellets, and syngas), bio-based material (composite, carbon fibres) for cements additive, asphalt additive, feed binder. Furthermore, large quantities of poly-aromatic structure make this compound to serve as a future aromatic source for the green chemicals (vanillin, phenols, building block for polymer such as polyester and polyurethanes) (de Wild *et al.*, 2009) .

Hemicellulose is the second most abundant polymer that composed polymers of pentoses (xylose, arabinose), hexoses (mannose, glucose, and galactose) and acetylated sugars. It is stored within plant cell wall and coated on cellulose fibrils where pretreatment severity must be control carefully to maximize sugar recovery, and avoid over degradation of products that inhibit a further process such as furfural (Zhang *et al.*, 2013). The typical industrial applications of hemicellulose include barrier materials for food packaging or biopolymers with new properties. Xylan with large molecular weight and high affinity to cellulose always is the best choice as strengthening agent in paper and bio-composite. Furthermore, modification of xylan can make self-supporting barrier films for food packaging (Mikkonen & Tenkanen, 2012). Cellulose is an organic compound from polysaccharide family with the formula of $(C_6H_{10}O_5)_n$, which consist of a linear chain of D-glucose units that linked by ß-1,4 glycosidic bond, with a degree of polymerization of approximately 10,000 for cellulose chains in nature and 15,000 for native cellulose cotton (Azizi Samir *et al.*, 2005). Generally, cellulose always exits in two major forms, which is cellulose I (native cellulose-original from plants in its natural form) and cellulose II (regenerated from cellulose 1 under chemical treatment)(Dumitriu, 2004; Eichhorn *et al.*, 2005). The properties of cellulose bio-polymer are unique in terms of its mechanical properties (strength, stiffness, and dimensional stability), thermal stability, chemical resistance, surface appearance, optical properties and electrical conductivity. The presence of strong mechanical strength of cellulose is due to the formation of hydrogen bonding, which strongly affect the multi-scale microfibrillated structure and hierarchical organization (crystalline vs. amorphous regions) (Dumitriu, 2004; Lindman *et al.*, 2010). Table 2.2 showed the comparison of strength and modulus in between commercial fibres and wood-based cellulose, where bio-cellulose show similar tensile strength as glass fiber (given their lower density), although are not as strong as either aramid or carbon fibres(Khalil *et al.*, 2012) . Thus from Table 2.2,it can be concluded that

cellulose fiber is a potential candidate for the application of textiles, alternative green reinforcing material for polymers such as glass, carbon and aramid fibres, or talc.

Table 2.2: Comparison of strength and modulus in commercial fibres and biomass-based cellulose

Material	Modulus (GPa)	Density (Mg m^{-3})	Specific Modulus (GPa/ Mg^{-1} m^3)	References
Aluminium	69	2.7	26	(Ashby & Jones, 2013)
Steel	200	7.8	26	(Ashby & Jones, 2013)
Glass	69	2.5	28	(Eichhorn *et al.*, 2010)
Crystalline cellulose	138	1.5	92	(Eichhorn *et al.*, 2010)
Alumina	350	3.8	92	(Eichhorn *et al.*, 2010)
Kevlar 29	1.44	83	58	(Peng *et al.*, 2011)
Kevlar 49	1.44	124	86	(Peng *et al.*, 2011)
Kevlar 149	1.47	179	122	(Peng *et al.*, 2011)
Twaron	1.44	80	56	(Peng *et al.*, 2011)
Twaron High Modulus(HM)	1.45	124	86	(Peng *et al.*, 2011)
Carbon fiber	1.68	221	132	(Peng *et al.*, 2011)

2.2 Nanocellulose

Despite being the most available natural polymer on earth, it has been only recently that cellulose has gained prominence as a nanostructured material. Increment of petroleum prices, high energy intensity of chemicals and polymers production, together with market sustainability trend have motivated the exploitation of nanostructured cellulose, e.g. crystalline nanocellulose (CNC), cellulose nanofibrils(CNF) and bacterial cellulose (BC). The growing attention is related to their unsurpassed quintessential physical and chemical features. The major advantages of nanocellulose are the excellent mechanical strength, non-toxic, biodegradable, broad availability with various functionalities. Like the characteristic of cellulose, the nanoscale of this biopolymer changes dramatically. It is stronger than steel, stiffer than Kevlar® (with specific Young's modulus 65 Jg^{-1} for microfibrils and 85 Jg^{-1} for nanocrystals)(Wu *et al.*, 2007), high elasticity, lighter in weight, conductive, extremely absorbent and so on(Dufresne, 2012; Wu *et al.*, 2007) . With all these superior properties, nanocellulose has great potential in applications such as strength enhancers in paper, as additives to composites, polymer reinforcement, in emulsions, films and barrier coating, water treatment, as oxygen barriers for food packaging, electronics, cosmetic, pharmaceuticals and biomedical devices (e.g. scaffolds in tissue engineering, artificial skin and cartilage, wound healing and vessel substitutes)(Dufresne, 2012; Peng *et al.*, 2011) (Figure 2.2).

With advance conversion and separation technologies, the hierarchy biomass structure can be unlocked and integrated into bio-based nanoproducts. Biomass pretreatment is an important step to enhance the efficiency of nanocellulose preparation step. Generally the pretreatment step is carried out before acid hydrolysis process.The pretreatment process breaks down the tangled network structure of lignocelluloses to make cellulose fibrils accessible for further hydrolysis to nanostructure. Cellulose fibres are formed by several groups of macrofibril, which generated from bundle groups of microfibril (diameter at 5-

50 nm and length in micrometers) that was connected by approximately of 36 individual cellulose molecule chains via hydrogen bonding (Eichhorn *et al.*, 2005; Khalil *et al.*, 2012; Peng *et al.*, 2011). The structures of microfibrils cellulose are arranged randomly into amorphous (disordered) and crystalline (highly ordered) regions. Crystalline celluloses are stiff as compared to amorphous phases, this is because the polysaccharide chain packed together with strong intra- and inter-molecular hydrogen bond network. Thus, the weak amorphous regions in cellulose microfibrils easily break down into shorter crystalline part when lignocellulosic biomass subjected to depolymerization treatment such as mechanical shearing, chemical or enzymatic treatment (Beck-Candanedo *et al.*, 2005).

The depolymerisation process of microfibrillated cellulose will produce cellulose nanocrystals (CNCs) or it can be named as microcrystals, whiskers, nanoparticles, microcrystallites, nanofibres, or nanofibrils. Nanocellulose can be produced by palm biomass-derived cellulose sources and the chemical methods for the preparation of nanofibres will be deliberated later. Nanocellulose can be categorized to BC, CNC and CNF (Xu *et al.*, 2013).

BC is a product of microbes' primary metabolic processes(Dufresne, 2013) . Generally, BC is produced by acetic acid bacteria in both synthetic and non-synthetic medium through oxidative fermentation process. Due to high cost and low yield of BC production, there is limited number of industrial production of BC and its commercial application as compared to CNC and CNF(Esa *et al.*, 2014).

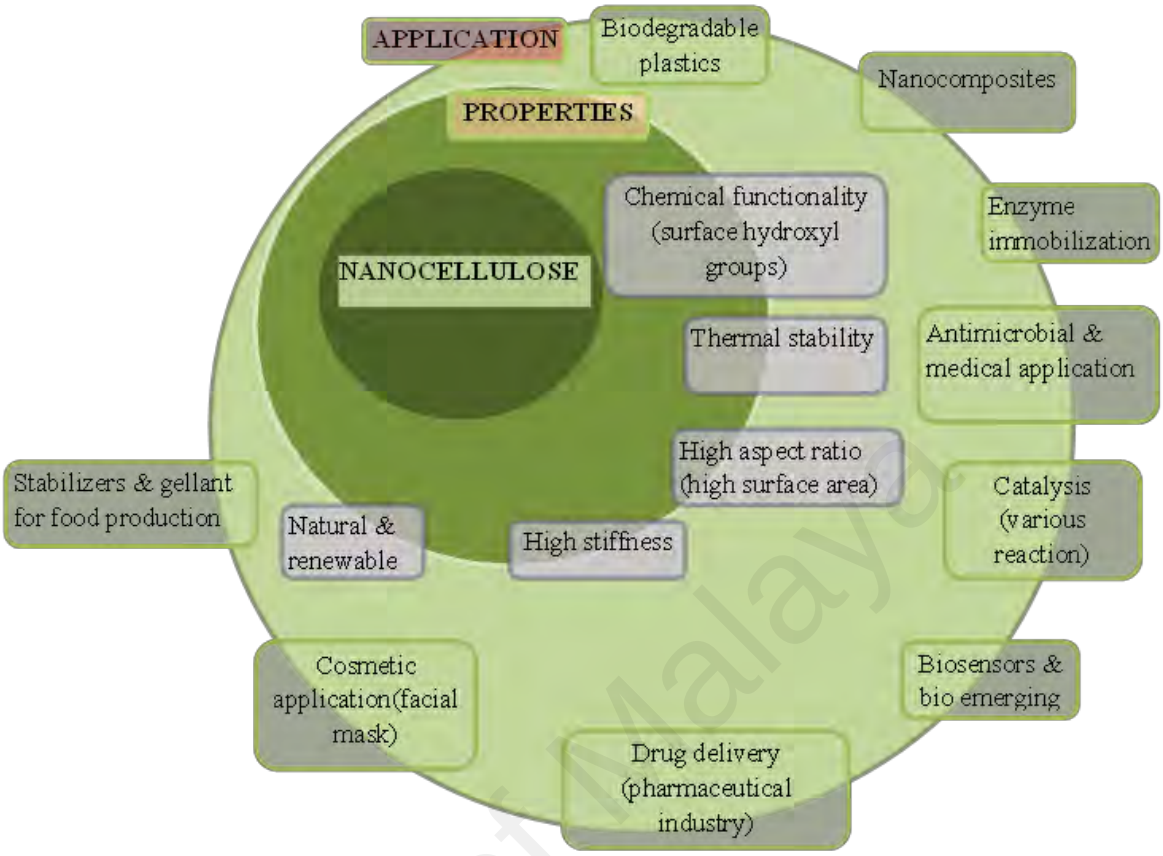

Figure 2.2: Nanocellulose characteristics and applications (Henriksson *et al.*, 2008)

CNCs are needle-like cellulose crystals of 10−20 nm in width and several hundred nanometres in length. It composed high purity of crystalline phase of cellulose, where non-cellulosic content and amorphous cellulose are eliminated (Xu *et al.*, 2013). CNFs formed long flexible fibre networks with both fibril diameters longer and crystallinity lower than CNCs. It contains a large amount of amorphous cellulose, while surface morphologies and dimensions of CNF can vary substantially, depending on the degrees of fibrillation and any pre-treatment involved (Xu *et al.*, 2013).

2.3 Conversion of Palm-Based Lignocellulosic Biomass to Nanocellulose

2.3.1 Biomass Pretreatment: Isolation of Cellulose Compound

Generally, the biomass recalcitrance is mainly due to the presence of highly complex phenolic polymer lignin, which resists degradation of polysaccharides from plant cell wall, and thus reduces the accessibility to cellulose. Hence, removal of lignin is the key processing step during the extraction of cellulose fibres. In chemical pretreatment, non-cellulosic components (lignin and hemicellulose) need to be dissolved from the lignocellulose and subsequently separated from the production process. However, the fact that non-linear polymer lignin is built in chemically diverse and poorly reactive linkages, which require costly and harsh pretreatment to degrade this component. The major influences on the operation costs are involved the reduction of lignocellulose particle size and subsequent depolymerisation process. Thus, effectively overcoming the biomass recalcitrance structure and releasing the locked polysaccharides is the crucial task for the emerging of nanocellulose industries.

The biomass pretreatment is aimed to reduce the degree of polymerization of cellulose (glucose congregated forming a polymer molecule) by breaking the lignocellulosic complex, solubilized the lignin and hemicellulose, increase porosity and surface area of hidden cellulose, and reduce the crystallinity of cellulose (Paulien Harmsen *et al.*, 2010).This fractionation process makes the cellulose accessible to hydrolysis reaction and improves depolymerisation of the cellulose chain into nano-dimension (Figure 2.3) (Kumar *et al.*, 2009)

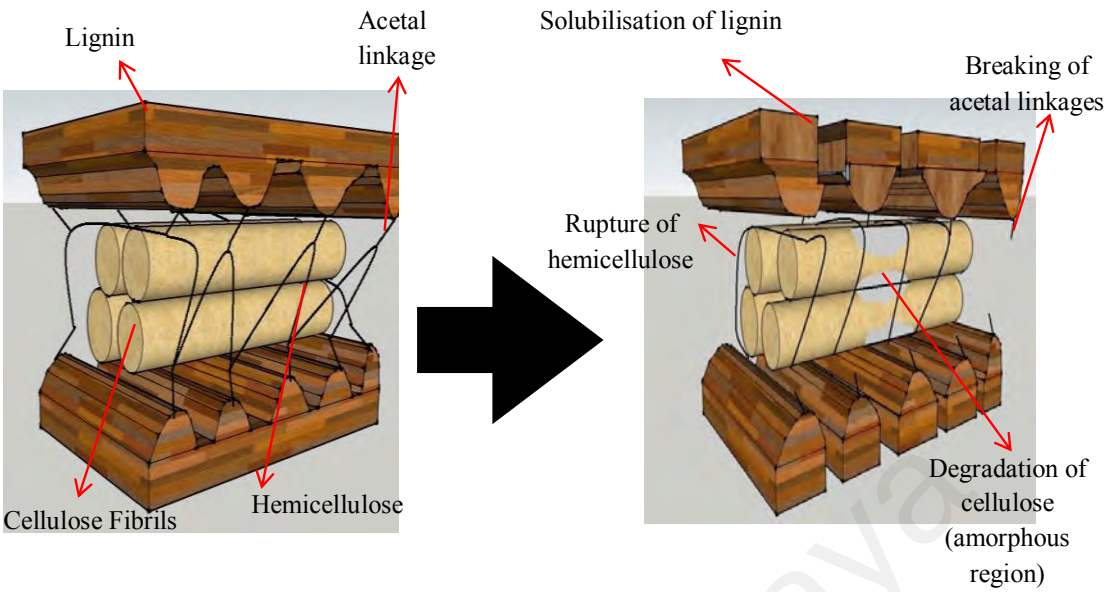

Figure 2.3: Schematic diagram of biomass pretreatment to unlock biopolymer stored within the plant

The biomass pretreatment process is categorized into three main classes in terms of pH: (i) Acidic; (ii) Alkaline and (iii) Neutral (Organosolv and ionic liquid treatments)(PFH Harmsen *et al.*, 2010). However, most of the processes suffer from unsatisfactory separation of cellulose and lignin, where over-degradation lead to the formation of by-product (polysaccharide is changed to sugars rather than nanocellulose).

Furthermore, the usage of severe reaction conditions (high temperature and pressure) makes the operation cost higher and increase the investment risks, as larger capital investments are required compared to pulp and paper manufacturing (PFH Harmsen *et al.*, 2010). Therefore, a suitable biomass pretreatment technology with the aims of mild reaction condition and effective at cellulose recovery is highly targeted in order to decrease utility consumption, lower down energy demand, rmazeduce capital cost, and reduce sugar degradation (PFH Harmsen *et al.*, 2010).

The advantages and disadvantages of chemical processes for lignocellulosic biomass pretreatment were shown in Table 2.3. It is crucial to indicate that different type of

chemicals functioning selectively in the biomass separation process. Although the main goal of pretreatment is to acquire a good quality cellulose product, it is important to preserve the structure of lignin and hemicellulose as well. The best way to maintain high recovery of lignin for value-added chemical process is organosolv treatment, which minimal degradation of aromatic compounds can be observed. Other than solvent process, alkaline route with the presence of oxidation agent is another potential route to remove lignin (major) and hemicellulose (minor) with minimum formation of inhibitors, especially during fermentation sugar to bioethanol. In case of direct acid treatment, a controllable amount of acid is the key point to solubilize cellulose and hemicellulose compounds to sugar products. However, it is unsuitable to be used for fractionation of cellulose as high recovery of cellulose in required for further nanocellulose synthesis. Ionic liquid treatment is another green process that fit well into the cellulose isolation with high recovery of all bio-compounds; however, using ionic liquid for biomass pretreatment is not economically friendly as it is expensive in cost.

Table 2.3: Advantages and disadvantages of lignocellulosic biomass pretreatment via chemical routes

Chemical	Mode of Action	Advantages	Disadvantages/limitation	Remarks	References
			Dilute Acid		
H_2SO_4, H_3PO_4	Removal of hemicellulose	1. Higher reaction rates 2. Increase the accessibility of cellulose	1. Presence of fermentation inhibitors 2. High cost, expensive construction material due to acidic environment.	Minimal degradation of lignin and hemicellulose.	(Zheng *et al.*, 2013)
			Concentrated Acid		
H_2SO_4, H_3PO_4	Solubilisation of hemicellulose and direct hydrolysis of cellulose to glucose.	1.Suitable to all types of biomass	1.Uncontrolled hydrolysis products	Saccharification of biomass	(Sathitsuksanoh *et al.*, 2012)
			Alkaline		
NaOH, CaOH	1. Removal of lignin (major) 2. Removal of hemicellulose 3. Cellulose swelling	1. High solubilisation of lignin 2. Low fermentation inhibitors formed	1. High cost of chemical 2. Alteration of lignin structure	Suitable for direct fermentation	(McIntosh & Vancov, 2010)

Chemical	Mode of Action	Advantages	Disadvantages/limitation	Remarks	References
			Organosolvent		
Mixture of organic solvent and water	1. Extraction of lignin 2. Complete solubilisation of hemicellulose	1. High quality lignin that is low molecular weight and sulphur free. 2. Organic solvent used can be recycled and reused. 3. Size reduction of biomass feedstock is not necessary. 4.Selective pretreatment method	1. High cost of chemicals 2. Containment vessels to prevent leakage of volatile organic solvents.	Suitable for producing a high quality lignin for specialty chemical	(Cybulska *et al.*, 2012)
			Ionic Liquid		
Imidazolium salts	1. Extraction of lignin 2. Decrease the cellulose crystalinity index 3. Carbohydrate dissolution	1. IL is high thermal stability and low volatility	1. High cost of chemicals.	The effects towards hemicellulose and lignin are depending on the nature of ionic liquid used.	(Fu & Mazza, 2011)
			Oxidative		
H_2O_2	1. Solubilisation of lignin. 2. Bleaching effect to the pulp	1. High removal of lignin 2. Increase biomass digestibility	1. High costs of chemicals.	Bleaching effect to the biomass, hemicellulose might be degraded	(Correia *et al.*, 2013)

2.4 Isolation of Micro- and Nano-Cellulose from Palm-Based Biomass

There are various approaches were reported for micro- and nano-cellulose synthesis, it can either in chemical, biological fermentation, mechanical, physical or mixed processes (Table 2.4) (Saratale & Oh, 2014).

2.4.1 Chemical Acid hydrolysis

Generally, acid hydrolysis is the leading process for nanocellulose isolation. The acid hydrolysis involves depolymerization of the cellulose chain by hydrolytically cleavage the glyosidic bond between two anhydroglucose units. The cellulose depolymerization occurs randomly and uncontrollable, where acid tends to attack amorphous cellulose as compared to the crystalline region, resulted in the formation of non-uniform sizes of CNC (L. Brinchi *et al.*, 2013). Furthermore, different cellulosic material also possesses a diverse dimension of crystalline to an amorphous region. Therefore, the nanocellulose obtained has an enormous variety of nano-scale dimension. The nanocellulose is high in crystallinity index (Crl) (Saratale & Oh, 2014) based on X-ray diffraction analysis, and Transmission Electron Microscope (TEM) or High Resolution Transmission Electron Microscope (HR-TEM) can show a rigid rod –like particle or whisker like structure.

By using sulfuric acid (H_2SO_4) for hydrolysis process, the intra- and inter-hydrogen bonds were broken and lead to the formation of sulfate coated cellulose complex. Hydrolyzing cellulose with H_2SO_4 involves esterification of hydroxyl groups, which generated acid half-ester or cellulose sulfate in nanocellulose product. The presence of sulfate groups on the surface of nanocellulose results in negatively charged surfaces above acidic pH. The surface of nanocellulose with negative charge will lead to anionic stabilization, where repulsion forces of electrical double layers able to prevent aggregation of nanocellulose driven by hydrogen bonding (Saratale & Oh, 2014). In

addition, mechanical treatment (sonication) sometime used to enhance the disintegration of cellulose structure into nanocrystalline form (J. Li *et al.*, 2015).

In the year of 1999, researcher had reported that large content of cellulose was successfully isolated from empty fruit bunches by using acid hydrolysis with removal of 0.9%- 6.6% of lignin and 11.9-17.3% of hemicellulose (Sun *et al.*, 1999). Wattaya's team further reduced the size of cellulose to microcystalline cellulose (MCC) in order to apply as reinforce material with rice starch film. The cellulose was extracted from palm pressed fiber through alkaline treatment using 10% of sodium hydroxide (NaOH) under 100ºC for 1 hr, followed by bleaching process via sodium chlorite ($NaClO_2$). The bleached pulps were then hydrolysed using H_2SO_4 (64%) at 45ºC for 4 hr prior to sonicate for 15min. The excess H_2SO_4 remained in suspension was neutralized with 0.5 M of NaOH and further washes via dialysis process. Based on the SEM analysis, the microcrystalline cellulose press fiber (MCPF) rendered dimension of 0.480±0.023 μm (Wittaya, 2009).

Similar works were done by Hafiz et al. (2013) and Battisya et al. (1950) (Mohamad Haafiz *et al.*, 2013). Oil palm empty fruit bunch (OPEFB) was hydrolysed by 2.5 N of hydrochloric acid (HCl) at 105°C for 30 min with the pulp to liquor ratio of 1:20. After completion of acid hydrolysis, sample was washed several times before proceed to neutralization by ammonium hydroxide (NH_4OH). The dried MCC was then ground into fine powder by using rotary ball miller. The crystalinity index for OPEFB-MCC is 87%, which is higher as compared to OPEFB (80%) and commercialized microcrystalline cellulose (C-MCC) (79%). This indicated that the amorphous region of cellulose was removed by acid hydrolysis and remained individual crystallite phases. The crystalinity is directly proportional to cellulose rigidity, thus this showed that OPEFB-MCC consisted of higher mechanical properties. SEM analysis for OPEFB pulp, OPEFB-MCC and C-MCC was reported by Hafiz's group. The morphology of OPEFB-pulp showed individual

and uniform fibres indicated that hemicellulose and lignin had been removed, while OPEFB-MCC and C-MCC rendered aggregated, irregular shaped fibrils with rough surface.

Bono et al. (2009) selected palm kernel cake (PKC) as the initial feedstock for cellulose extraction (Bono *et al.*, 2009). The cellulose was further functionalized into carboxymethyl cellulose (CMC), which was useful in anti-caking agent, emulsifier, stabilizer, dispersing agent, thickener, and gelling agent. PKC was first grind into smaller particles (600 μm) in order to ease the pretreatment process by increase the biomass accessibility to chemicals. Furthermore, soxhlet extraction using isopropanol (C_3H_7OH) was performed to enhance the chemical attack by removes the coating layers (wax, lipids, fats) (Cunha *et al.*, 2004)on the biomass surface. The bounded hemicellulose and lignin were later solubilised by NaOH and NaClO solution, respectively. Final CMC sample was substantially produced via alkalization (NaOH), followed by esterification of cellulose using sodium monochloroacetate (SMCA). The slurry was soaked in methanol (CH_3OH) for overnight and neutralized using 10% acetic acid (CH_3COOH) until pH 6-8 (Bono *et al.*, 2009).

Other than MCC, some of the study was continued to push forward the synthesis of nanocellulose. Fahma et al., (2010) was successfully produced nanocellulose from oil palm empty fruit bunches (OPEFB) via acid hydrolysis (Fahma *et al.*, 2010). As similar to other's studies, OPEFB was mashed into 0.5-1 cm, followed by dewaxing process via soxhlet extraction using ethanol (C_2H_5OH) and benzene (C_6H_6) with the ratio of 1:2, respectively. The process continued by delignification with $NaClO_2$ (pH 4-5) under 70 ºC for 1 h, while hemicellulose was removed using 6% potassium hydroxide (KOH) at 20 ºC for 24 h. The cellulose fibres were subsequently stored in a refrigerator for further process. Nanocellulose suspension was later hydrolysed by 64 % of H_2SO_4 for 15, 30, 60,

and 90 min, and the reaction was immediately terminated by using cold water to prevent over hydrolysis of cellulose into sugar. The particle sizes of nanocellulose under different treatment time were studied by SEM analysis, where the results are 2.51 ± 1.03, 2.05 ± 0.95, 2.05 ± 0.89, and 1.96 ± 0.85 nm, respectively. The crystalinity index (CrI) of nanocellulose with 15 min treatment showed highest index (58.78 ± 0.70%), followed by 30, 60 and 90 min (53.83 ± 2.03%) (Fahma *et al.*, 2010). Generally, acid will easily attacked amorphous region as compared to crystalline region of cellulose, this increased the crystalinity index of product after mild acid treatment. When drastic hydrolysis condition (high concentration of acid and longer treatment time) was applied, both amorphous and crystalline region would partially destroy. This is the reason of the crystalinity of nano-fibre tend to decrease as acid continuously attack the crystalline part of cellulose. For Souza's group, nanowhiskers cellulose was derived from pressing mesocarp oil palm fibres via similar chemical process ($NaOH$-H_2O_2-H_2SO_4) (Souza *et al.*, 2013).The nanocellulose product render the length (L) of 171.76 ± 14.91 nm while the diameter (D) is average of 5.48 ± 0.48 nm, with aspect ratio (L/D) of 35.35 ± 3.37 (Souza *et al.*, 2013)

Although acid hydrolysis is efficiently to depolymerise cellulose into nanocellulose, however, controllable concentration of acid and treatment time are important to achieve higher yield of nanocellulose with high crystalinity index.

2.4.2 Physical-Chemical Route

Physical-chemical treatment was proposed by Yan's group for nanocellulose synthesis (Yan *et al.*, 2009)Palm Kernel Cake (PKC) was initially pretreated under hot liquid oxidation process, where water (H_2O) was used as a mild acid agent at temperature of 160-180 ºC under saturated vapourpressure for 30 min (Yan *et al.*, 2009). In this reaction, the biomass undergoes an explosive decompression, where hemicellulose was degraded

(yielding a dark brown material) to organic acid and saccharides, resulted in lignin matrix disruption (Paulien Harmsen *et al.*, 2010; Ramos, 2003). The cellulose extraction was continued by using the same method (hot water oxidation on treated PKC) in the presence of chemical (30 % of H_2O_2) for 600-1440min at temperature of 60-80°C. The maximum yield of nanocellulose (45 %) was obtained within 600min of reaction under 75 ^{O}C (Yan *et al.*, 2009).

2.4.3 Mechanical-Chemical Route

Conversion of empty fruit bunches (EFB) to nanocellulose was performed by chemical-milling techniques in Jonoobi's study (Jonoobi *et al.*, 2011). The EFB fibres was treated by sodium hydroxide-anthraquinone (NaOH-AQ), followed by oxidation by $NaClO_2$ and CH_3COOH hydrolysis reaction(Jonoobi *et al.*, 2011). These pulping and bleaching processes are used to preserve the cellulose structure, while selectively solubilize the lignin and hemicellulose in the fibres (Jonoobi *et al.*, 2011). During pulping process, NaOH-AQ acted as a pre-swelling agent, which increases the accessibility of the core cellulose for hydrolysis action. The oxidation agent ($NaClO_2$) and acid agent (CH_3COOH) were selectively penetrated into fibres to oxidized lignin and cleave the glyosidic bond of cellulose, respectively (Kalia *et al.*, 2011). Mechanical treatment was subsequently performed by using mechanical grinder and high pressure homogenization (HPH) treatment. The grinding process allows the cellulose to refine uniformly, and HPH treatment reduced the particle sizes of cellulose due to the presence of cleavage energy derived from homogenization pressure to break down the fibres bonding(Jonoobi *et al.*, 2011; Kalia *et al.*, 2011).

Table 2.4 showed the summary of nanocellulose production from palm-based biomass. Based on the overall studies, it is concluded that chemical route is important to unleash nanocellulose from complex biomass.

Table 2.4: Summary of nanocellulose production from palm-based biomass

Raw material	Final product	Chemicals	Temperature (°C)	Time (min)	Product yield (%)	Crystalinity index	Particle sizes (L & D) (2)/ aspect ratio (L/D) (3)	References
			Chemical Route					
OPEFB	MCC	2.5 N HCl 5 % NH_4OH	105 ± 2	30	N/A	Pulp (80%) MCC (87%) C-MCC (79%)	50µm	(Mohamad Haafiz *et al.*, 2013)
PKC	CMC	C_3H_7OH (Soxhlet)	82.4		67%	N/A	N/A	(Bono *et al.*, 2009)
		7.5% NaOH	25	60				
		CH_3COOH and $NaClO_2$	75	120				
		95% C_2H_5OH and D.I						
		C_3H_7OH						
		17.5% NaOH	30	60				
		SMCA	50	120				
OPEFB	CNF	C_2H_5OH:C_6H_6	80.1	2880	18.46 -91.89	53.83-58.97	1.96-2.51nm	(Fahma *et al.*, 2010)
		$NaClO_2$	70	60				
		KOH	20	60				
		H_2SO_4	45	15, 30, 60,90				
Oil palm fibres	NC	NaOH	80	120 min	N/A	70.90%	35.35 ± 3.37	(Souza *et al.*, 2013)
		H_2O_2 and NaOH	55	90 min.				
		H_2SO_4 60%	45	150 min				
Palm pressed fiber	MCC	NaOH	45	60	15.00-40.00%	N/A	0.480±0.023µm	
		NaCl H_2SO_4 (175 ml, 64%) NaOH	45	240				

Raw material	Final product	Chemicals	Temperature (°C)	Time (min)	Product yield (%)	Crystalinity index	Particle sizes (L & D) (2)/ aspect ratio (L/D) (3)	References
				Physical chemical route				
Palm kernel	Cellulose	Hot water treatment	160-180	30	45%	N/A	N/A	
		6gram grinded PKC and 300ml distilled water filled inside micro pressure reactor C_2H_5OH(washing)						(Yan *et al.*, 2009)
		2 gram of pretreated PKC was mixed with 30% H_2O_2	60-80	600-1440				
				Mechanical chemical route				
EFB	CNF	Chemical treatments		160	105	Cellulose: 91 ±1 (%)	EFB fibres (40%)	(Jonoobi *et al.*, 2011; Kalia *et al.*, 2011)
		NaOH		70	180	Hemicellulose: 4± 1(%)	bleached pulp fibres (61%)	
		NaOH-AQ (12%+1%)		160	105	Lignin: 1.0 ± 0.5(%)	Nanofibres (69%)	
		$NaClO_2$and CH_3COOH (1.25%+3%)		70	180			
		NaOH and H_2O_2 (1.5%+1%)		70	90			
		$NaClO_2$ and CH_3COOH (1.5%+3%)		70	90			
		Physical treatment						
		Grinding			15			
		High Pressure Homogenization		500 bar (pressure)				

Currently, researchers and scientists had improved the chemical process by applying mechanical or physical treatment, in order to bring significant performance with the concern of higher selectivity of the product, energy saving and cost effectiveness. Although physical and mechanical treatments showed high improvement of the conversion process, unfortunately, it requires longer treatment time as compared to acid hydrolysis reaction, which a maximum of 180min was used for the nanocellulose synthesis as compared to acid treatment. Thus, greener nanocellulose preparation route was developed in order to overcome the limitation of current technologies

2.5 Inorganic salt catalyzed mild hydrolysis

Generally, nanopolymeric cellulose can be isolated *via* biological hydrolysis (enzyme) or chemical acid hydrolysis (strong acid) of the glycosidic bonds of cellulose fibres (L Brinchi *et al.*, 2013). However, isolation techniques are still problematic because of the presence of strong intra- and intermolecular hydrogen bonding and van der Waals forces linking the cellulose fiber network. This highly organized bonding can create a defensive barrier to protect the plant structure (Lindman *et al.*, 2010).

The enzymatic hydrolysis of lignocellulosic materials requires several days to digest the structural barriers before the hydrolysis process. In the case of strong acid treatment, hydronium ions can efficiently break down or attack intermolecular and intramolecular bonds in cellulose. This treatment is more effective in comparison to enzymatic treatment. However, the use of a strong acid is usually accompanied by over-degradation of cellulose and has drawbacks such as equipment corrosion. Thus, diluted or organic acids have been suggested for milder reactions, but such treatments have been found to be less effective in reacting to the plant's structure (H. Lee *et al.*, 2014). Inorganic salts in the categories of trivalent ($FeCl_3$, $Fe_2(SO_4)_3$, $Al(NO_3)_3$), divalent ($CaCl_2$, $FeCl_2$, $FeSO_4$), and monovalent (NaCl, KCl) have been considered by others as potential catalysts for

hydrolysis treatment for several purposes: i) degradation of hemicellulose and cellulose in biomass (Kamireddy *et al.*, 2013; Liu *et al.*, 2009; López-Linares *et al.*, 2013; Zhao *et al.*, 2011a); ii) conversion of cellulose to glucose (Zhang *et al.*, 2015); and iii) extraction of micro- or nano-crystalline cellulose (Hamid *et al.*, 2014; Jinbao Li *et al.*, 2015; Lu *et al.*, 2014). It has been reported that the valence state of metal ion is the key factor to influence the hydrolysis efficiency, where acidic solution (H^+) was generated during polarization between metal ions with water molecules (Kamireddy *et al.*, 2013). A higher valence state will generate more H^+ ions, which act effectively in the co-catalyzed acid hydrolysis reaction in the presence of metal ion.

At present, acid hydrolysis of cellulose is still considered to be the most efficient pathway for high-yield nanocellulose production. To achieve a technically feasible, selective, and controllable hydrolysis process, a transition metal-based catalyst can be used because of its mild acidity. Transition metal-based catalysts, such as an iron-based catalyst, were found to contain Lewis acid sites and can perform the hydrolysis of cellulose efficiently (H. Lee *et al.*, 2014). Iron metal-based catalyst with its Lewis acid site is potentially to perform as catalyst for acid hydrolysis. Several studies reported that this catalyst could increase hydrolysis rate for biomass fractionation and nanocellulose preparation. Iron-based inorganic salts eg: $FeCl_3$ and $Fe_2(SO_4)_3$ had been selected as catalyst to accelerate the degradation of hemicellulose in corn stover. Based on the study, $FeCl_3$ significantly increased the hemicellulose degradation in aqueous solutions under temperature of 140- 200^{0}C with high xylose recovery (~90%) and low cellulose removal(<10%,). The hemicellulose removal increased 11-fold when the corn stover was pretreated with 0.1 M $FeCl_3$ as compared to pretreatment with hot water under the same conditions, which was 6-fold greater than pretreatment with dilute H_2SO_4 at the same pH (Liu *et al.*, 2009).

This fact was supported by Liu's group (Liu & Wyman, 2006), where $FeCl_3$ treatment significantly increases the hemicellulose (xylose and xylotriose) degradation at 180^0C. The result showed that 0.8% of $FeCl_3$ with acid pH of 1.86 rendered 3-fold and 7-fold greater of xylose and xylotriose degradation, respectively, than that for treatment with dilute H_2SO_4 with similar pH value. The study suggested that different mechanism may exist for the reaction; first, the presence of $FeCl_3$ may induce the formation of H^+ ion from water for hydrolysis; second, $FeCl_3$ may catalyze the dehydration of carbohydrates. Other than $FeCl_3$, $FeSO_4$ catalyst also showed strong hydrolysis effects on the pretreatment of corn stover, where hemicellulose significantly degrades to xylose (60.3%) with high recover of cellulose (89.8%) under temperature of 180^0C within 20 min. According to Zhao et al. (Zhao *et al.*, 2011b), $FeSO_4$ pretreatment is capable of disrupting the ester linkages between cellulose and hemicellulose. It is a potential pretreatment that is able to enhance further hydrolysis reaction of lignocellulosic biomass by destructing chemical composition and altering structural features. In acid hydrolysis, proton (H^+ from HCl or H_2SO_4) plays an important role to weaken the glycosidic bond energy by attracting electron, making it easier for bone rupture.

The presence of inorganic metal ions also play same function as proton, which consist of more positive charge to pair with more electrons, but proton can only pair with one electron. This fact was in agreement with the studies above, where $FeCl_3$ (trivalent, Fe^{3+}) rendered better hydrolysis effect than $FeSO_4$ (divalent, Fe^{2+}), while acid solution performed less effect as compared to inorganic salts (Yan *et al.*, 1996).

Lately, researchers started to use transition metal based catalyst ($FeCl_3$) for preparing cellulose nanocrystal (CNC) via hydrolysis of cellulose. The results show that 22% of CNC was produced under 10% $FeCl_3$, temperature of 110^0C for 60 min, and ultrasonic time of 180 min. The CNC produced are shaped rod-like with the diameter of 20–50 nm,

the length of 200–300 nm, and crystallinity of 76.2%(Lu *et al.*, 2014). The research findings indicate that Fe^{3+} from the $FeCl_3$-catalyzed hydrolysis can selectively diffuse into the amorphous regions of cellulose and promote the cleavage of glycosidic linkages of cellulose chains into smaller dimensions. Furthermore, the presence of an acidic medium (HCl) or ultrasonic-assisted treatment can act synergistically to improve the accessibility of metal ions for the hydrolysis process (Karim *et al.*, 2014; Jinbao Li *et al.*, 2015; Lu *et al.*, 2014).

Abd Hamid's group reported that the cellulosic fiber extracted from palm tree trunk were successfully converted into more valuable products that is MCC by using $FeCl_3$ treatment. The result show that under response surface methodology (RSM) optimized at 97.98°C,4hr,0.8M of $FeCl_3$. The crystallinity index of MCC yielded was 68.66%(Abd Hamid *et al.*, 2014). Yahya's group were successfully prepare nanocellulose from MCC via Ni-salt catalyzed hydrolysis pathway under mild reaction conditions of 45°C for 15 min(Yahya *et al.*, 2015). The mild acid Ni-salt catalyzed hydrolysis was able to selectively depolymerized the amorphous regions of cellulose and retain its crystalline region thus improving the crystallinity of the treated product up to 80%. Furthermore, the synthesized Ni-treated nanocellulose products appeared in the form of cluster fragments with spider-web-like appearance (fiber diameter of 10 to 60 nm and fiber length of 300 to 600nm).Thus, this study concluded that nickel-based inorganic salt is an efficient and selective catalyst for the hydrolysis of MCC with high simplicity in operation and short preparation time. Table 2.5 summarizes all the study from the previous researchers of converting biomass into valuable products via transition metal salt hydrolysis.

Table 2.5: Transition metal salt hydrolysis

Feedstock	Catalyst	Acidity	Operation condition	Final product	References
Corn stover	$FeCl_3$	pH 1.68	0.1M $FeCl_3$, 140^0C, 20 min	91% removal hemicellulose 91% recovery of cellulose	(Liu *et al.*, 2009)
Hemicellulose compounds: xylose and xylotriose	$FeCl_3$	pH 1.86	0.8% of $FeCl_3$, 180^0C, 20 min	65% degrade of xylose, 78% degrade of xylotriose	(Liu & Wyman, 2006)
Corn stover	$FeSO_4$	N/A	0.1 mol/L $FeSO_4$, 180^0C, 20 min 10% $FeCl_3$,110^0C	60.3% degrade of hemicellulose, 89.8% recovery of cellulose 22% CNC	(Zhao *et al.*, 2011b)
Cellulose	$FeCl_3$	N/A	60min of reaction time, 180 min of ultrasonic time	Diameter = 20–50 nm, Length of 200–300 nm, crystallinity index = 76.2%	(L.Q. Lin, T. L. Rong, Y.H. Juan et al.,2014)
Cellulose	Zn-Ca-Fe based nanocatalyst	N/A	160^0C,12hr, 140^0C	29% of glucose	(Zhang *et al.*, 2011)
Palm tree trunk (PTT)	$FeCl_3$	N/A	0.8M $FeCl_3$,97.98^0C,4hr	Crystallinity index=68.66%	(Abd Hamid *et al.*, 2014)
MCC	$(Ni(NO_3)_2$	pH5.0-6.3	1.0M,0.5M and 0.05M $(Ni(NO_3)_2$ 45°C for 15 min	Nanocellulose Diameter=10nm-60nm Length=300nm-600nm	(Yahya *et al.*, 2015)

CHAPTER 3: RESEARCH METHODLOGY

3.1 Introduction

This section includes raw material, apparatus and equipment, research design and research procedure. It describes the experimental procedures to develop a separation technology in order to prepare nanocellulose from EFB fibres.

3.2 Research design

The process flow of this experiment is shown in Figure 3.1 for the Preparation of Nanocellulose from Oil Palm Biomass (EFB) via Chemical Route. There are three sections in this project which has been elaborated more in the below which a step-by-step account of procedure included:

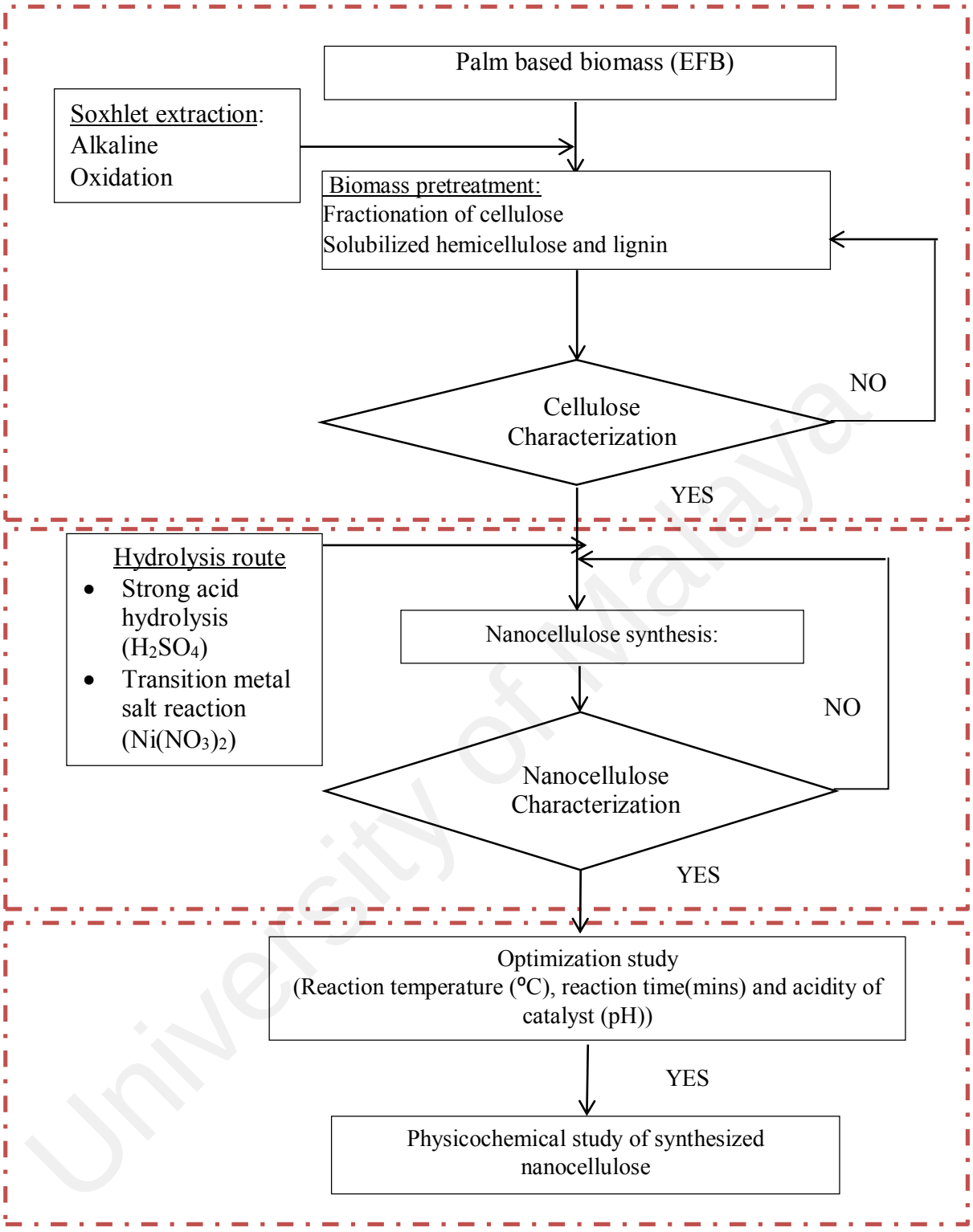

Figure 3.1: Production of Nanocellulose from Oil Palm biomass

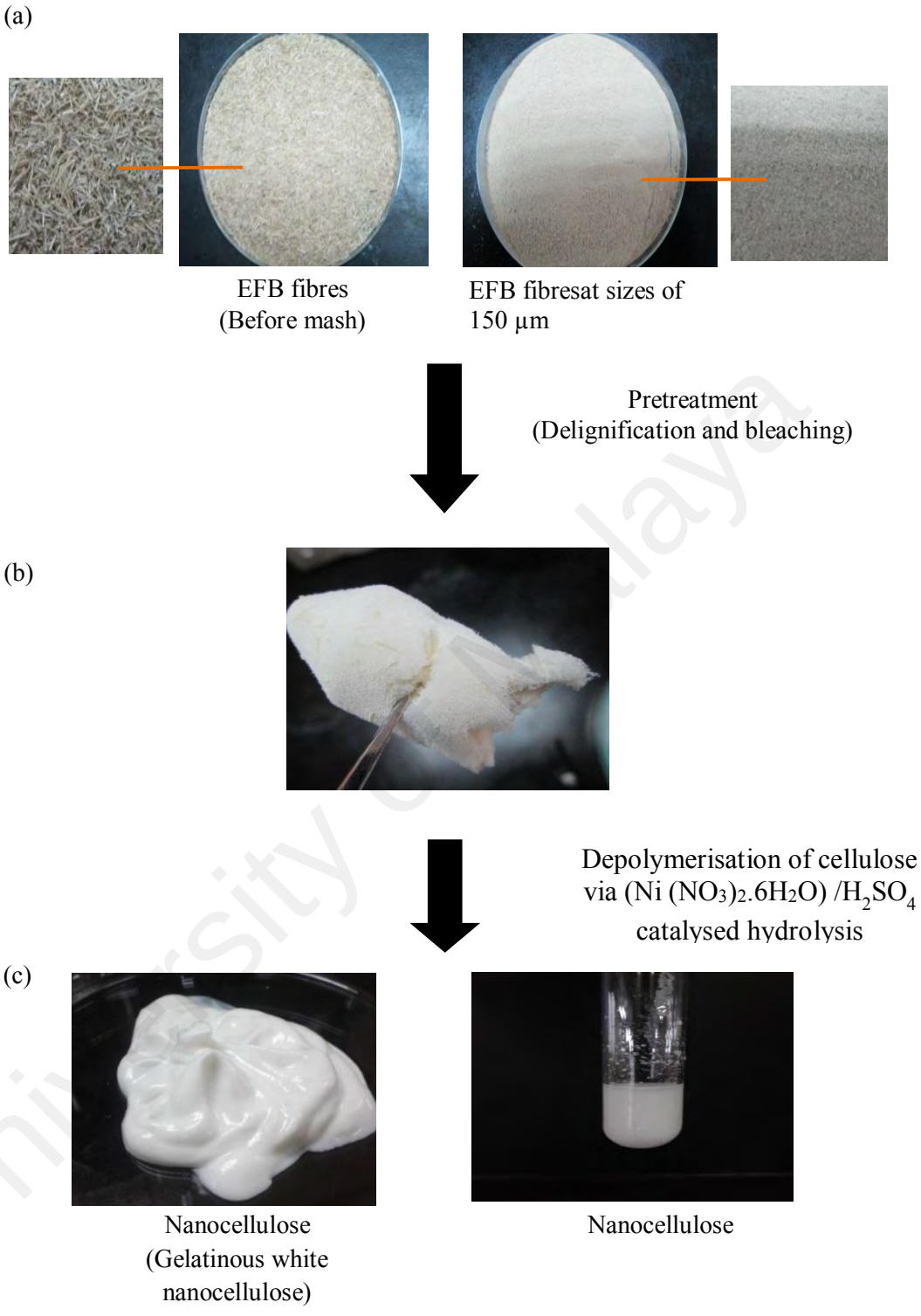

Figure 3.2: Visual observation: (a) Empty Fruit Bunch (EFB) fibres, (b) Cellulose, and (c) Nanocellulose

3.2.1 Raw Material

Empty Fruit Bunch (EFB) fibres were supplied from Malaysian Palm Oil Board (MPOB) (Figure 3.2a)

3.2.2 Equipment

Equipment	Model
Grinder machine	Daihan, HCP-750A
Magnetic stirring hotplate	Thermolyne, Cimarec hotplate stirrer
pH meter	Mettler Toledo, FE20
Orbital shaker	Lab Companion,SI-300R
Freeze drier	Labconco,75408-00
Sonicator	Daihan, WUC-A03H
Sieve shaker	Endecotts EFL, 2000

3.2.3 Chemicals

Chemical	Supplier
Toluene (C_7H_8)	R&M Chemical.
Ethanol (C_2H_7OH)	R&M Chemical.
Nickel (II) Nitrate Hexahydrate ($Ni(NO_3)_2.6H_2O$)	Systerm
Hydrogen peroxide (H_2O_2) (35%)	R&M Chemical.
Sulfuric acid (H_2SO_4)(97%)	R&M Chemical.

3.2.4 Powdering biomass

The Oil Palm Fiber (EFB) was collected from Malaysian Palm Oil Board (MPOB) Bandar Baru Bangi Selangor. It was then milled, sieved and separated in smaller sizes using a grinder and test sieve shaker (Endecotts EFL, 2000). This grinding process was carried out to make sure the size of EFB fibres is in similar size (100-150 μm) for further treatments.

3.3 Catalytic conversion of lignocellulosic biomass into nanocellulose

(i) Extraction of cellulose from Empty Fruit Bunch (EFB) biomass

Figure 3.1 and 3.2 clearly showed the process flow and visual observation for the production of nanocellulose respectively from EFB fibres. Empty Fruit Bunch (EFB) biomass was mashed and sieved to EFB powder (150 μm of particle sizes) prior for soxhlet extraction treatment. Under soxhlet extraction, the EFB fibres was immersed into mixture of toluene (C_7H_8) and ethanol (C_2H_7OH) with a ratio of 2:1 for 360 min as mentioned in literature studies (Abe & Yano, 2009; Agbor *et al.*, 2011; Fahma *et al.*, 2010; Iwamoto *et al.*, 2007). The dewaxed EFB fibres was aged in 2 M Potassium Hydroxide (KOH) and then bleached by 10 % (v/v) of hydrogen peroxide (H_2O_2) solution at 75 °C for several times by using orbital shaker. The process was stoped when the sample color turn into pearl white from brown colour. The extracted cellulose slurry (named as cellulose derived EFB fibers) was rinsed for few times with deionized water until it reached neutrality (pH6-pH7). The chemical composition of EFB fibres, alkali pretreated and bleached cellulose sample is enlisted in Table 3.1.

Table 3.1 Chemical composition of raw EFB fibres, alkali pretreated EFB sample and bleached cellulosic sample

EFB Fiber Sample	Holocellulose (%)	Cellulose (%)	Hemicellulose (%)	Lignin (%)	Wax (%)
Raw EFB Fiber	18.0	48.4	30.4	18.1	3.1
Alkali Pretreated EFB	44.75	65.4	20.7	13.9	-
Cellulose derived EFB	95.27	97.38	2.11	0.51	-

(ii) Preparation of CNC cellulose

Productions of nanocellulose from EFB-derived cellulose will be prepared by chemical route: inorganic acid:H_2SO_4 (Strong acid) and inorganic salt:Ni-salt solution (mild acid). Cellulose was added into prepared Ni-salt solution and H_2SO_4 respectively at 45 ^{O}C within 15 mins duration. After hydrolysis, the gelatinous white product was washed repeatedly by using deionized water to remove the residue of H^+,SO_4^{2-}, Ni^{2+} or NO_3^- ions that attached on the surface of product. Then the gelatinous white nanocellulose were dialyze for a week until the pH is constant (pH 7) to ensure that the H^+,SO_4^{2-} , Ni^{2+} or NO_3^- ions have been removed. The slurry was further treated with 40 kHz sonication for 40 min in a sonicator (WUC-A03H, DAIHAN, Korea) to disperse the nanofibres in water. Finally, the products were dried in a freeze dryer to obtain a fine white powder from H_2SO_4 (SA-NC) and Ni-salt (Ni-NC) hydrolysis.

3.4 Characterization techniques

3.4.1 Fibers characterization

The composition of extractives, cellulose, holocellulose, hemicellulose and lignin of the samples (EFB fibres, alkaline pretreated EFB and cellulose derived EFB) was analyzed according to Technical Association of Pulp and Paper Industry (TAPPI) standards.

- **Holocellulose content**

The holocellulose content (α-cellulose and hemicellulose) of the fibres and cellulose was determined by treating the fibres and cellulose with a $NaClO_2$ and 10 %(v/v) CH_3COOH mixture solution (Schuerch, 1968). The sample was diluted in distilled water under magnetic agitation (70^OC, 30min). Then, $NaClO_2$ and 10 %(v/v) CH_3COOH mixture solution were added. This procedure repeated for 3 hour reaction. Finally, the resultant mass was filtered and oven dried at 100^OC untill the mass is constant. The content of holocellulose was calculated according to Equation 3.1. M_H represent dry of mass fibres (g), M_{HOLO} is dry mass of holocellulose (g) and (%) P_{HOLO} is the content of holocellulose(Schuerch, 1968).

Equation 3.1:

$$P_{HOLO}\ (\%) = M_{HOLO}/M_H \times 100\%$$

- **α-cellulose content**

The α-cellulose content was determined by treating the extracted holocellulose samples with 17.5 %(v/v) NaOH solution(Technical Association of the & Paper, 1973). After 3.5min, soak the sample with CH_3COOH. Lastly, the resultant mixture was filtered and oven dried for 24hour at $48^OC\pm2$. Put in desiccator for 15min (Technical Association of the & Paper, 1973). The content of α-cellulose was calculated according to Equation 3.2. M_C represent dry mass of α-cellulose (g), W_{HOLO} is extracted holocellulose samples (g) and (%) $P_{CELLULOSE}$ is the content of α-cellulose.

Equation 3.2:

$$P_{CELLULOSE}\ (\%) = M_C/W_{HOLO} \times 100\%$$

- **Lignin determination**

The lignin content of the fibres and cellulose was found by treating them with a 72(%) v/v H_2SO_4 solution (15min,2hr) (Technical Association of the & Paper, 1973). Then, distilled water were added under reflux. Finally, the samples was oven dried at 100^{O}C until constant mass was attained. The content of lignin was defined in Equation 3.3; where M_F is the dry mass of fibres (g), M_L is the mass of dry lignin (g) and P_{LIGNIN} (%) is the content of lignin in the sample.

Equation 3.3:

$$P_{LIGNIN}\ (\%) = M_L / M_F x100\%$$

- **Hemicellulose determination**

The hemicellulose content was obtained by subtracting the percentage of α-cellulose from holocellulose content (Joaquim *et al.*, 2009; Lai & Idris, 2013a). $P_{CELLULOSE}$ (%) is the α-cellulose content (Equation 3.2) and P_{HOLO}(%) is the holocellulose content (Equation 3.1). P_{HEMI} (%) is the percentage of hemicellulose content (Equation 3.4).

Equation 3.4:

$$P_{HEMI}\ (\%) = P_{CELLULOSE}\ (\%) - P_{HOLO}\ (\%)$$

3.4.2 Physiochemical properties characterization

- **X-Ray diffraction (XRD)**

XRD patterns were obtained within a 2θ range from 5 to 40° by using Shimadzu diffractometer model XRD 6000, with CuKα radiation at the operating voltage of 2.7 kW. The crystallinity index (CrI) of samples was calculated based on the intensity between (002) and (101) lattice diffraction peaks using Segal's method (Segal, Creely, Martin, & Conrad, 1959) (Equation 3.5). I_{002} represents both crystalline and amorphous region of

cellulose (maximum intensity at 2θ = 22°) while Iam represents only amorphous phase (intensity of diffraction at 2θ = 18^{O}):

Equation 3.5:

$$CrI\ (\%) = (I_{002}\text{-}I_{am})/I_{002} \times 100\%$$

- **Fourier Transform Infrared Spectroscopy (FTIR)**

FTIR was performed by using Perkin Elmer spectrometer (Spectrum Two) in the range 4000-500cm^{-1} with a scanning resolution of 4cm^{-1}. Ground samples were mixed with potassium bromide (KBr) and then pressed into ultra-thin transparent pellets (approximately 4mm thickness) for analysis.

- **High Resolution Transmission Electron Microscopy (HR-TEM)**

The dimensional measurements were determined by using HR TEM JEOL JEMP-2100F at an acceleration voltage of 200kV. The CNF samples diluted in ethanol (C_2H_6OH) solution was deposited on the surface of copper grid and allowed to dry at room temperature. Aspect ratios in terms of length to diameter (L/D) of treated samples were determined based on the HR-TEM measurement.

- **Field Emission-Scanning Electron Microscopy (FESEM)**

The surface morphology were studied by using FESEM, Fei Quanta 200F and operated at 10 kV and 100 Paunder low vacuum conditions. The samples were mounted with conductive carbon tape and coated with 5nm thickness of gold before FESEM viewing process.

- **Thermogravimetric analysis (TGA)**

Thermal analysis were studied by using TGA Q-500 (TA Instruments,United States of America). 1 mg of each sample was heated at 10°C/min from 25°C to 900°C under nitrogen (N_2) gas at the flow rate of 200mL/min.

- **Atomic Force Microscopy (AFM)**

In order to prevent the formation of aggregates, a short sonication (30minutes) were done. A drop of dilute samples (EFB fibres,EFB derived cellulose,SA-NC and Ni-NC) suspensions were deposited onto glass slides. After dried at ambient temperature (24hours) to allow the films to dried, AFM observation were carried out using a Bruker's ScanAsyst Mode technology.

- **Particle Size Distribution (PSD)**

The nanocellulose suspension at 4% (w/v) was diluted in water at the ratio of 1:100 (v/v) and ultrasonicated for 30 min in an ultrasonic bath (WUC-A03H, DAIHAN, Korea). Measurements were made using a Malvern 3600 Zetasizer NanoZS (Malvern Instruments, UK). This equipment uses dynamic light scattering to measure the diffusion of particles moving under Brownian motion, and converts this to size and size distribution.

3.5 Optimization study for nanocellulose production via Response Surface Methodology (RSM)

The nanocellulose synthesis was developed and optimizes using response surface methodology (RSM) provided by Design expert software 6.0.8 (Stat-Ease Inc., Minneapolis,USA). A standard RSM design tool known as Face Central Composite Design (FCCD) was applied to study the acid catalyzed hydrolysis reaction variables (Ni salt catalyzed reaction). Three identified independent variables are A: acidity of catalyst

(pH), B: reaction time (minute) and C: reaction temperature (°C). The response chosen was nanocellulose yields (%) which were obtained from the reaction. Table 3.1 lists the ranges and the levels of the independent variables with actual and coded levels of each parameter. The independent variables are coded to two levels namely: low (-1) and high (+1). A three level, three factor face central composite design was develop to fit second order response surface model which require 20 experiments including 8 factorial, 6 center and 6 axial at the center points were employed in this study.

The experiment result obtained from FCCD was analyzed using response surface methodology. The second order polynomial equation variables for prediction of the optimal point between the response variable (nanocellulose yield, %) and the independent variables of hydrolysis reaction is expressed by Equation 3.6 where Y is the predicted response; n is the number os experiments; βo, βi, βii and βij are regression coefficients for constant, linear, quadratic and interaction coefficient, respectively; Xi and Xj are the coded independent variables or factors.

Equation 3.6:

$$Y=\beta_0+\sum_{i=1}^{n}\beta iXi+\sum_{i=1}^{n}\beta ii\times Xi^2\times X_i+\sum_{i=1}^{n}\sum_{j>1}^{n}\beta_{ij}\times Xi\,X_j$$

The quality of fit for the reaction model was studied by the coefficients of variances (R^2) and its regression coefficient significant (analysis of variances (ANOVA)) were determined with Fisher's test (F-test). Response surfaces and contour plots were plotted using the quadratic polynomial equation obtained from regression analysis of experiment by keeping one of the independent variables at a constant value while changing the other two variables.

Table 3.2: Range of independent variables and the experimental domain

Factor	Name	Units	Low Actual	High Actual	Low Coded	High Coded
A	Acidity of catalyst	pH	2	4	-1	1
B	Reaction time	mins	20	100	-1	1
C	Reaction temperature	°C	25	65	-1	1

Table 3.3: The CCD matrix of experimental and yield response

Type	A: Acidity of catalyst(pH)	B: Reaction time (min)	C: Reaction temperature (°C)	Response (Yield %)
Factorial	2	20	25	40.55
Factorial	4	20	25	40.61
Factorial	2	100	25	19.91
Factorial	4	100	25	33.62
Factorial	2	20	65	60.01
Factorial	4	20	65	56.82
Factorial	2	100	65	50.15
Factorial	4	100	65	62.26
Axial	2	60	45	60.95
Axial	4	60	45	72.1
Axial	3	20	45	70.54
Axial	3	100	45	66.41
Axial	3	60	25	63.91
Axial	3	60	65	82.21
Center	3	60	45	79.89
Center	3	60	45	80.92
Center	3	60	45	83.51
Center	3	60	45	82.91
Center	3	60	45	80.54
Center	3	60	45	80.55

CHAPTER 4: RESULTS AND DISCUSSION

The present study was divided into three sections: (i) First section is the extraction of cellulose from palm based lignocellulosic biomass (EFB); (ii) Preparation of nanocellulose from the EFB derived cellulose via acid hydrolysis reaction (H_2SO_4 and Ni-salt hydrolysis);(iii)Optimization study for nanocellulose preparation. The physicochemical properties of raw material, intermediate cellulose and final product were also been investigated. The physicochemical properties of the EFB derived cellulose and nanocellulose included the particle size distribution, crystallinity index, chemical functional group, morphology and thermal stability study which will be discussed in this chapter.

4.1 X-Ray Diffraction Analysis

Figure 4.1 shows the XRD profiles of EFB fibres, EFB derived cellulose and SA-NC and Ni-NC. All samples exhibited similar XRD patterns at diffraction peaks of 2θ = 15°, 16°, 22.8°, and 35°, which can be attributed to the crystallographic planes (101), $(10\bar{1})$, (021), (002), and (040) respectively (Park *et al.*, 2010). According to French (2014), the main contributors of intensity to the three main peaks for cellulose Iβ have miller indices of (1-10),(110) and (200) (French, 2014). Furthermore, the main crystal structure of cellulose derived EFB was retained and do not altered during the sulfuric acid and Ni-salt catalyzed hydrolysis process.

Based on the crystallinity profile (Table 4.1), the crystallinity index of samples was in the order of EFB fibres < EFB derived cellulose < SA-NC < Ni-NC. The increase in crystallinity index of treated samples showed a significant removal of amorphous regions and increased exposure of the crystalline regions of cellulose (Dhepe & Fukuoka, 2008).

As for industrial applications, crystallinity of nanocellulose is an important factor determining its mechanical and thermal properties. Higher crystallinity in nanocellulose is generally associated with higher tensile strength, which is expected to be beneficial for producing high-strength composite materials (Bhatnagar & Sain, 2005).

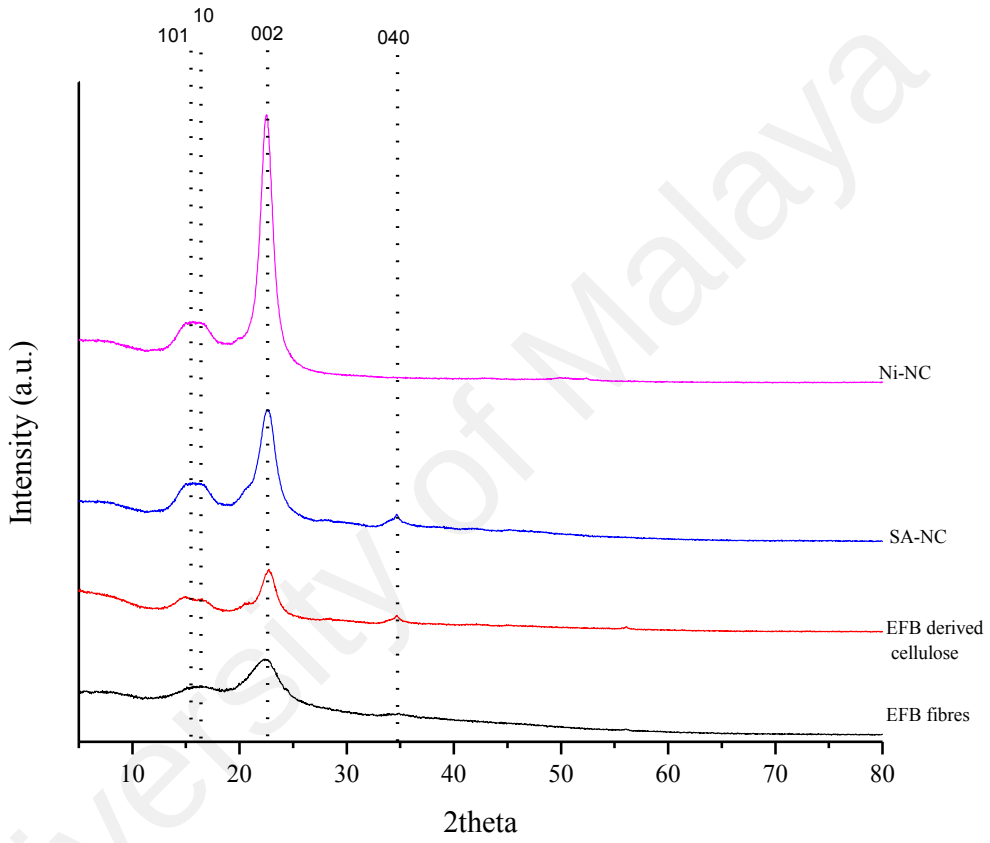

Figure 4.1: X-ray diffraction patterns of (a) EFB fibres (b) EFB derived cellulose, (c) SA-NC, and (d) Ni-NC

As shown in Table 4.1, the crystallite size was increased after hydrolysis, following the order of EFB fibres < EFB derived cellulose < SA-NC < Ni-NC. Similar cases in which the crystallite size was increased have been reported (Das *et al.*, 2010; Sèbe *et al.*, 2012; Shahabi-Ghahafarrokhi *et al.*, 2015). It is believed that the cellulose with smaller crystallites with disorderly phases were easily degraded by Ni-solution, which resulted in high exposure of thicker crystallite phases (Sèbe *et al.*, 2012). Furthermore, the

recrystallization of defective crystallites during the hydrolysis reaction may change the crystallite sizes of nanocellulose (Tang *et al.*, 1996).

Table 4.1: .Crystallinity Index (Crl) and Crystallite Sizes of EFB fibres, EFB derived cellulose, SA-NC and Ni-NC

Sample	2θ(°)	FWHM (°)	Crystallite size, D (nm) (perpendicular to 200 plane)	Crystallinity index, Crl (%)
EFB fibres	22.14	4.00	2.00	46.04
EFB derived cellulose	22.19	3.29	2.43	68.35
SA-NC	22.41	2.03	3.94	73.17
Ni-NC	22.81	0.8600	9.44	80.75

Mild inorganic acid hydrolysis (Ni-salt) able to enhance the hydrolysis selectivity of nanocellulose compared to strong inorganic acid hydrolysis (H_2SO_4). The reason is that Ni^{2+} capable to diffuse into the amorphous region and surfaces of crystalline region of cellulose fibres, and disrupt the intermolecular hydrogen bonds and intramolecular glyosidic bonds of cellulose, which leads to physical swelling with the chemical degradation of cellulose. Swelling of the cellulose will increase the contact area between acids and cellulose, thus enhances the hydrolysis performances. Under mild acid hydrolysis conditions (Ni-salt inorganic acid), the rate of cellulose hydrolysis is relatively low because only a selective amount of the amorphous nanocellulose was degraded into sugar. This explains of higher nanocellulose yield from Ni salt inorganic acid hydrolysis compared to strong inorganic H_2SO_4 hydrolysis. The possible mechanism is that metal ions such as Ni^{2+} able to dissociate into complex ions in aqueous solvent such as water. They form coordinate covalent bond with six water molecules. The nomenclature of metals ions ligand complexes is given as $[M (H_2O) n]^{Z+}$ (where M is the metal ion, z is the cation oxidation state and n is solvation number). Six water molecules form monodentate ligands with the central metal cation. The central metal cation polarizes (withdraws electron density) from the water molecules. This makes the hydrogen atoms

in O-H bonds more electropositive. The complex ions $[M(H_2O)n]^{Z+}$ are then deprotonated by hydroxonium ions H_3O^+ causing the solution to be acidic. This phenomenon can be explained using Ni^{2+} cation as an example (shown in Equation 4.1). This process continues until there is no charge on the metal complex.

Equation 4.1:

$$Ni(NO_3)_2 + 6H_2O \leftrightharpoons [Ni(H_2O)_6]^{2+} + 2NO_3^- \quad (4.1.1)$$

$$[Ni(H_2O)_6]^{2+} + H_2O \leftrightharpoons [Ni(H_2O)_5(OH)]^+ + H_3O^+ \quad (4.1.2)$$

$$[Ni(H_2O)_6]^+ + H_2O \leftrightharpoons [Ni(H_2O)_5(OH)] + H_3O^+ \quad (4.1.3)$$

Due to the formation of sophisticated metal ions (Equation 4.1.1 to 4.1.3), more H_3O^+ was produced. Therefore, the concentration of H_3O^+ was increased due to the presence of metal ions. Thus, the results clearly showed that different metal ions concentration (pH) gives differences in nanocellulose yield.

4.2 Fourier Transform Infrared Spectroscopy (FTIR)

The chemical functional groups of EFB fibres, EFB derived cellulose, SA-NC and Ni-NC were studied using FTIR analysis (Figure 4.2). The four samples had similar FTIR patterns, which indicated that the chemical structure of synthesized nanocellulose remained unchanged after H_2SO_4 and Ni-catalyzed hydrolysis. Furthermore, the absence of NO^-_3 and SO^{2-}_4 peaks at 1384 cm^{-1} and 1109 cm^{-1} indicated that the nitrate and sulfate ions was completely removed during the washing and dialysis process (Bhatt *et al.*, 2008; Grube *et al.*, 2006; Smidt *et al.*, 2005).

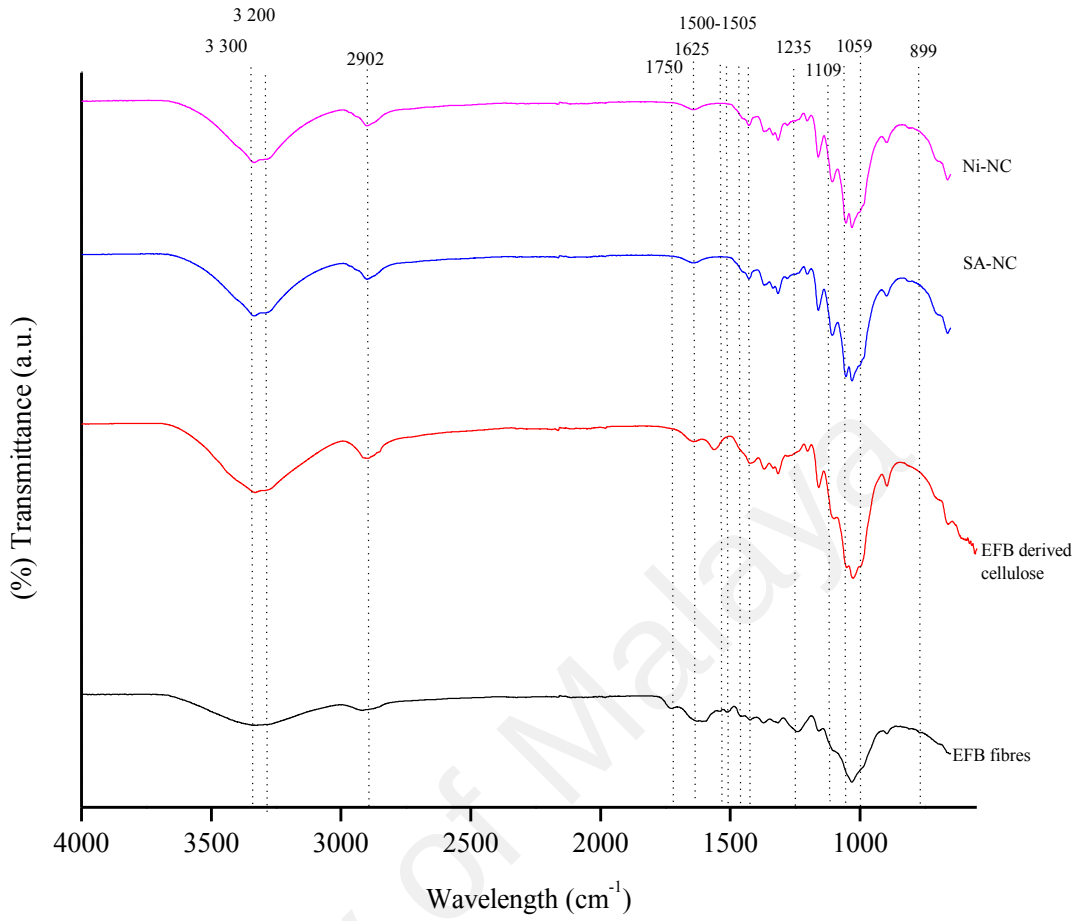

Figure 4.2: FTIR spectra of EFB fibres, EFB derived cellulose, SA-NC and Ni-NC

FTIR spectra of the EFB fibres showed an absorption peak at 1750cm^{-1}, which is -C=O (saturated aldehyde) that attributed to vibration of xylan (hemicellulose)(Lai & Idris, 2013b). The respective peak was noticeable absence after the pretreatment process, which indicating that hemicellulose was successfully removed from the complex biomass structures(Gibson, 2012). In addition, non-cellulosic lignin's chemical functional groups appeared at the band of 1505 cm^{-1} and 1500 cm^{-1}, which attributed to aromatic skeletal vibration in lignin(Lai & Idris, 2013b), while FTIR band at 1235cm^{-1} attributed to syringyl ring and CO stretch in lignin and xylan. These respective peaks also disappeared after the bleaching treatment, thus confirming that lignin and small part of hemicellulose were eliminated.The dominant peak in the region between 3700 and 3000 cm^{-1} is

attributed to O-H stretching. A slight decrease in the peak intensity showed the disruption of intramolecular and intermolecular hydrogen bonding (Alemdar & Sain, 2008; Yang *et al.*, 2011).The FTIR peak at 2,800 cm^{-1} corresponds to the presence of C–H stretching vibration and $–CH_2–$(C6)– bending vibration (Alemdar & Sain, 2008; Yang *et al.*, 2011). The weak intensity of the FTIR band at 1640 to 1645 cm^{-1} can be attributed to the cellulose-water interaction, *i.e.*, the –OH bending of absorbed water. The chemical structure of C–O–C pyranose ring skeletal vibration of cellulose was observed in the FTIR peak at 1,050 cm^{-1} (Jahan *et al.*, 2011). Furthermore, the absorption bands near 1058 to1060 cm^{-1} can be attributed to C-O and C-H stretching vibrations, which confirms the presence of cellulose structures (cellulose I as cellulose Iβ). The increasing peak intensity of these groups indicated an increase in sample crystallinity (Man *et al.*, 2011; Zain *et al.*, 2014). The peak at 885 cm^{-1} is attributed to the characteristic ß-glycosidic linkages between the glucose units of cellulose chains (Sun *et al.* 2004; Zhang *et al.*2011).

4.3 Field-Emission Scanning Electron Microscopy (FESEM)

The surface morphology of EFB fibres, cellulose derived EFB, SA-NC and Ni-NC was determined using FESEM analysis (Figure 4.3). FESEM images clearly displayed significant changes of EFB fibres structure after being treated under alkali, bleaching and acid condition. Based on Figure 4.3a, EFB fibres showed bundles of individual fibres which was coated with extractive materials such as waxes, pectin, hemicellulose, lignin and other impurities. Wax and pectin acted as a protective layer for palm fiber's surfaces (Johar *et al.*, 2012), thus soxhlet extraction treatment was performed to remove this hydrophobic layer in order to increase the accessibility of cellulose towards chemical attack. Figure 4.3b showed the de-lignified and bleached cellulose derived from EFB. It was observed that the treated fiber appeared in smoother and individualized fibrils as most of the non-cellulosic content and impurities were removed from the fiber surface via soxhlet extraction, delignification and bleaching. These processes has broken the

lignocellulosic complex, solubilized the lignin and hemicellulose and increase the surface area of hidden cellulose. Thus, the cellulose will be more accessible to hydrolysis reaction to produce nanocellulose.

The structures for SA-NC (Figure 4.3c) showed the aggregations of cellulosic fibres were reduced. Furthermore, the presence of cellulose crystallites (in the form of rice shape) indicating that the intra-fibrillar structure was disintegrated into individual cells as the amorphous region of cellulose has been decomposed (Kumar *et al.*, 2014; Nazir *et al.*, 2013). The Ni-treated products showed the significant changes of structure as compared to EFB fibres and EFB derived cellulose, where the fibres were degraded into narrower and less orderly fragments with cracks on the surface.

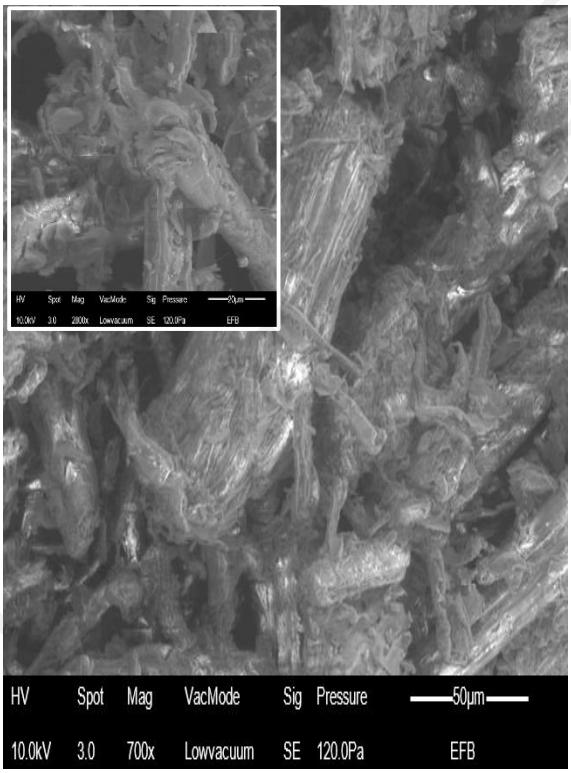

(a) EFB fibres

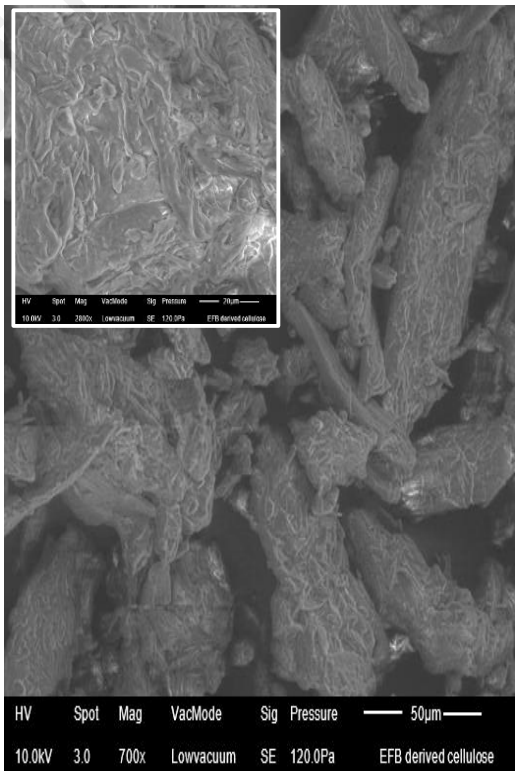

(b) EFB derived cellulose

Continued on next page

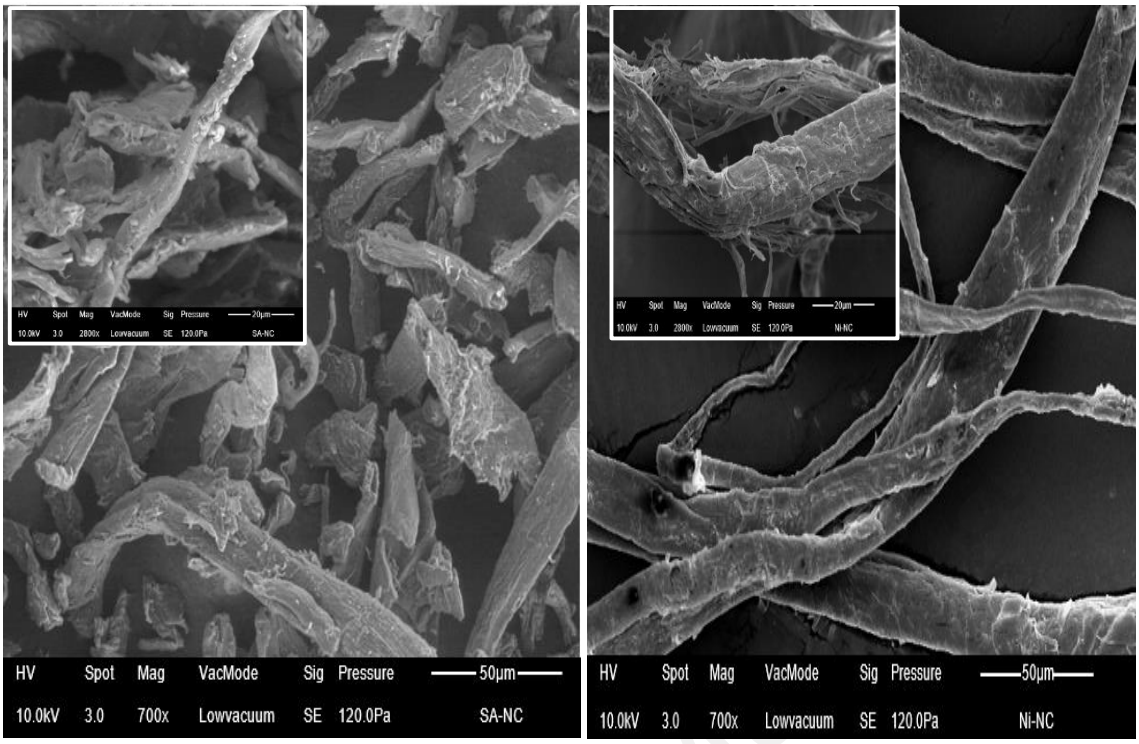

(a) SA-NC (d)Ni-NC

Figure 4.3: The morphology of (a) EFB fibres (b) EFB derived cellulose (c) SA-NC and (d) Ni-NC

This confirmed the destruction of amorphous fraction remaining in cellulose by means of mild Ni-hydrolysis, the compact structure of cellulose derived from EFB was significantly changed to finer fibril and with a longer structure. This indicated that most of the cellulose fiber was selectively cleaved into smaller sizes during hydrolysis reaction. It is expected that Ni^{2+} ions diffused into surface of cellulose fibres and attack the glycosidic bonding of cellulose chains, which lead to the breakage of amorphous regions of cellulose fibres (J. Li *et al.*, 2015), thus increased fiber's surface area. This led to the breakage of the amorphous regions of cellulose fibres thus resulted in smaller particle sizes compared to EFB fibres and EFB derived cellulose. Several researchers also proved that from FESEM images, the destruction of amorphous leaving crystallite region at the nanocellulose can be observed (Kumar *et al.*, 2014; Nazir *et al.*, 2013). This hypothesis were further supported by XRD data, which showed the CrI of SA-NC and Ni-NC is higher than the EFB fibres, and cellulose derived EFB.

4.4 High Resolution Transmission Electron Microscopy (HR-TEM)

HR-TEM images of SA-NC and Ni-NC are shown in Figure 4.4. The Ni-salt-catalyzed hydrolysis rendered an interconnected of individual cellulose nanocrystals with spider web-like structure (Fig. 4a-c). Furthermore, the nanocellulose are presented in fine diameter (10 to 60 nm) and length at 70 to 300 nm according to the results,which implied that the Ni ion successfully diffuse into the rigid structure of cellulose and resulted in selective fragmentation of crystal into smaller sizes.

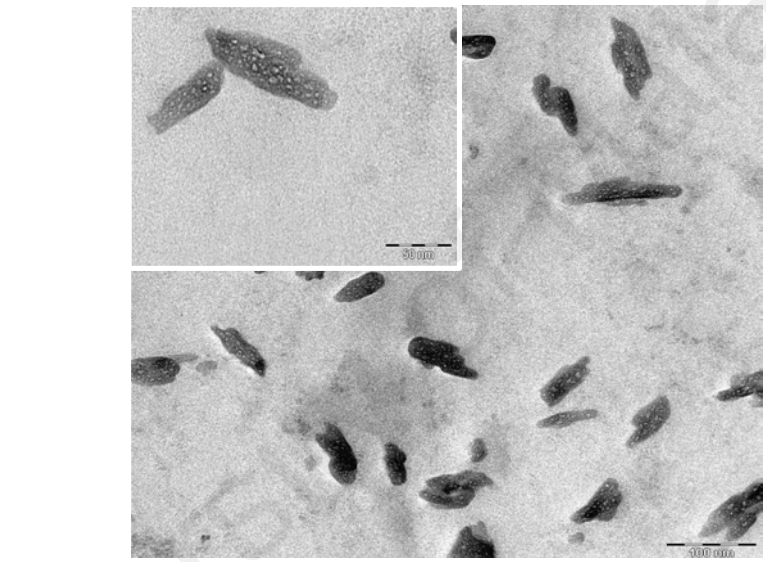

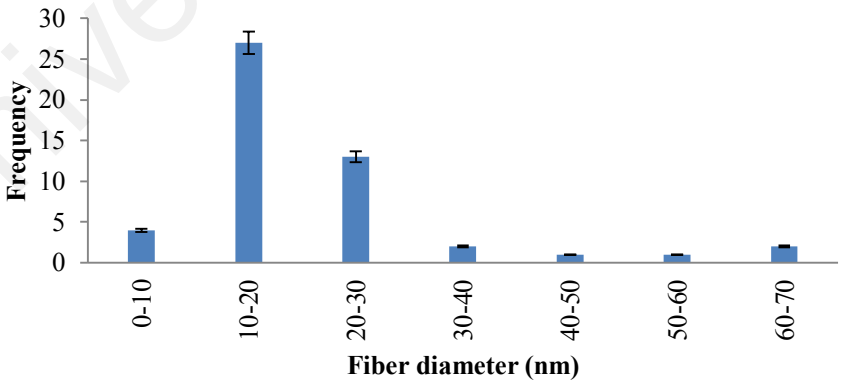

Continued on next page

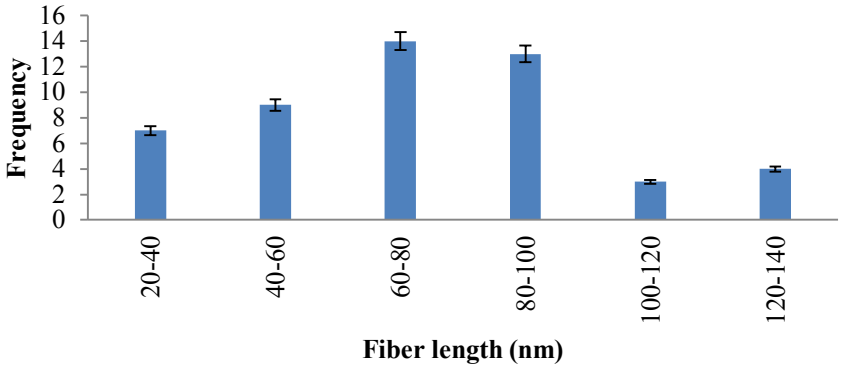

(a) SA-NC

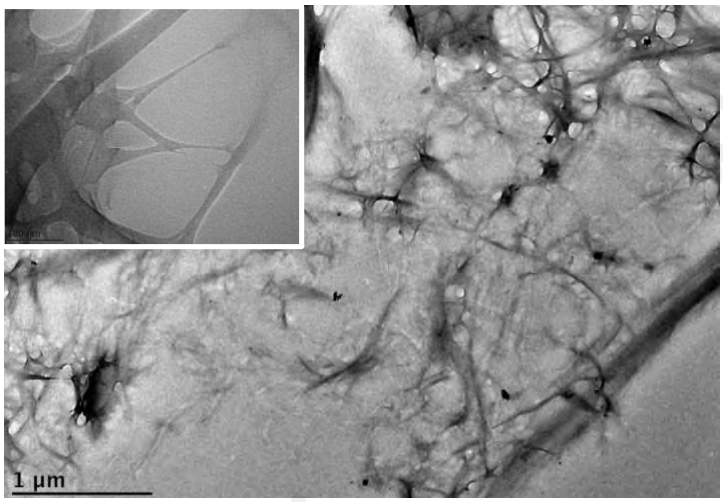

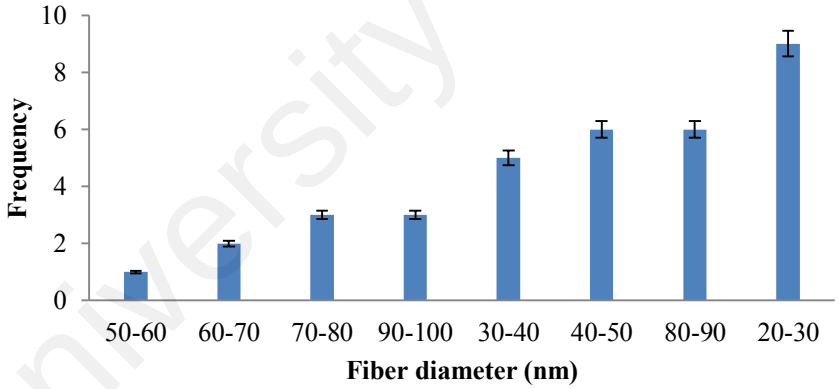

Continued on next page

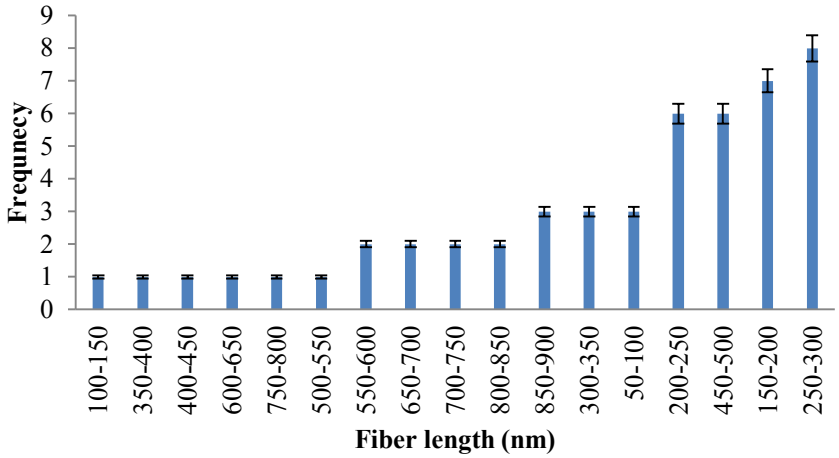

(b) Ni-NC

Figure 4.4: HR-TEM micrographs and particle size distribution profile of (a) SA-NC and (b)Ni-NC

A comparison study was performed for both inorganic metal salt (Ni^{2+}) and inorganic acid (H_2SO_4) catalyzed hydrolysis process. H_2SO_4-treated nanocellulose (SA-NC) was performed (Figure 4.4). The HR-TEM images clearly revealed the rice-shape structures of the cellulose crystals with nano-scale diameter (10 to 30 nm) and shorter length (60 to 100 nm). Besides, dimensional profiles of Ni-treated and H_2SO_4-treated nanocellulose samples were determined by studying the aspect ratio of length (*L*) to diameter (*D*): *L*/*D* (Table 4.2).

The aspect ratio of prepared nanocellulose increases in the order SA-NC< Ni-NC. SA-NC rendered shorter length of nanocrystal while Ni-NC showed fine width with controllable length of products. This indicated that Ni-inorganic salt capable to selectively control the hydrolysis as compared to sulphuric acid reaction although low acid concentration was used.

Table 4.2: Dimensional Profile of Prepared Nanocellulose for HR-TEM images

Sample	Length (L, nm)	Diameter (D, nm)	Aspect ratio (L/D)
SA-NC	72.7±2.0	21.5±2.0	3.4
Ni-NC	383.7±34.1	42.1±3.9	9.1

4.5 Atomic Force Microscopy (AFM)

The morphological characteristics and nanostructured dimension of produced nanocelluloses were studied by using AFM analysis. The AFM images of nanocellulose products that prepared by H_2SO_4 and Ni-salts catalyzed acid hydrolysis were shown in Figure 4.5(a) and 4.5(b). Theoretically, acid hydrolysis of cellulose have resulted in reduction of fibres diameter from microns to nanometers as most of the amorphous region in cellulose was solubilized by chemical (Azizi Samir *et al.*, 2005; Yahya *et al.*, 2015). Based on the results, the average dimension for SA-NC was 27.5±1.1nm and 93.8±3.7nm for diameter and length, respectively (Table 4.3). For Ni-NC, the average dimensional profile was 36.6±1.7nm and 637.3±55.4nm for diameter and length, respectively (Table 4.3). As a result, aspect ratio (length/diameter ratio) for Ni-NC was higher compared to SA-NC, which was 17.4 from 3.4 respectively.

From the AFM images, SA-NC showed a shorter dimension of fragmented fibres as compared to Ni-NC. This was due to the harsher condition of strong inorganic acid (H_2SO_4) catalyzed depolymerisation process and shortens the crystallite (Salas *et al.*, 2014) with more charged surface half ester groups at the surface. Furthermore, Prodyut's group reported that the energy of adhesion of two crystallite is proportional to the contact area of fibres; thus less contact leads to easier separation of thinner and shorter particles into cellulose nanocrystals via strong acid hydrolysis (H_2SO_4) (Prodyut *et al.*, 2014; Salas *et al.*, 2014)compared to mild acid hydrolysis (Ni-salts). This also indicates that Ni-

inorganic salt hydrolysis capable to selectively control the hydrolysis as compared to sulfuric acid reaction.

Table 4.3: Dimensional Profile of Prepared Nanocellulose for AFM images

Sample	Length (L, nm)	Diameter (D, nm)	Aspect ratio (L/D)
SA-NC	93.8±3.7	27.5±1.1	3.4
Ni-NC	637.3±55.4	36.6±1.7	17.4

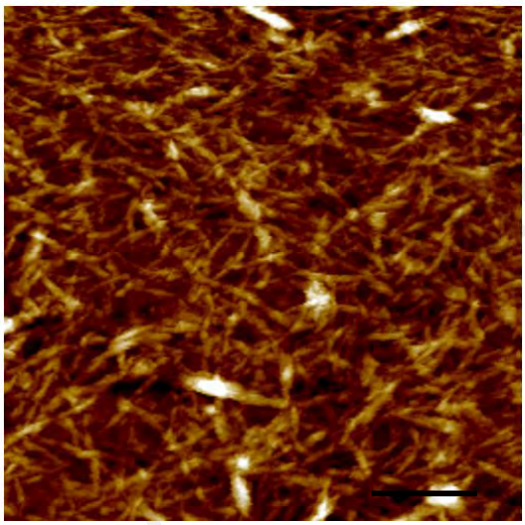

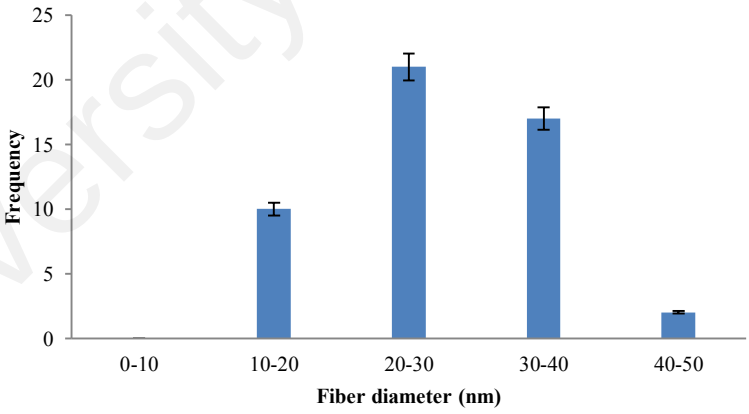

Continued on next page

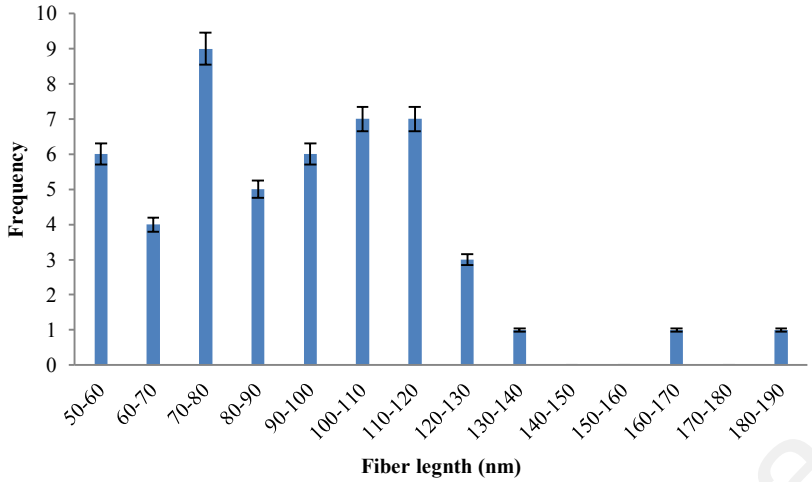

(a)SA-NC

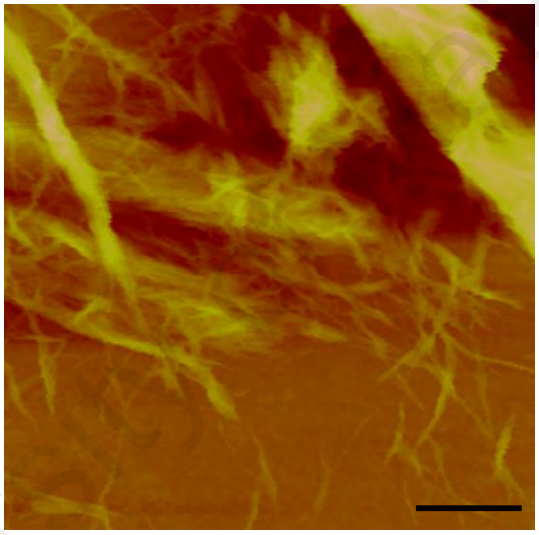

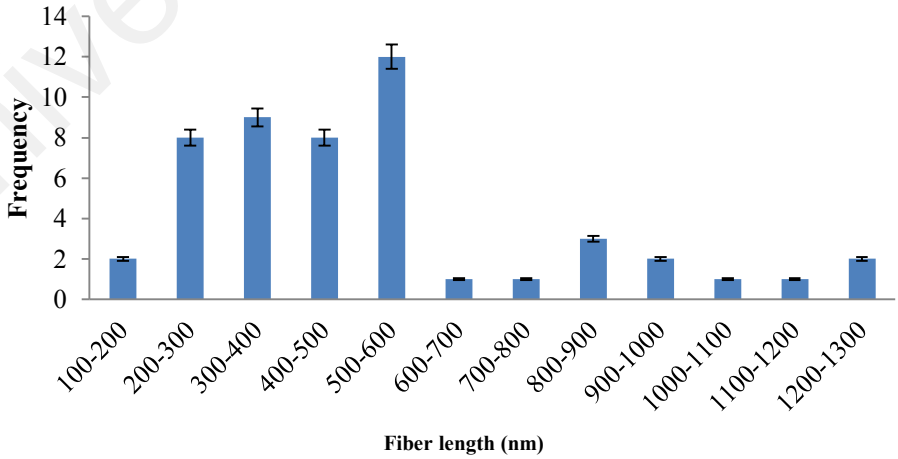

Continued on next page

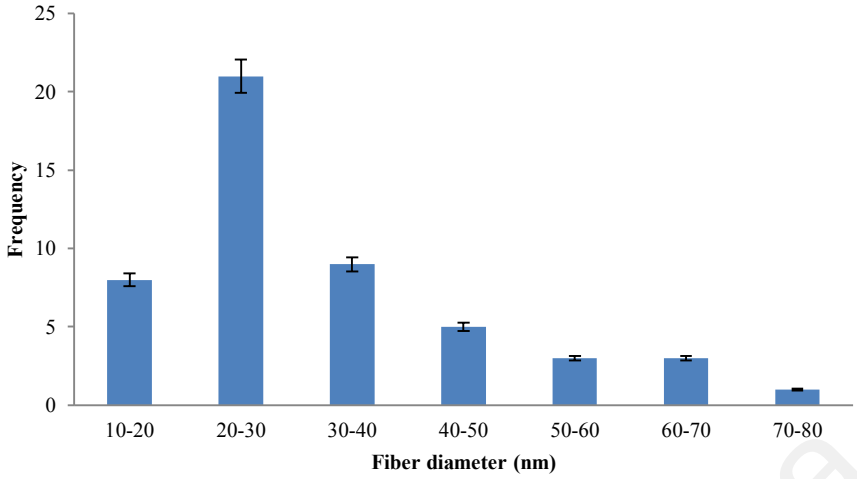

(b)Ni-NC

Figure 4.5: AFM images and dimention analysis for (a) SA-NC and (b) Ni-NC

4.6 Particle Size Distribution (PSD)

PSD or Dynamic Light Scattering (DLS) is a well establish, on-invasive method to measure particles in a dispersed liquid medium. It use to measures transitional diffusion coefficient of particles in dispersion medium, which undergo Brownian movement. Brownian movement motion is a random motion of particles suspended in a fluid (liquid or gas) resulting from their collision with the quick atom or molecules in the gas or fluid. A light scattering device (Malvern Zetasizer NanoZS) will determine various dimensions in average measurement as the particles flow randomly through the light beam, producing a distribution of sizes from the smallest to the largest dimensions(Instruments, 2012).

Figure 4.6 shows the particle size distribution of EFB, cellulose derived EFB,SA-NC and Ni-NC. As shown from the results, the particle size distribution for EFB fibres was present in the sizes at range of 458.7nm to 5560nm, where the majority region of sizes was exhibit in microscale region of 4568.7nm (Figure4.6a).

The extracted cellulose fibres derived from EFB fibres showed smaller range of size compared to EFB fibres. Figure 4.6b revealed the particle size distribution ranging from

396.1nm to 6439nm, with the majority of particle size in the region of 712.4nm. The smaller size of cellulose reflects that the non-cellulosic compound such as lignin and hemicellulose was successfully removes from the cellulosic fibres (Gibson, 2012).

In contrast, nanocellulose that treated by sulfuric acid (SA-NC) and Ni-salt (Ni-NC) rendered smallest nano range of particle size distribution at 32.67nm to 458.7nm (Figure 4.6c) and 37.84nm to 91.28nm (Figure4.6d) respectively. Both nanocellulose products showed the majority sizes at regions of 50.75nm (SA-NC) and 91.28nm (Ni-NC) respectively. Apparently, the particles size distribution of nanocellulose analysed by PSD analysis was bigger in size range as compared to the results of for HRTEM (10-60nm(D),70-300nm (L)) and AFM analysis (20-40nm (D), 90-600 (L)). This is due to the occurence of Brownian movement motion and electroviscious effects (presence of counter ions in double layer) during PDS analysis, which resulted in particles agglomeration into spherical aggregates, thus increased the sizes range of particle size distribution of the product. The reduced sizes of cellulose to nanocellulose is because the acids cleaves the amorphous region of microfibrils transversely, resulting in reduction in fiber diameter from microns to nanometers (Azizi Samir *et al.*, 2005; Yahya *et al.*, 2015).

(a)

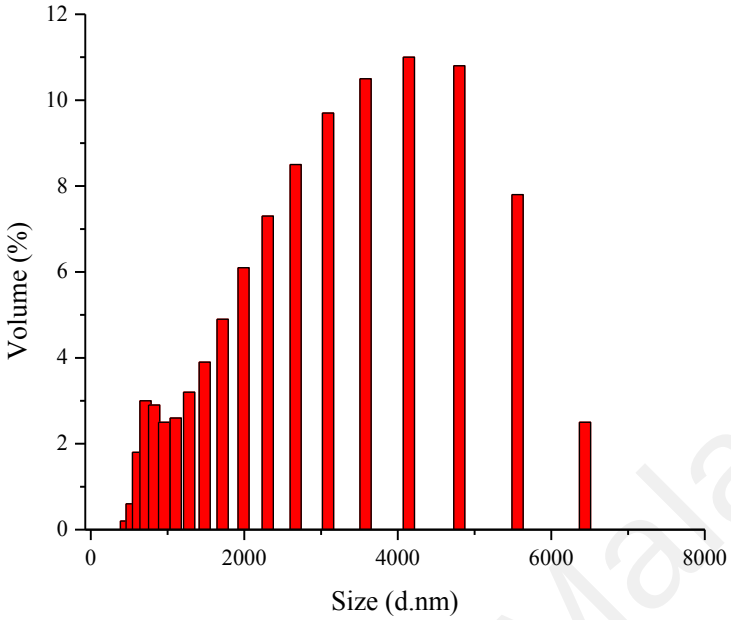

(b)

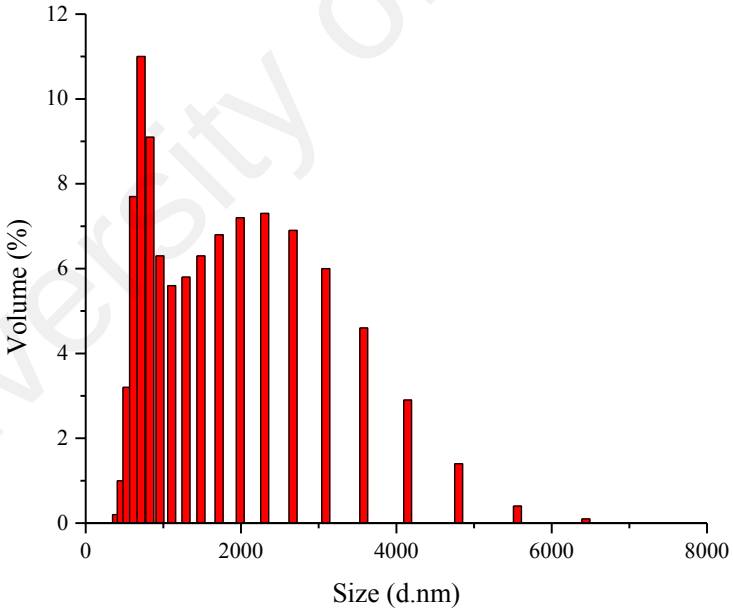

Continued on next page

(c)

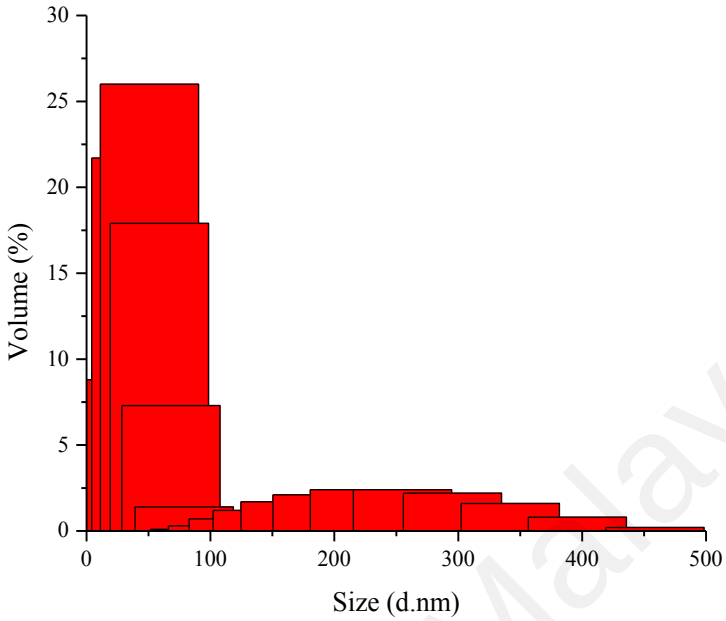

(d)

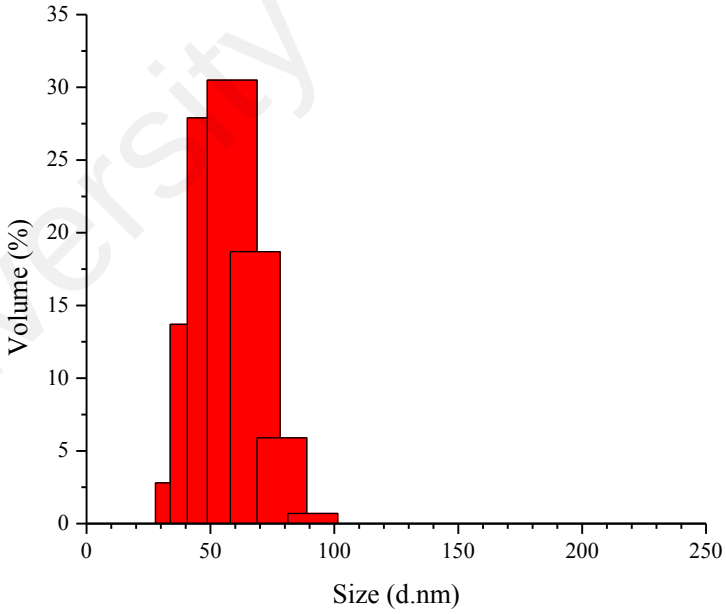

Figure 4.6: Particle size distribution for (a)EFB fibres, (b)EFB derived cellulose, (c)SA-NC and (d)Ni-NC

4.7 Thermogravimetric (TG) and Differential Thermogravimetric (DTG) Analysis

Figures 4.7a and b show that the thermal decomposition peaks with maximum weight loss for EFB, cellulose derived EFB,SA-NC and Ni-NC appeared at 232.31°C, 215.46°C, 174.93°C, and 332.74 °C, respectively. The presence of hemicellulose and lignin in EFB fibres consumed more energy to decompose the non-cellulosic content, especially of lignin, which require higher temperature (230 ºC -400 ºC) and longer time to break the heavily crossed linked aromatic rings(Poletto *et al.*, 2012). This confirmed the existence of complex hemicellulose and lignin in EFB, which resulted in higher decomposition temperatures as compared to the cellulose derived EFB. Cellulose in nanodimension (SA-NC and Ni-NC) showed significant differences of thermal decomposition behaviour from cellulose fibrils. The long-chain polymer structure of cellulose arranged in well order and strongly linked with hydrogen bonding consisted of higher thermal stability that is 215.46°C as compared to SA-NC (Yang *et al.*, 2007), this makes extra energy to cleave the chemical linkages.The nanocellulose product treated with Ni-salt had the highest thermal stability (332.74°C). According to the literature, the thermal stability of nanocellulose prepared by sulfuric acid hydrolysis of ionic liquids (composed of sulfate compounds) is lower than that of native cellulose (Chen *et al.*, 2009; Fahma *et al.*, 2010; Man *et al.*, 2011; Wang *et al.*, 2007). Sulfate content is thus one of the factors affecting the thermal stability of prepared nanocellulose. The presence of sulfate (residual H_2SO_4) adsorbed on the outer surfaces of cellulose hydroxyl crystals increases the reactivity of the material with increasing temperature, causing the decomposition of nanocellulose chains at low temperatures (Wang *et al.*, 2007). In comparison, nanocellulose prepared by Ni-salt-catalyzed hydrolysis exhibits much higher thermal stability. This is due to the lesser amount of damage in the crystalline regions of cellulose structure under mild

conditions. Thus, the high thermal stability of Ni-NC means that it has many potential applications in composite materials that require high thermal stability.

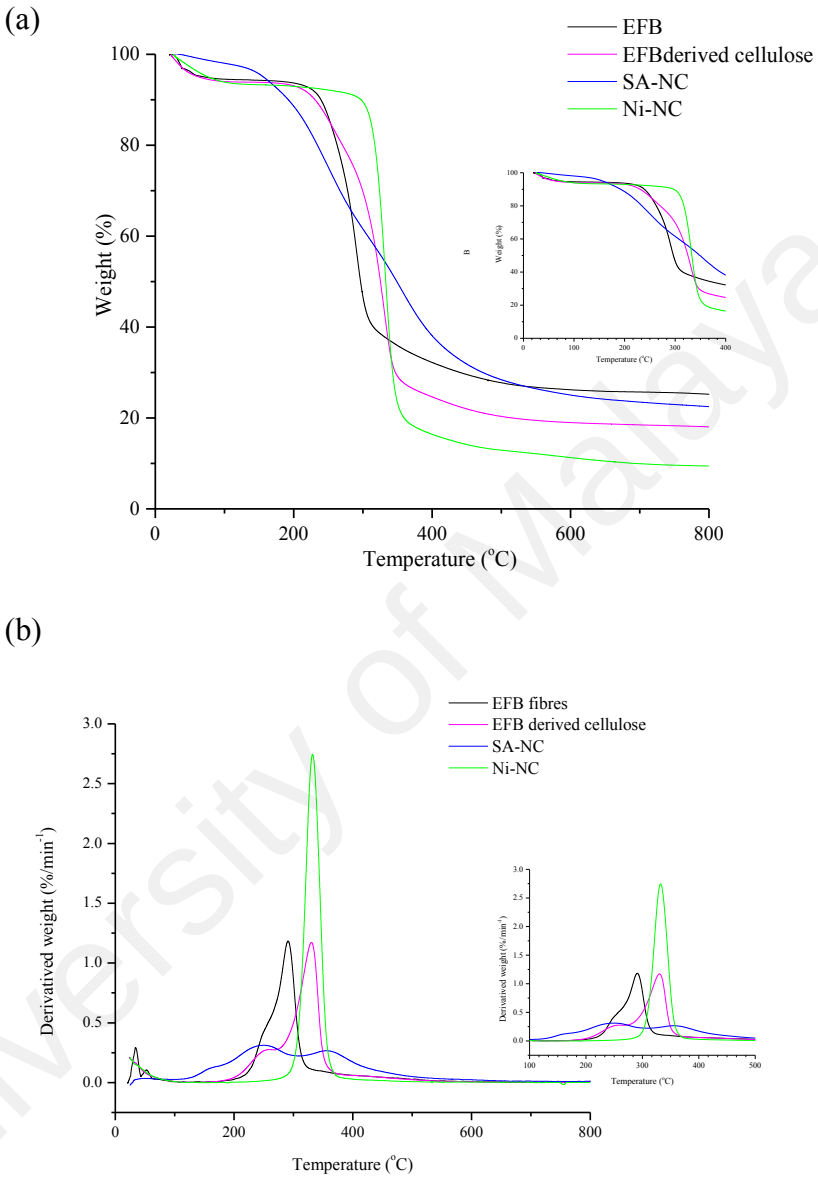

Figure 4.7: (a) TGA and (b) DTG spectra for EFB fibres, EFB derived cellulose, SA-NC and Ni-NC

4.8 Optimization study for nanocellulose production via Response Surface Methodology (RSM)

In this project, response surface methodology simulation focused on the effect of acidity of catalyst (pH), reaction temperature (°C) and reaction time (mins) towards nanocellulose yield. These three effective reaction variables were selected with each parameter being examined at a different level. The reaction times for hydrolysis process were varied from 20 min-100 min while reaction temperatures were varied in range of 25 to 65 °C and the acidity of catalyst (Ni-salt) was studied from pH2 to pH4 A maximum nanocellulose yield (%) was obtained using optimization process by RSM technique. The model equation based on the coded values (A, B, and C as acidity of catalyst, reaction time, and reaction temperature, respectively) for the nanocellulose production was expressed by Equation 4.2.

Positive sign in front of the reaction terms indicates synergistic effect in nanocellulose yields (%), whereas negative sign indicates unfavorable effect. The reaction model) indicated that positive coefficients of A, C, AB and BC rendered a linear effect to increase the nanocellulose yield. However, quadratic term of B, A^2, B^2 , C^2 and AC had negative effects that decrease the nanocellulose yield.

Equation 4.2:

$$\text{Nanocellulose yield, } Y = 81.36 + 3.38A - 3.62B + 11.29C - 14.79A^2 - 12.84B^2 - 8.25C^2 + 3.62AB - 0.61AC + 2.90BC$$

The result of statistical analysis of variance (ANOVA) was performed to determine the significant and fitness of quadratic reaction model as well as the effect of significant individual hydrolysis terms and their interaction towards the nanocellulose yield was presented in Table 4.4. The variables incorporated in the Model-F value of 177.24 with p –value <0.0001 implies that the model is significant at 95% confidence interval. The p-value (probability of error value) is used as a tool to check the significance of each regression coefficient, which also indicates the interaction effect of each cross product. The smaller the p-value, the bigger the significance of the corresponding coefficient is (Lee *et al.*, 2011). In the case of model terms, the p-value less than 0.05 indicated that the particular model terms were statistically significant.

From the ANOVA results, the reaction model suggested that variables with significant influence on nanocellulose yield response were acidity of catalyst (A), reaction time (B), reaction temperature (C), A^2, B^2, $C^2$and the interaction terms were found to exist between the main factors (AB, AC and BC). A low value of coefficient of variation (CV= 3.17) indicated a high degree of precision and good deal of reliability of the experimental values. The lack of fit test with p-value of 0.1429, which is not significant (p-value>0.05 is not significant) showed that the model satisfactorily fitted to experimental data. Insignificant lack of fit is most wanted as significant lack of fit indicates there might be contribution in the regressor-response relationship that is not accounted for by the model (Lee *et al.*, 2011).

Table 4.4: ANOVA for nanocellulose yield

Source	Sum of squares	[a]DF	Mean square	F-value	p-value	
Model	6458.52	9	717.61	177.24	< 0.0001	significant
A	114.51	1	114.51	28.28	0.0003	
B	130.9	1	130.9	32.33	0.0002	
C	1273.51	1	1273.51	314.54	< 0.0001	
A2	601.32	1	601.32	148.52	< 0.0001	
B2	453.19	1	453.19	111.93	< 0.0001	
C2	187.28	1	187.28	46.25	< 0.0001	
AB	104.76	1	104.76	25.87	0.0005	
AC	2.94	1	2.94	0.73	0.4141	
BC	67.34	1	67.34	16.63	0.0022	
Residual	40.49	10	4.05			
Lack of Fit	29.78	5	5.96	2.78	0.1429	not significant
Pure Error	10.7	5	2.14			
[b]SD	2.01217785		R-squared	0.99377003		
Mean	63.4185		[c]Ad R-squared	0.98816307		
C.V	3.17285626		[d]Pr R-squared	0.96149893		
			[e]Adeq R-squared	45.2078178		

[a] Degree of freedom
[b] Standard deviation
[c] Adjusted R-Squared
[d] Predicted R-Squared
[e] Adequate R-squared

The predicted values versus actual values for nanocellulose yield with adjusted-R^2 value of 0.99 indicate the model with 100% variability (Figure 4.8). Furthermore, the R^2 value closed to unities, which mean that the data fit, will with the model and given a convincingly good estimate of response for the system in the range studied. In addition, investigation on residuals to validate the adequacy of the model was discussed. Residual is the difference between the observed response and predicted response.

This analysis was examined using normal probability plot of the residuals (Figure 4.9a) and the plot of the residuals versus predicted response (Figure 4.9b). The normal

probability plot of the residuals indicates that the errors are distributed normally in a very straight line.

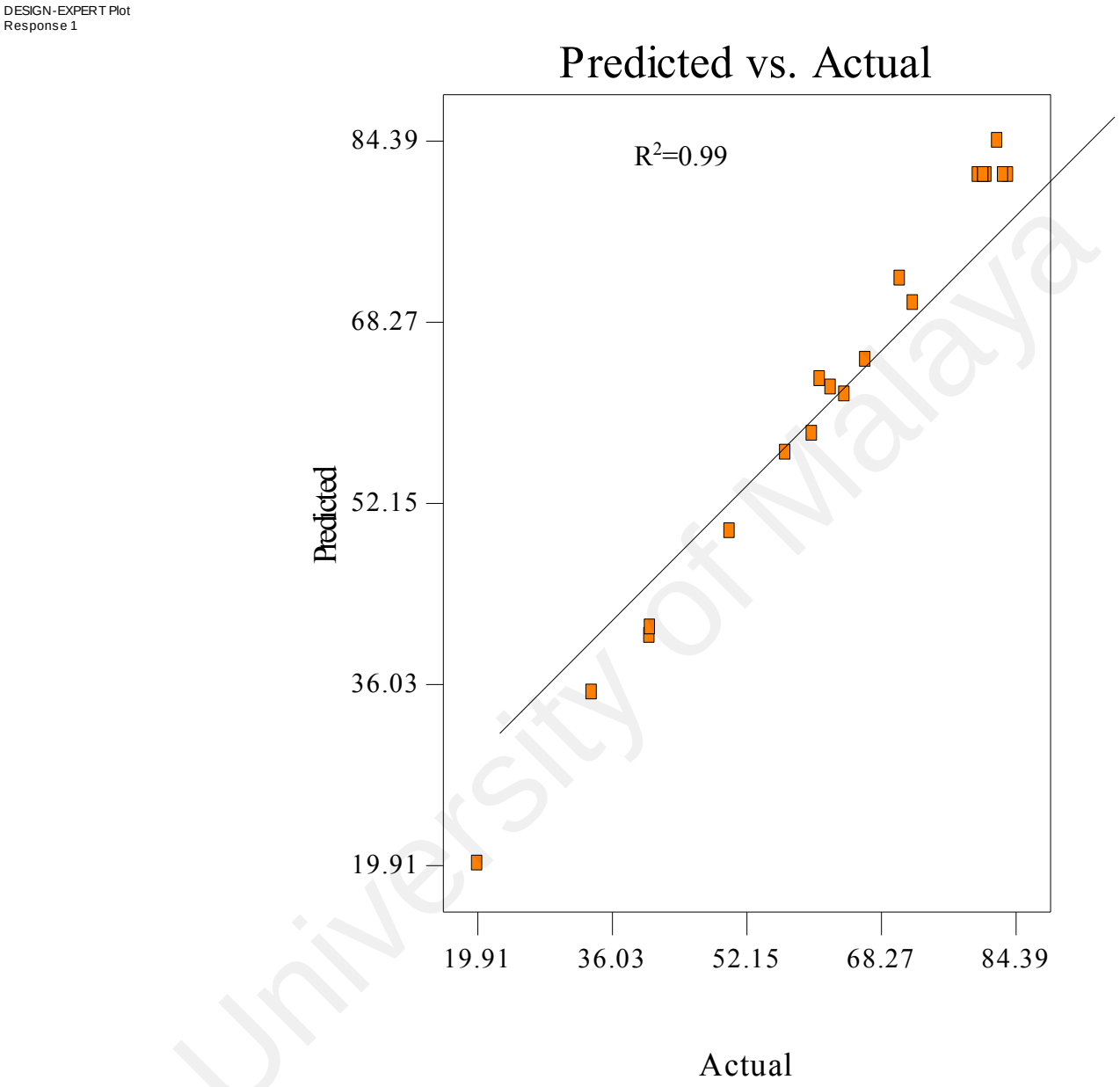

Figure 4.8: Predicted versus actual nanocellulose yield

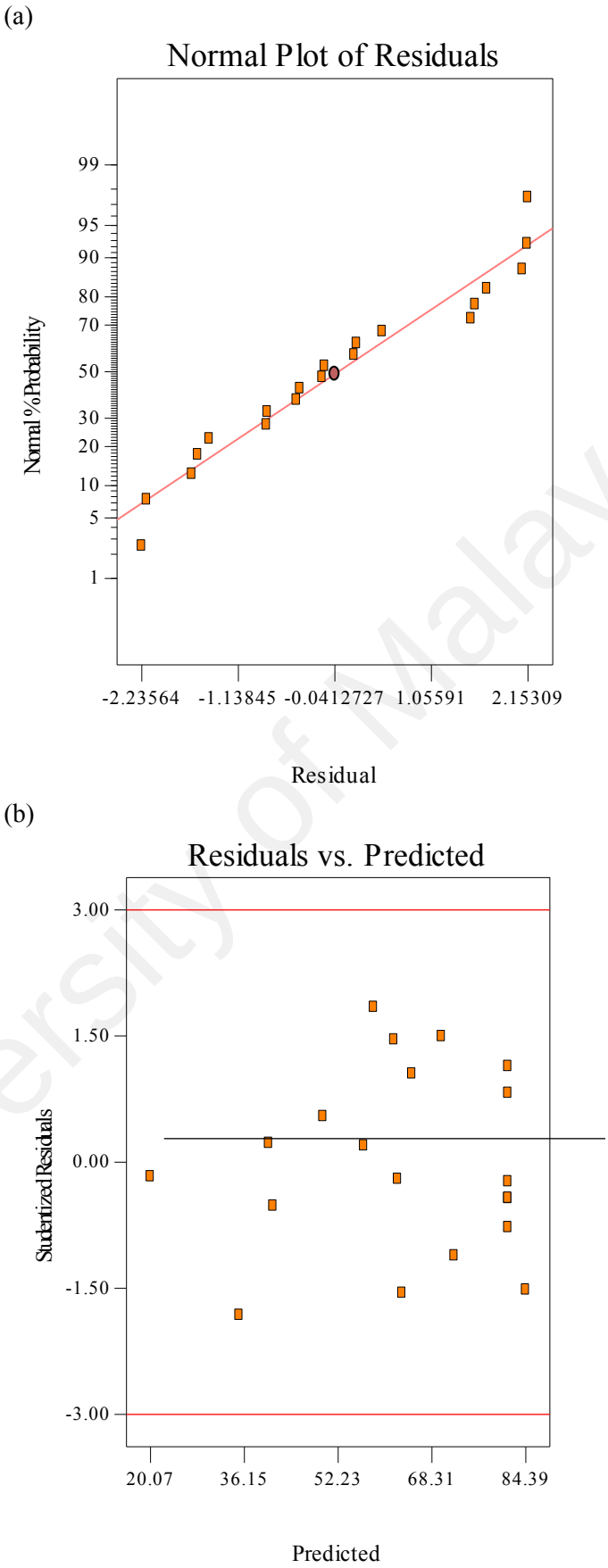

Figure 4.9: Normal probability plots of the residuals (a) and plot of the residuals versus the predicted response (b)

Figure 4.10 (a) and (b) showed the 3D RSM plot and contour plot for the interaction effect between acidity of catalyst (A) and reaction time (B) toward nanocellulose yield. The reaction temperature (°C) was fixed at 45°C. The 3D response surface revealed that increment of reaction time from 20 to 60 min was lead to increase of nanocellulose yield (~60%-~80%), further prolong the reaction time to 100 min caused decreased of nanocellulose yield (~50%). Reaction time plays an important role in the process of cellulose depolymerization. In the initial step, long period required to soften and solubilized the amorphous region that present in cellulose fiber (Lu *et al.*, 2014). When the reaction period reached certain level, the hydrolysis reaction gained enough of energy to cleave the glycosidic bond of cellulose chain (Abd Hamid *et al.*, 2014; H. V. Lee, S. B. Hamid*, et al.*, 2014). Furthermore, effects of acidity of catalyst (pH) at different reaction duration towards nanocellulose yield (%) were investigated. The results shown that increment of pH2 to pH 3(decrease of acidity) was lead to increase of nanocellulose yield (~55%-~80%), further decrease of acidity to pH 4 caused a decreased of nanocellulose yield (~55%). Acidity of pH plays an important role in the hydrolysis process for cellulose depolymerization. Utilizing lower concentration of Ni ions (pH 4-lowest acidity), the hydrolysis of cellulose was not occurred effectively, which gives lower yield of nanocellulose product. However, employing higher acidity of catalyst (pH2-pH3) lead to Ni^{2+} ions diffused into surface of cellulose fibres and attacks the glyosidic bonding of cellulose chains to produce cellulose in nanodimention. The interaction between reaction time (mins) and acidity of catalyst (pH) have been found to gives positives effect in this study. However, prolong reaction of time (B) occurred with high acidity of catalyst (A),cellulose was broken into its component sugar molecule by hydrolysis reaction (Lu *et al.*, 2014). This process was in agreement with Kumar's study which nanocellulose yield increase with the use of different catalyst of increasing acidity

due to increase in the acid centers which is mainly responsible for the hydrolysis process (Kumar & Singh, 2014).

(a)

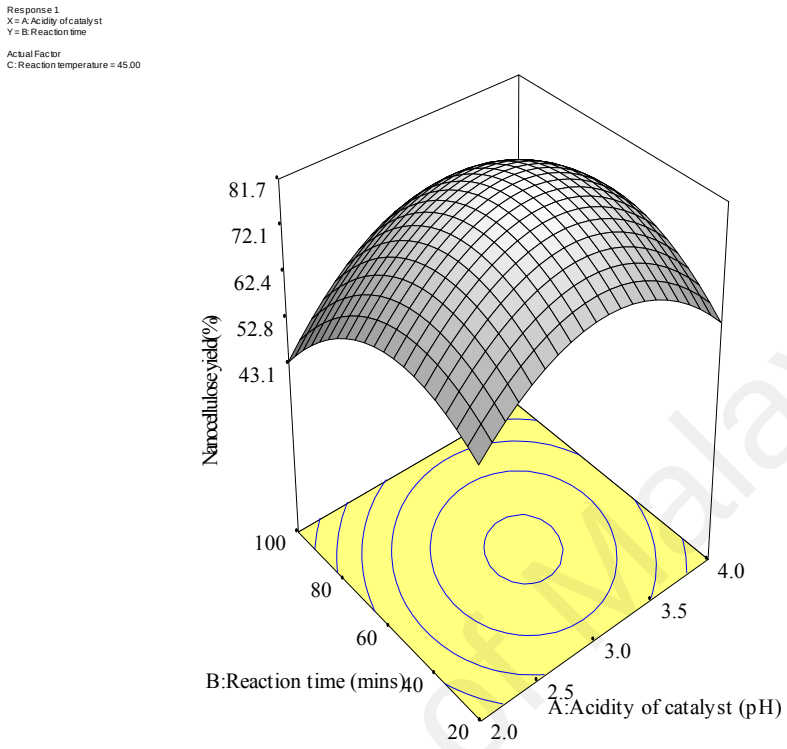

(b)

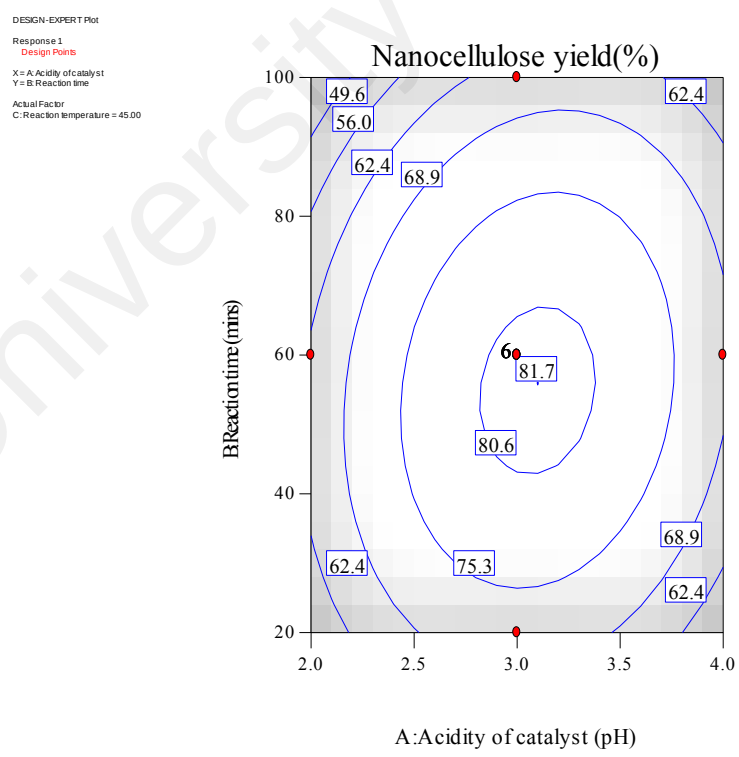

Figure 4.10: Effect of acidity of catalyst (A) and reaction time (B) toward nanocellulose yield, reaction temperature =45°C (a)3D response surface plot and (b) 2D Contour plot

Figure 4.11 (a) showed the 3D plot and (b) contour plot for the interaction effect between reaction temperature (C) and acidity of catalyst (A) toward nanocellulose yield. The reaction time was fixed at 60 mins. At low level of acidity of catalyst (pH2), the increase of reaction temperature from room temperature to 55 °C showed a positive effect towards the nanocellulose yield (~40%-~60%). It was observed that the nanocellulose yield showed better effect at acidity of catalyst (pH4) at high level of temperature, which rendered ~50% to 70% nanocellulose yield . Among the interaction terms that influenced the nanocellulose yield response, the interaction effect of acidity of catalyst-reaction temperature gave the most significant influence toward the yield of nanocellulose. This interaction effect showed unfavorable influence on nanocellulose yield (Equation 4.2) which suggests that the interaction between reaction temperature–acidity of catalyst reduced the nanocellulose yield. This may due to the high acidity of catalyst with high reaction temperature that favors byproducts formation (glucose) as over-hydrolysis occurred, thus reduced the nanocellulose yield (Abd Hamid *et al.*, 2014). Subsequently, it is suggested that the reaction was to perform at optimal condition whereby the nanocellulose yield will achieve the best value (~80%) at pH3,45°C and for 60min

(a)

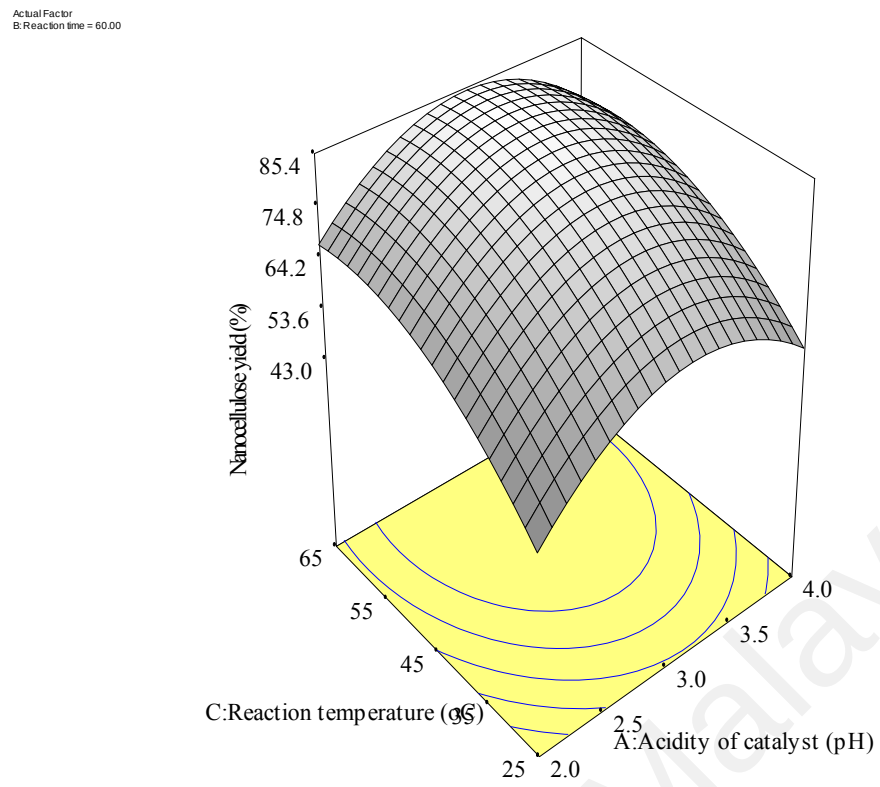

(b)

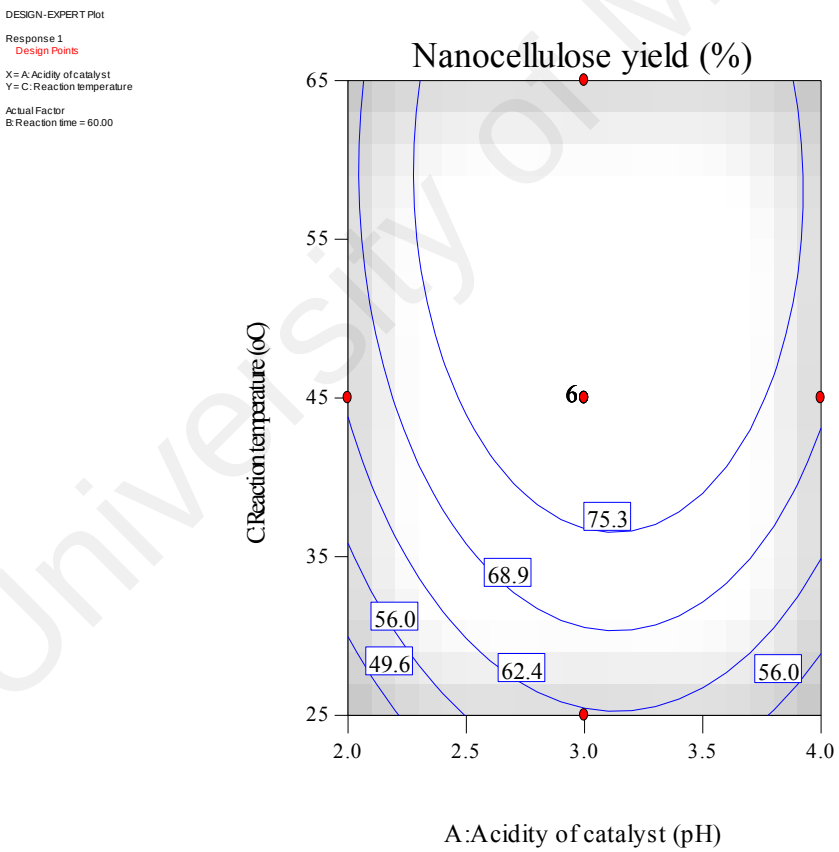

Figure 4.11: **:** Effect of acidity of catalyst (A) and reaction temperature (C) toward nanocellulose yield, reaction time=60mis (a)3D response surface plot and (b) Contour plot

Figure 4.12 a and b showed the 3D plot and contour plot for the relationship between reaction time (B) and reaction temperature (C) toward nanocellulose yield. The acidity of catalyst was fixed at pH3. The 3D response surface revealed that increment of reaction temperature from low level (25°C) to high level (65°C) leads to the increase of nanocellulose content (62-84 %) with reduced reaction time (20-60 mins). On the contrary, the increase of reaction time does not improve the nanocellulose yield at low reaction temperature level. The decreased of nanocellulose yield at longer reaction time was due to the over-reaction, which convert nanocellulose product into glucose rather than nanocellulose intermediate (Lu *et al.*, 2014). Results showe that nanocellulose yield remained <65% with the reaction time increased from 20 to 40 min at the temperature of 25-35 °C. However, the nanocellulose content was raised apparently to >70% at intermediate level (45 °C) to high level at 65 °C. The nanocellulose content reached plateau point when both of the reaction temperature and reaction time rise to optimum level. This might indicate that the hydrolysis reaction process reached ideal condition (55°C, 60mins), further proceeds the reaction that may lead to decomposition of nanocellulose (glucose formation) thus reduced the nanocellulose content. Reaction time and temperature plays an important role in the degradation of cellulose. In a short period of time and t, the hydrolysis of cellulose could not happen effectively(Lu *et al.*, 2014).

(a)

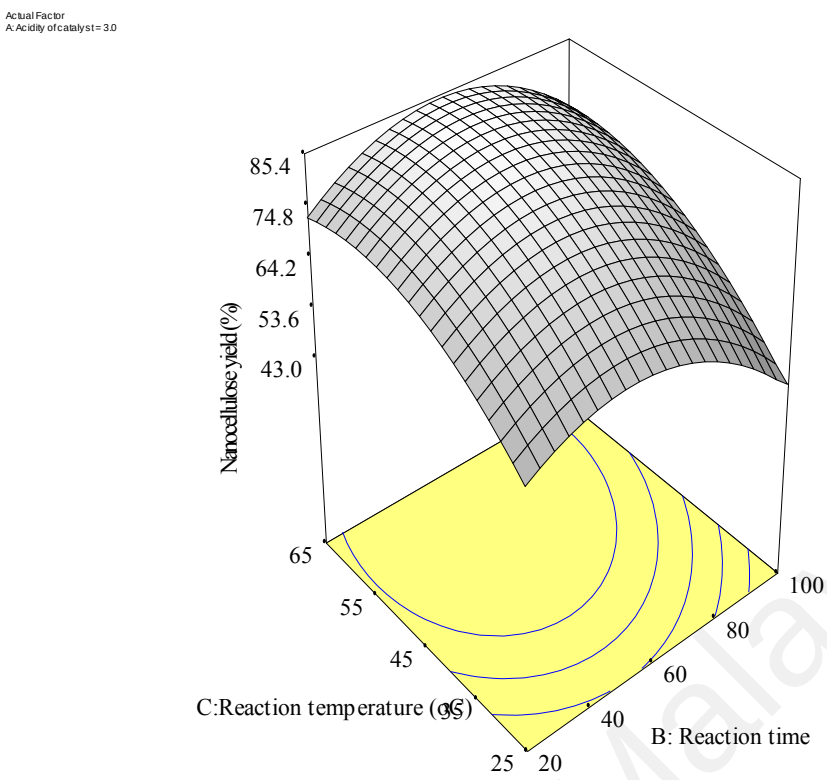

(b)

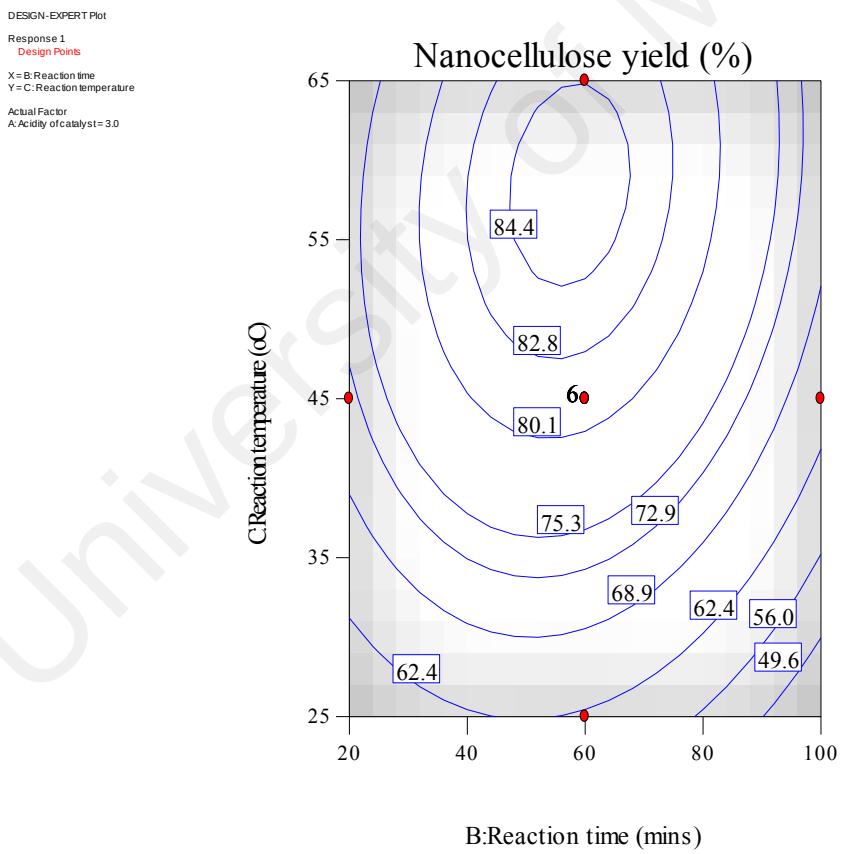

Figure 4.12: Effect of reaction temperature (C) and reaction time (B) toward nanocellulose yield, acidity of catalyst=3 (a) 3D response surface plot and (b) Contour plot

There are several previous studies successfully extracted nanocellulose by using transition metal salt (Fe and Cr based metal salt) hydrolysis with the yield between >50%. Abd Hamid et. al (2016) successfully hydrolyzed palm tree cellulose (PTC) and alpha cellulose (AP) to nanocellulose by using HCl-$FeCl_3$ assisted with ultrasonication process. From XRD analysis results, the isolated CNC from PTC and AC showed higher CrI of 73.51% and 89.03%, with a diameter of 20-70nm and 15-50nm respectively. The yield of CNC from PTC and AC is 80.88% and 81.20% respectively(Abd Hamid *et al.*, 2016). Further investigation were made by Chen et. al (2016), which they successfully produced nanocellulose via chromium nitrate ($Cr(NO_3)_3$) assisted H_2SO_4 hydrolysis and was optimized using RSM. Based from the optimum condition of producing nanocellulose (82.2°C,0.22M $Cr(NO_3)_3$and 0.80M H_2SO_4, 1 hr), the CrI and yield of nanocellulose is 85.35% and 82.42% respectively with a average diameter of 18.4±7.3nm (Chen *et al*., 2016). The above perusal of literature reflects that several studies have been conducted for the preparation of nanocellulose using transition metal based gives higher yield as compared to strong acid hydrolysis. As such, Ni salt hydrolysis process shows that the yield of nanocellulose is ~40- 80%.

4.9 Optimization of nanocellulose yield

In this project, the optimization of the nanocellulose hydrolysis process was done to search for optimal operating conditions in which the highest nanocellulose yield is reached. The variables (acidity of catalyst, reaction temperature and reaction time) were set in a range between low and high levels which coded −1 and +1 to obtained ultimate response for the nanocellulose yield (Table 4.5a). The overall average optimized conditions for nanocellulose yield were obtained as follows: acidity of catalyst (pH3), reaction time (60 mins), and reaction temperature (45 °C) with nanocellulose yield of 81.37% (Table 4.5b). The predicted nanocellulose yield was 81.40%. This means that the experimental value achieved was reasonably near to the predicted value calculated from

the model (0.69% of standard error mean). It can be concluded that the generated model is near to predictability and close to precision for the nanocellulose yield in the experimental conditions used.

Table 4.5: (a) Optimization criteria for ideal nanocellulose yield and (b) Results of model validation at the optimum level

[(a)]**Name**	**Goal**	**Lower Limit**	**Upper Limit**	**Lower Weight**	**Upper Weight**	**Importance**
Acidity of catalyst	Is in range	2	4	1 (-1)	1(+1)	3
Reaction time	Is in range	20	100	1 (-1)	1(+1)	3
Reaction temperature	Is in range	25	65	1 (-1)	1(+1)	3

[(b)]**Acidity of catalyst (pH)**	**Reaction time (mins)**	**Reaction temperature (^{0}C)**	**Predicted nanocellulose yield (%)**	**Experimental nanocellulose yield (%)**	**Standard error mean**
3	60	45	81.40	81.37	0.69

CHAPTER 5: CONCLUSION

5.1 Conclusion

This project was devoted to study the catalytic synthesis of nanocellulose from oil palm lignocellulosic biomass. Nanocellulose were successfully extracted from EFB fibres by conventional chemical pretreatment and mild acid hydrolysis process from inorganic acid (H_2SO_4) and inorganic salt (Ni-salt). The physicochemical properties of EFB-drived nanocelluloses were in terms of product's crystallinity index, chemical characteristic, surface chemical functional group, surface morphology and structure, particle size distribution and thermal stability profile were determined by using analytical instruments such as TGA and DTG, FT-IR, FESEM ,HRTEM, AFM, PSD and XRD.

XRD analysis was performed to investigate the crystallinity index and crystallite sizes of cellulose samples. The crystallinity (Crl) of SA-NC (73.17%) and Ni-NC(80.75%) were higher as compared to raw EFB fibres (46.04%) and EFB-derived cellulose (68.45%). This shows that the amorphous region of cellulose was successfully attacked by acid and resulted in higher CrI of SA-NC and Ni-NC than EFB fibres and EFB derived cellulose. The results also indicated those biomasses pretreatment are successfully removes non-cellulosic content (lignin and hemicellulose) in EFB fibres and thus, the CrI of EFB-derived cellulose was higher than EFB. Furthermore, the changes of chemical composition for all samples (EFB, EFB-derived cellulose, SA-NC and Ni-NC) were evaluated using FTIR analysis. FTIR results revealed that non-cellulosic contents were successfully removed from EFB fibres via alkali and bleaching treatments. Based from the XRD and FTIR analysis, there was an absence of Ni-metal and NO_3^- ions after the washing and dialysis processes of nanocellulose, which rendered a higher thermal stability of nanocellulose product as compared to EFB-derived cellulose. Thermogravimetric and derivatives thermal analysis shows that the order of starting decomposition temperature decreased in the trend of Ni-NC > EFB fibres > EFB-derived

cellulose > SA-NC, which was 332.74 °C, 232.31 °C, 215.46 °C and 179.93 °C, respectively. The Ni-NC exhibits higher thermal decomposition as compared to SA-NC, which indicated the content of damage in the crystalline regions of Ni-NC structure is lesser as compared to SA-NC structure.

The morphological changes of micro- and nano-structured of all samples were performed by using FESEM analysis. FESEM images clearly display that outer layer (waxes, pectins and fats) of EFB fibres has been removed after pretreatment process. The pretreatment methods eventually enhance the hydrolysis process (SA-NC and Ni-NC) to produce nano-scale dimension. Furthermore, HR-TEM and AFM analysis indicated that acid hydrolysis was capable to depolymerize cellulose micro-chain into nano-crystallites, in which SA-NC and Ni-NC rendered average nano-dimensions in fibres length (< 700 nm) and fibres width dimension (< 50 nm). In addition, PSD results clearly showed the particle sizes had been reduced from EFB-derived cellulose to nanocellulose products (SA-NC and Ni-NC). The particle size distribution of EFB fibres in micro-sizes were reduced to nanocellulose sizes from <5500 nm to <90.00 nm. The presence study concluded that Ni-salts is an efficient and selective catalyst for the hydrolysis of cellulose with high simplicity in operation as compared to inorganic acid (H_2SO_4).

In order to achieve high yield of nanocellulose, optimization study for Ni-salt catalyzed hydrolysis of EFB-derived cellulose reaction was investigated via response surface methodology (RSM). The hydrolysis parameters were selected for the optimization study were reaction temperature (°C), reaction time (min) and acidity of catalyst (pH). The reaction model suggested that all the hydrolysis parameters playing an significant role to influence the nanocellulose yield. Furthermore, based on the reaction model generated from RSM-CCD, the predicted nanocellulose yield was 81.40 % under reaction condition of 60 min of reaction time, 45 °C for reaction temperature and acidity

of catalyst at pH3. Meanwhile, the experimental value (81.37 %) achieved was reasonably near to the predicted value generated from the model (0.69% of standard error mean). It can be concluded that the generated model is near to predictability and close to precision for the nanocellulose yield in the experimental conditions used.

In summary from the results above, it shows that nano scale of cellulose (Ni-NC and SA-NC) were successfully produced, characterize as well as optimized from oil palm biomass (EFB) via Ni-Salt and H_2SO_4 catalyzed treatment.

5.2 Recommendation

The future production of bio-based chemicals and bio-based materials from lignocellulosic biomass will grow continuously, whereby shifting society's dependence from petroleum-based to renewable biomass-based resources. However, the hardest challenge of this transformation is the separation technology of chemical components from complexity of biomass with high recovery of each individual valuable component for production of advanced chemicals in the application of food, energy, health and environment. The lignocellulosic biomass is composed mainly of cellulose, hemicellulose and lignin. The presence of highly cellulose content in biomass is potentially converted to nanocellulose, which is a promising bio-polymer that useful for various industrial applications, such as personal cares, chemicals, foods, pharmaceuticals and bio-composites.

In order to secure the continuous supply of nanocellulose materials for various applications, an economy- and environmental-friendly synthesis process is required to provide long term manufacturing process without processing problems. In this study, mild acid hydrolysis of cellulose using inorganic-salt (Ni-salt) was developed for the preparation of nanocellulose. The finding showed potential process in preparing high yield of nanocellulose products under milder reaction condition as compared to inorganic

acid process, with less equipment corrosion issues and generation of acid water during post-treatment process. Further studies are recommended to standardize the range of features and properties of nanocellulose product achieved from Ni-salt hydrolyzed reaction. It is important to produce a contants and desired range of nanocellulose's properties (crystallinity index, particles' structure, surface morphology, particle sizes, and aspect ratio) for certain application. Furthermore, reaction kinetic study and large scale study of nanocellulose production by using Ni-catalyzed reaction is recommended in order to confirmed the suitability of this new developed technology for the large scale manufacturing process.

REFERENCES

Abd Hamid, S. B., Chowdhury, Z. Z., & Karim, M. Z. (2014). Catalytic Extraction of Microcrystalline Cellulose (MCC) from Elaeis guineensis using Central Composite Design (CCD). *BioResources*, *9*(4), 7403-7426. doi:10.15376/biores.9.4.7403-7426

Abd Hamid, S. B., Chowdhury, Z. Z., Karim, M. Z., & Ali, M. E. (2016). Catalytic Isolation and Physicochemical Properties of Nanocrystalline Cellulose (NCC) using HCl-FeCl3 System Combined with Ultrasonication. *BioResources, 11*(2), 3840-3855. doi:10.15376/biores.11.2.3840-3855

Abe, K., & Yano, H. (2009). Comparison of the characteristics of cellulose microfibril aggregates of wood, rice straw and potato tuber. *Cellulose*, 16(6), 1017-1023. doi: 10.1007/s10570-009-9334-9

Agbor, V. B., Cicek, N., Sparling, R., Berlin, A., & Levin, D. B. (2011). Biomass pretreatment: Fundamentals toward application. *Biotechnology Advances*, 29(6), 675-685. doi: http://dx.doi.org/10.1016/j.biotechadv.2011.05.005

Alemdar, A., & Sain, M. (2008). Isolation and characterization of nanofibers from agricultural residues – Wheat straw and soy hulls. *Bioresource Technology*, 99(6), 1664-1671. doi: http://dx.doi.org/10.1016/j.biortech.2007.04.029

Ashby, M. F., & Jones, D. R. H. (2013). General Introduction. In M. F. A. R. H. Jones (Eds.), *Engineering Materials* (pp. xvii-xx). Boston: Butterworth-Heinemann.

Azizi Samir, M. A. S., Alloin, F., & Dufresne, A. (2005). Review of Recent Research into Cellulosic Whiskers, Their Properties and Their Application in Nanocomposite Field. *Biomacromolecules*, 6(2), 612-626. doi: 10.1021/bm0493685

Beck-Candanedo, S., Roman, M., & Gray, D. G. (2005). Effect of Reaction Conditions on the Properties and Behavior of Wood Cellulose Nanocrystal Suspensions. *Biomacromolecules*, 6(2), 1048-1054. doi: 10.1021/bm049300p

Bhatnagar, A., & Sain, M. (2005). Processing of Cellulose Nanofiber-reinforced Composites. *Journal of Reinforced Plastics and Composites*, 24(12), 1259-1268. doi: 10.1177/0731684405049864

Bhatt, N., Gupta, P. K., & Naithani, S. (2008). Preparation of cellulose sulfate from α-cellulose isolated from Lantana camara by the direct esterification method. *Journal of Applied Polymer Science*, 108(5), 2895-2901. doi: 10.1002/app.27773

Bono, A., Sarbatly, R., Krishnaiah, D., Muei, C., Yan, F. Y., & Ying, P. (2009). Synthesis and characterization of carboxymethyl cellulose from palm kernel cake. *Advances in Natural and Applied Sciences*, 3(1), 5-11.

Bozell, J. J., O'Lenick, C. J., & Warwick, S. (2011). Biomass Fractionation for the Biorefinery: Heteronuclear Multiple Quantum Coherence–Nuclear Magnetic Resonance Investigation of Lignin Isolated from Solvent Fractionation of Switchgrass. *Journal of Agricultural and Food Chemistry*, 59(17), 9232-9242. doi: 10.1021/jf201850b

Brinchi, L., Cotana, F., Fortunati, E., & Kenny, J. (2013). Production of nanocrystalline cellulose from lignocellulosic biomass: technology and applications. *Carbohydrate Polymer*, 94(1), 154-169.

Chen, Y., Liu, C., Chang, P. R., Cao, X., & Anderson, D. P. (2009). Bionanocomposites based on pea starch and cellulose nanowhiskers hydrolyzed from pea hull fibre: Effect of hydrolysis time. *Carbohydrate Polymer*, 76(4), 607-615. doi: http://dx.doi.org/10.1016/j.carbpol.2008.11.030

Chen, Y. W., Lee, H. V., & Abd Hamid, S. B. (2016). A Response Surface Methodology Study: Effects of Trivalent Cr3+ Metal Ion-Catalyzed Hydrolysis on Nanocellulose Crystallinity and Yield. *BioResourse*, *11*(2), 4645-4662. doi:10.15376/biores.11.2.4645-4662

Correia, J. A. d. C., Júnior, J. E. M., Gonçalves, L. R. B., & Rocha, M. V. P. (2013). Alkaline hydrogen peroxide pretreatment of cashew apple bagasse for ethanol production: Study of parameters. *Bioresource Technology*, 139, 249-256. doi: http://dx.doi.org/10.1016/j.biortech.2013.03.153

Cunha, I., Sawaya, A. C., Caetano, F. M., Shimizu, M. T., Marcucci, M. C., Drezza, F. T., . . . Carvalho, P. d. O. (2004). Factors that influence the yield and composition of Brazilian propolis extracts. *Journal of the Brazilian Chemical Society*, 15(6), 964-970.

Cybulska, I., Brudecki, G., Rosentrater, K., Julson, J. L., & Lei, H. (2012). Comparative study of organosolv lignin extracted from prairie cordgrass, switchgrass and corn stover. *Bioresource Technology*, 118, 30-36. doi: 10.1016/j.biortech.2012.05.073

Das, K., Ray, D., Bandyopadhyay, N. R., & Sengupta, S. (2010). Study of the Properties of Microcrystalline Cellulose Particles from Different Renewable Resources by XRD, FTIR, Nanoindentation, TGA and SEM. *Journal of Polymers and the Environment*, 18(3), 355-363. doi: 10.1007/s10924-010-0167-2

de Wild, P., Van der Laan, R., Kloekhorst, A., & Heeres, E. (2009). Lignin valorisation for chemicals and (transportation) fuels via (catalytic) pyrolysis and hydrodeoxygenation. *Environmental Progress & Sustainable Energy*, 28(3), 461-469. doi: 10.1002/ep.10391

Dhepe, P. L., & Fukuoka, A. (2008). Cellulose conversion under heterogeneous catalysis. *ChemSusChem*, 1(12), 969-975. doi: 10.1002/cssc.200800129

Doherty, W. O. S., Mousavioun, P., & Fellows, C. M. (2011). Value-adding to cellulosic ethanol: Lignin polymers. *Industrial Crops and Products*, 33(2), 259-276. doi: http://dx.doi.org/10.1016/j.indcrop.2010.10.022

Dufresne, A. (2013). *Nanocellulose: from nature to high performance tailored materials*. Berlin, Germany: De Gruyter.

Dumitriu, S. (2004). *Polysaccharides: structural diversity and functional versatility(2nd ed.)*. Canada:Taylor & Francis.

Eichhorn, S. J., Dufresne, A., Aranguren, M., Marcovich, N. E., Capadona, J. R., Rowan, S. J., Peijs, T. (2010). Review: current international research into cellulose nanofibres and nanocomposites. *Journal of Materials Science*, 45(1), 1-33. doi: 10.1007/s10853-009-3874-0

Eichhorn, S. J., Young, R. J., & Davies, G. R. (2005). Modeling Crystal and Molecular Deformation in Regenerated Cellulose Fibers. *Biomacromolecules*, 6(1), 507-513. doi: 10.1021/bm049409x

Esa, F., Tasirin, S. M., & Rahman, N. A. (2014). Overview of Bacterial Cellulose Production and Application. A*griculture and Agricultural Science Procedia*, 2, 113-119. doi: http://dx.doi.org/10.1016/j.aaspro.2014.11.017

Fahma, F., Iwamoto, S., Hori, N., Iwata, T., & Takemura, A. (2010). Isolation, preparation, and characterization of nanofibers from oil palm empty-fruit-bunch (OPEFB). *Cellulose*, 17(5), 977-985. doi: 10.1007/s10570-010-9436-4

French, A. (2014). Idealized powder diffraction patterns for cellulose polymorphs. *Cellulose,* 21(2), 885-896. doi: 10.1007/s10570-013-0030-4

Fu, D., & Mazza, G. (2011). Aqueous ionic liquid pretreatment of straw. *Bioresource Technology*, 102(13), 7008-7011. doi: 10.1016/j.biortech.2011.04.049

Gibson, L. J. (2012). The hierarchical structure and mechanics of plant materials. *J R Soc Interface*, 9(76), 2749-2766. doi: 10.1098/rsif.2012.0341

Grube, M., Lin, J. G., Lee, P. H., & Kokorevicha, S. (2006). Evaluation of sewage sludge-based compost by FT-IR spectroscopy. *Geoderma*, 130(3–4), 324-333. doi:10.1016/j.geoderma.2005.02.005

Harmsen, P., Huijgen, W., Bermudez, L., & Bakker, R. (2010). *Literature review of physical and chemical pretreatment processes for lignocellulosic biomass*. Wageningen, Netherland: Food & Biobased Research.

Henriksson, M., Berglund, L. A., Isaksson, P., Lindström, T., & Nishino, T. (2008). *Biomacromolecules*, 9, 1579.

Himmel, M. E., Ding, S.-Y., Johnson, D. K., Adney, W. S., Nimlos, M. R., Brady, J. W., & Foust, T. D. (2007). Biomass Recalcitrance: Engineering Plants and Enzymes for Biofuels Production. Science, 315(5813), 804-807. doi: 10.1126/science.1137016

Instruments, H.A. (2012). Guidebook to Particle Size Analysis.*Understanding and interpreting particle size distribution*. Retrived from http://www.horiba. com/fileadmin/uploads/Scientific/Documents/PSA. PS A_Guidebook

Iwamoto, S., Nakagaito, A. N., & Yano, H. (2007). Isolation, preparation, and characterization of nanofibers from oil palm empty-fruit-bunch (OPEFB). *Appl. Phys*. A, 89, 461.

Jahan, M. S., Saeed, A., He, Z., & Ni, Y. (2011). Jute as raw material for the preparation of microcrystalline cellulose. *Cellulose*, 18(2), 451-459. doi: 10.1007/s10570-010-9481-z

Joaquim, A. P., Tonoli, G. H. D., Santos, S. F. D., & Savastano Junior, H. (2009). Sisal organosolv pulp as reinforcement for cement based composites. *Materials Research,* 12, 305-314.

Johar, N., Ahmad, I., & Dufresne, A. (2012). Extraction, preparation and characterization of cellulose fibres and nanocrystals from rice husk. *Industrial Crops and Products,* 37(1), 93-99. doi: http://dx.doi.org/10.1016/j.indcrop.2011.12.016

Jonoobi, M., Khazaeian, A., Tahir, P. M., Azry, S. S., & Oksman, K. (2011). Characteristics of cellulose nanofibers isolated from rubberwood and empty fruit bunches of oil palm using chemo-mechanical process. *Cellulose*, 18(4), 1085-1095.

Kalia, S., Dufresne, A., Cherian, B. M., Kaith, B., Avérous, L., Njuguna, J., & Nassiopoulos, E. (2011). Cellulose-based bio-and nanocomposites: a review. *International Journal of Polymer Science*, 2011(1),30-35.

Kamireddy, S. R., Li, J., Tucker, M., Degenstein, J., & Ji, Y. (2013). Effects and mechanism of metal chloride salts on pretreatment and enzymatic digestibility of corn stover. *Industrial & Engineering Chemistry Research*, 52(5), 1775-1782.

Karim, M. Z., Chowdhury, Z. Z., Hamid, S. B. A., & Ali, M. E. (2014). Statistical Optimization for Acid Hydrolysis of Microcrystalline Cellulose and Its Physiochemical Characterization by Using Metal Ion Catalyst. *Materials*, 7(10), 6982-6999.

Khalil, H. P. S. A., Jawaid, M., Hassan, A., Paridah, M. T., & Zaidon, A. (2012). *Oil Palm Biomass Fibres and Recent Advancement in Oil Palm Biomass Fibres Based Hybrid Biocomposites* (Hu, N.Ed.). Croatia: InTech

Kumar, A., Negi, Y. S., Choudhary, V., & Bhardwaj, N. K. (2014). Characterization of Cellulose Nanocrystals Produced by Acid-Hydrolysis from Sugarcane Bagasse as Agro-Waste. *Journal of Materials Physics and Chemistry*, 2(1), 1-8.

Kumar, P., Barrett, D. M., Delwiche, M. J., & Stroeve, P. (2009). Methods for pretreatment of lignocellulosic biomass for efficient hydrolysis and biofuel production. *Industrial & Engineering Chemistry Research*, 48(8), 3713-3729.

Kumar, S., & Singh, R. K. (2014). Optimization of process parameters by response surface methodology (RSM) for catalytic pyrolysis of waste high-density polyethylene to liquid fuel. *Journal of Environmental Chemical Engineering,* 2(1), 115-122. doi: http://dx.doi.org/10.1016/j.jece.2013.12.001

Lai, L.-W., & Idris, A. (2013b). Disruption of oil palm trunks and fronds by microwave-alkali pretreatment. *BioResources*, 8(2), 2792-2804.

Lange, J.-P. (2007). Lignocellulose conversion: an introduction to chemistry, process and economics. *Biofuels, Bioproducts and Biorefining*, 1(1), 39-48. doi: 10.1002/bbb.7

Lee, H. V., Hamid, S. B. A., & Zain, S. K. (2014). Conversion of Lignocellulosic Biomass to Nanocellulose: Structure and Chemical Process. *The* Scientific World Journal, 2014, 20. doi: 10.1155/2014/631013

Lee, H. V., Yunus, R., Juan, J. C., & Taufiq-Yap, Y. H. (2011). Process optimization design for jatropha-based biodiesel production using response surface methodology. *Fuel Processing Technology*, 92(12), 2420-2428. doi: http://dx.doi.org/10.1016/j.fuproc.2011.08.018

Li, J., Zhang, X., Zhang, M., Xiu, H., & He, H. (2015). Ultrasonic enhance acid hydrolysis selectivity of cellulose with HCl-FeCl3 as catalyst. *Carbohydr Polym*, 117, 917-922. doi: 10.1016/j.carbpol.2014.10.028

Lindman, B., Karlström, G., & Stigsson, L. (2010). On the mechanism of dissolution of cellulose. *Journal of Molecular Liquids*, 156(1), 76-81. doi: http://dx.doi.org/10.1016/j.molliq.2010.04.016

Liu, C., & Wyman, C. E. (2006). The enhancement of xylose monomer and xylotriose degradation by inorganic salts in aqueous solutions at 180 C. *Carbohydrate research,* 341(15), 2550-2556.

Liu, L., Sun, J., Cai, C., Wang, S., Pei, H., & Zhang, J. (2009). Corn stover pretreatment by inorganic salts and its effects on hemicellulose and cellulose degradation. *Bioresource Technology*, 100(23), 5865-5871.

López-Linares, J. C., Romero, I., Moya, M., Cara, C., Ruiz, E., & Castro, E. (2013). Pretreatment of olive tree biomass with FeCl 3 prior enzymatic hydrolysis. *Bioresource Technology*, 128, 180-187.

Lu, Q., Tang, L., Lin, F., Wang, S., Chen, Y., Chen, X., & Huang, B. (2014). Preparation and characterization of cellulose nanocrystals via ultrasonication-assisted FeCl3-catalyzed hydrolysis. *Cellulose*, 21(5), 3497-3506. doi: 10.1007/s10570-014-0376-2

Man, Z., Muhammad, N., Sarwono, A., Bustam, M. A., Kumar, M. V., & Rafiq, S. (2011). Preparation of cellulose nanocrystals using an ionic liquid. *Journal of Polymers and the Environment*, 19(3), 726-731.

McIntosh, S., & Vancov, T. (2010). Enhanced enzyme saccharification of Sorghum bicolor straw using dilute alkali pretreatment. *Bioresource Technology*, 101(17), 6718-6727. doi: http://dx.doi.org/10.1016/j.biortech.2010.03.116

Mikkonen, K. S., & Tenkanen, M. (2012). Sustainable food-packaging materials based on future biorefinery products: Xylans and mannans. *Trends in Food Science & Technology*, 28(2), 90-102. doi: http://dx.doi.org/10.1016/j.tifs.2012.06.012

Mohamad Haafiz, M. K., Eichhorn, S. J., Hassan, A., & Jawaid, M. (2013). Isolation and characterization of microcrystalline cellulose from oil palm biomass residue. *Carbohydr Polym*, 93(2), 628-634. doi: 10.1016/j.carbpol.2013.01.035

Morais, J. P. S., Rosa, M. d. F., Nascimento, L. D., do Nascimento, D. M., & Cassales, A. R. (2013). Extraction and characterization of nanocellulose structures from raw cotton linter. *Carbohydr Poly*m, 91(1), 229-235.

Nazir, M. S., Wahjoedi, B. A., Yussof, A. W., & Abdullah, M. A. (2013). Eco-Friendly Extraction and Characterization of Cellulose from Oil Palm Empty Fruit Bunches *BioResourse*, *8*(2), 2161-2172. doi:10.15376/biores.8.2.2161-2172

Ng, W. P. Q., Lam, H. L., Ng, F. Y., Kamal, M., & Lim, J. H. E. (2012). Waste-to-wealth: green potential from palm biomass in Malaysia. *Journal of Cleaner Production*, 34(0), 57-65. doi: http://dx.doi.org/10.1016/j.jclepro.2012.04.004

Park, S., Baker, J. O., Himmel, M. E., Parilla, P. A., & Johnson, D. K. (2010). Research cellulose crystallinity index: measurement techniques and their impact on interpreting cellulase performance. *Biotechnol Biofuels*, 3(10),68.

Peng, B. L., Dhar, N., Liu, H. L., & Tam, K. C. (2011). Chemistry and applications of nanocrystalline cellulose and its derivatives: A nanotechnology perspective. *The Canadian Journal of Chemical Engineering*, 89(5), 1191-1206. doi: 10.1002/cjce.20554

Poletto, M., Zattera, A. J., Forte, M. M. C., & Santana, R. M. C. (2012). Thermal decomposition of wood: Influence of wood components and cellulose crystallite size. *Bioresource Technology,* 109(0), 148-153. doi: http://dx.doi.org/10.1016/j.biortech.2011.11.122

Prodyut, D., Umesh, B., Amit, K., & Vimal, K. (2014). Cellulose Nanocrystals: A Potential Nanofiller for Food Packaging Applications Food Additives and Packaging. *American Chemical Society*, 1162, 197-239:

Química NovaRamos, L. P. (2003). The chemistry involved in the steam treatment of lignocellulosic materials. *Química Nova*, 26, 863-871.

Rosnah, M., Ghazali, A., Wan Rosli, W., & Dermawan, Y. (2010). Influence of alkaline peroxide treatment duration on the pulpability of oil palm empty fruit bunch. *World Applied Sciences Journal,* 8(2), 185-192.

Salas, C., Nypelö, T., Rodriguez-Abreu, C., Carrillo, C., & Rojas, O. J. (2014). Nanocellulose properties and applications in colloids and interfaces. *Current Opinion in Colloid & Interface Science*, 19(5), 383-396. doi: http://dx.doi.org/10.1016/j.cocis.2014.10.003

Saratale, G. D., & Oh, S. E. (2014). Lignocellulosics to ethanol: The future of the chemical and energy industry. *African Journal of Biotechnology*, 11(5), 1002-1013.

Sathitsuksanoh, N., Zhu, Z., & Zhang, Y. H. P. (2012). Cellulose solvent-based pretreatment for corn stover and avicel: concentrated phosphoric acid versus ionic liquid [BMIM]Cl. *Cellulose*, 19(4), 1161-1172. doi: 10.1007/s10570-012-9719-z

Scheller, H. V., & Ulvskov, P. (2010). Hemicelluloses. *Annu Rev Plant Biol*, 61, 263-289. doi: 10.1146/annurev-arplant-042809-112315

Schuerch, C. (1968). *Methods of wood chemistry*. (B. L. Browning, Ed.). New York:Wiley.

Sèbe, G., Ham-Pichavant, F., Ibarboure, E., Koffi, A. L. C., & Tingaut, P. (2012). Supramolecular Structure Characterization of Cellulose II Nanowhiskers Produced by Acid Hydrolysis of Cellulose I Substrates. *Biomacromolecules*, 13(2), 570-578. doi: 10.1021/bm201777j

Shahabi-Ghahafarrokhi, I., Khodaiyan, F., Mousavi, M., & Yousefi, H. (2015). Preparation and characterization of nanocellulose from beer industrial residues using acid hydrolysis/ultrasound. *Fibers and Polymers,* 16(3), 529-536. doi: 10.1007/s12221-015-0529-4

Shinoj, S., Visvanathan, R., Panigrahi, S., & Kochubabu, M. (2011). Oil palm fiber (OPF) and its composites: A review. *Industrial Crops and Products*, 33(1), 7-22.

Shuit, S. H., Tan, K. T., Lee, K. T., & Kamaruddin, A. H. (2009). Oil palm biomass as a sustainable energy source: A Malaysian case study. *Energy*, 34(9), 1225-1235. doi: http://dx.doi.org/10.1016/j.energy.2009.05.008

Singh, P., Sulaiman, O., Hashim, R., Peng, L. C., & Singh, R. P. (2013). Using biomass residues from oil palm industry as a raw material for pulp and paper industry: potential benefits and threat to the environment. *Environment, development and sustainability,* 15(2), 367-383.

Smidt, E., Eckhardt, K. U., Lechner, P., Schulten, H. R., & Leinweber, P. (2005). Characterization of different decomposition stages of biowaste using FT-IR spectroscopy and pyrolysis-field ionization mass spectrometry. *Biodegradation*, 16(1), 67-79.

Song, J., Fan, H., Ma, J., & Han, B. (2013). Conversion of glucose and cellulose into value-added products in water and ionic liquids. *Green Chemistry*, 15(10), 2619-2635. doi: 10.1039/C3GC41141A

Souza, N., Pinheiro, J., Brígida, A., Morais, J., Filho, M. S., & Rosa, M. (2013, Nov). *Cellulose Nano Whiskers from Oil Palm Fibers*. Paper presented at the International Association of Embrapa Agroindústria de Alimentos-Artigo em anais de congresso (ALICE),Mexico.

Sulaiman, F., Abdullah, N., Gerhauser, H., & Shariff, A. (2011). An outlook of Malaysian energy, oil palm industry and its utilization of wastes as useful resources. *Biomass and bioenergy*, 35(9), 3775-3786.

Sun, R., Fang, J., Mott, L., & Bolton, J. (1999). Extraction and characterization of hemicelluloses and cellulose from oil palm trunk and empty fruit bunch fibres. *Journal of wood chemistry and technology*, 19(1-2), 167-185.

Tang, L.-G., Hon, D. N. S., Pan, S.-H., Zhu, Y.-Q., Wang, Z., & Wang, Z.-Z. (1996). Evaluation of microcrystalline cellulose. I. Changes in ultrastructural characteristics during preliminary acid hydrolysis. *Journal of Applied Polymer Science*, 59(3), 483-488. doi: 10.1002/(SICI)1097-4628(19960118)59:3<483::AID-APP13>3.0.CO;2-V

Technical Association of the, P., & Paper, I. (1973). TAPPI directory / Technical Association of the Pulp and Paper Industry. doi: Technical Association of the Pulp and Paper Industry. Washington, DC: Technical Association of the Pulp & Paper.

Umar, M. S., Jennings, P., & Urmee, T. (2013). Strengthening the palm oil biomass Renewable Energy industry in Malaysia. *Renewable Energy*, 60, 107-115.

Wang, N., Ding, E., & Cheng, R. (2007). Thermal degradation behaviors of spherical cellulose nanocrystals with sulfate groups. *Polymer*, 48(12), 3486-3493.

Wittaya, T. (2009). Microcomposites of rice starch film reinforced with microcrystalline cellulose from palm pressed fiber. *International Food Research Journal,* 16(4), 493-500.

Wu, Q., Henriksson, M., Liu, X,& Berglund, L. (2007). A high strength nanocomposite based on Microcrystalline cellulose and Polyurethane. *Biomacromolecules*, 8, 3687.

Xiao-shu, C., & Wen-xun, F. (1992). Studies of utilization and health effect of palm oil in China. *Nutrition Research*, 12, S23-S29. doi: 10.1016/S0271-5317(05)80447-6

Xu, X., Liu, F., Jiang, L., Zhu, J. Y., Haagenson, D., & Wiesenborn, D. P. (2013). Cellulose Nanocrystals vs. Cellulose Nanofibrils: A Comparative Study on Their Microstructures and Effects as Polymer Reinforcing Agents. *ACS Applied Materials & Interfaces*, 5(8), 2999-3009. doi: 10.1021/am302624t

Yahya, M. B., Lee, H. V., & Abd Hamid, S. B. (2015). Preparation of Nanocellulose via Transition Metal Salt-Catalyzed Hydrolysis Pathway. *BioResourse*, *10*(4), 7627-7639. doi:10.15376/biores.10.4.7627-7639

Yan, F. Y., Krishniah, D., Rajin, M., & Bono, A. (2009). Cellulose extraction from palm kernel cake using liquid phase oxidation. *J Engg Sci Tech*, 4, 57-68.

Yan, Y., Li, T., Ren, Z., & Li, G. (1996). A study on catalytic hydrolysis of peat. *Bioresource Technology*, 57(3), 269-273.

Yang, H., Yan, R., Chen, H., Lee, D. H., & Zheng, C. (2007). Characteristics of hemicellulose, cellulose and lignin pyrolysis. *Fuel*, 86(12–13), 1781-1788. doi: http://dx.doi.org/10.1016/j.fuel.2006.12.013

Yang, Q., Pan, X., Huang, F., & Li, K. (2011). Synthesis and characterization of cellulose fibers grafted with hyperbranched poly(3-methyl-3-oxetanemethanol). *Cellulose*, 18(6), 1611-1621. doi: 10.1007/s10570-011-9587-y

Zain, N., Yusop, S., & Ahmad, I. (2014). Preparation and Characterization of Cellulose and Nanocellulose From Pomelo (Citrus grandis) Albedo. *J Nutr Food Sci*, 5(334), 2.

Zhang, F., Deng, X., Fang, Z., Zeng, H., Tian, X., & Kozinski, J. (2011). Hydrolysis of microcrystalline cellulose over Zn-Ca-Fe oxide catalyst. *Petrochemical Technology*, 40(1), 43-48.

Zhang, S.-Y., Wang, C.-G., Fei, B.-H., Yu, Y., Cheng, H.-T., & Tian, G.-L. (2013). Mechanical Function of Lignin and Hemicelluloses in Wood Cell Wall Revealed with Microtension of Single Wood Fiber. *BioResourse*, *8*(2), 2376-2385. doi:10.15376/biores.8.2.2376-2385

Zhang, Y., Li, Q., Su, J., Lin, Y., Huang, Z., Lu, Y., Hu, H. (2015). A green and efficient technology for the degradation of cellulosic materials: structure changes and enhanced enzymatic hydrolysis of natural cellulose pretreated by synergistic interaction of mechanical activation and metal salt. *Bioresource Technology*, 177, 176-181.

Zhao, J., Zhang, H., Zheng, R., Lin, Z., & Huang, H. (2011a). The enhancement of pretreatment and enzymatic hydrolysis of corn stover by FeSO4 pretreatment. *Biochemical Engineering Journal,* 56(3), 158-164. doi: http://dx.doi.org/10.1016/j.bej.2011.06.002

Zheng, Y., Lee, C., Yu, C., Cheng, Y.-S., Zhang, R., Jenkins, B. M., & VanderGheynst, J. S. (2013). Dilute acid pretreatment and fermentation of sugar beet pulp to ethanol. *Applied Energy,* 105, 1-7. doi: http://dx.doi.org/10.1016/j.apenergy.2012.11.070

LIST OF PUBLICATIONS AND PAPERS PRESENTED

SCOPUS/ISI Cited Publications:

1. **Mazlita, Y**, H.V. Lee, S.B.A. Hamid and S.K. Zain (2015), Chemical Conversion of Palm-based Lignocellulosic Biomass to Nano- Cellulose: Review, Polymer Research Journal, 9(4), 1-22. (Published-*SCOPUS Cited Publication*)
2. **Yahya, M**., Lee, H. V., and Abd Hamid, S. B. (2015). Preparation of Nanocellulose via Transition Metal Salt- Catalyzed Hydrolysis Pathway. BioResource 10:7627-7639 (Published-*ISI Cited Publication*)
3. **Mazlita, Y.,** H.V Lee and S.B.A. Hamid (2016). Preparation of Cellulose Nanocrystals (CNCs) Bio-polymer from Agro-Industrial Wastes: Separation and Characterization. Polymer and Polymer Composites (Accepted-*ISI Cited Publication)*

Conference Proceedings:

1. **Mazlita, Y**, H.V. Lee, S.B.A. Hamid (2014). Chemical Conversion of Palm-based Lignocellulosic Biomass to Nano- Cellulose: Review. *Proceeding of 9th International Materials Technology Conference & Exhibition (IMTCE*), 3-4 May 2014, Kuala Lumpur, Malaysia.
2. **Mazlita, Y**, H.V. Lee, S.B.A. Hamid (2014). Extraction and Characterization of Cellulose and Nanocellulose from Palm Trunk Biomass via Chemical route. *Proceeding of Seminar on Palm Oil Milling, Refining, Environment and Quality (POMREQ*), 3-5 November 2014, Sarawak, Malaysia.
3. **Mazlita, Y**, H.V. Lee, S.B.A. Hamid (2015).Extraction and isolation of Nanocellulose via Nickel Nitrate catalyzed hydrolysis. *Proceeding of Malaysia Polymer International Conference (MPIC)*, 10-11 June 2015, Putrajaya, Malaysia

4. **Mazlita, Y**, H.V. Lee, S.B.A. Hamid (2015). A Novel Green Approach for The Preparation Of Nanocellulose From Oil Palm Biomass. *Proceeding of International Conference On Waste And Management (ICWME),* 20-22 August 2015, Kuala Lumpur. Malaysia
5. **Mazlita, Y**, H.V. Lee, S.B.A. Hamid (2015). A Renewable Source for The Production of Nanocellulose. *Proceeding of Malaysian Palm Oil Board International Palm Oil Congress and Exhibition (PIPOC) 2015,* 6-8 October 2015, Kuala Lumpur. Malaysia